Angewandte Chemie
Eine Zeitschrift der Gesellschaft Deutscher Chemiker

Supporting Information

A Bidentate Ligand Featuring Ditopic Lewis Acids in the Second Sphere for Selective Substrate Capture and Activation

*D. M. Beagan, J. J. Kiernicki, M. Zeller, N. K. Szymczak**

Table of Contents:

Experimental Procedures

General Considerations. All air- and moisture-sensitive manipulations were performed using standard Schlenk techniques or in an inert atmosphere drybox with an atmosphere of purified nitrogen. The drybox was equipped with a cold well designed for freezing samples in liquid nitrogen as well as a −35 °C freezer for cooling samples and crystallizations. Solvents were purified using a Glass Contour solvent purification system through percolation through a Cu catalyst, molecular sieves, and alumina. Solvents were then stored over sodium and/or sieves. Benzene-d_6 and chloroform-*d* were purchased from Cambridge Isotope Laboratories. Benzene-d_6 was dried with molecular sieves and sodium, and degassed by three freeze–pump–thaw cycles. Chloroform-*d* was distilled from CaH_2.

Metal halides, NaH, 9-borabicyclo[3.3.1]nonane, potassium bis(trimethylsilylamide), $NaNO_2$, KOAc, and KEt_3BH, $TBANO_2$, $TBANO_3$, TBAF were purchased from commercial vendors and used as received. Anhydrous hydrazine was purchased from Sigma Aldrich, degassed, and passed through activated alumina prior to use. $^{H}NN^{tBu}$ and ($^{allyl}NN^{tBu}$) were synthesized according to literature procedures.[1,2]

NMR spectra were recorded on Varian Vnmrs 700, Varian MR400, or Bruker Advance Neo 500 spectrometers. ^1H, ^{13}C, and ^{11}B chemical shifts are reported in parts per million (ppm) relative to

tetramethylsilane and referenced internally to the residual solvent peak. ^{11}B spectra were referenced on a unified scale, where the single primary reference is the frequency of the residual solvent peak in the ^{1}H NMR spectrum. ^{11}B spectra are referenced vs. $BF_3(OEt_2)$. Multiplicities are reported as follows: singlet (s), doublet (d), triplet (t), quartet (q), pentet (p), multiplet (m). When reported, purity of diamagnetic species was assessed using quantitative NMR with hexamethyldisiloxane (HMDSO) as an internal standard. Infrared spectra were recorded using a Nicolet iS10 FT-IR spectrometer equipped with Smart Diamond Attenuated Total Reflectance (ATR) sampling accessory. Samples were either diluted into dry KBr and recorded as pellets or collected using ATR sampling accessory. MALDI-TOF data were collected on a Bruker AutoFlex Speed with samples prepared under inert atmosphere in an anthracene matrix.

Samples for elemental analysis were crystallized from slow diffusion of pentane into concentrated THF solutions. After isolation of crystalline material, each sample was dried in vacuo for 5 hours before transfer to a glass ampoule fitted with a sealable adapter. The samples were transferred from the glovebox and attached to the Schlenk line. While under vacuum, each sample was flame sealed to ensure a rigorously moisture and air free transit. The samples were shipped to Atlantic Microlabs for analysis. Despite moisture/air free shipping conditions, the samples were analyzed under ambient conditions. For complexes 2, 2-N_2H_4, and ($^{ene}NN^{tBu}$)$FeBr_2$, the carbon content was anomalously high. The Fe/second-sphere borane complexes readily undergo hydrolysis, and we note that incorporation of hydrates significantly improves the elemental analysis data. For transparency, we report the elemental analysis data with *and* without hydrates.

Single crystals of ($^{(BBN)2}NN^{tBu}$), [$^{(BBN)2}NN^{tBu}$(OAc)](K-18-crown-6), [$^{(BBN)2}NN^{tBu}$(NO_2)](K-18-crown-6), [($^{(BBN)2}NN^{tBu}$)(H)]K, ($^{(BBN)2}NN^{tBu}$)$FeCl_2$, ($^{(BBN)2}NN^{tBu}$)$NiBr_2$, ($^{(BBN)2}NN^{tBu}$)$ZnCl_2$, ($^{(BBN)2}NN^{tBu}$)$NiBr_2(N_2H_4)$, ($^{(BBN)2}NN^{tBu}$)$ZnCl_2(N_2H_4)$, ($^{(BBN)2}NN^{tBu}$)$ZnBr(N_2H_3)$, ($^{(BBN)2}NN^{tBu}$)$ZnCl(N_2H_3)$, and ($^{(BBN)2}NN^{tBu}$)$FeBr(N_2H_2)$ were mounted on a Rigaku AFC10K Saturn 944+ CCD-based X-ray diffractometer equipped with Micromax-007HF Cu-target microfocus rotating anode (λ = 1.54187 Å) operated at 1.2 kW power (40 kV, 30 mA). The X-ray intensities were measured at 293 K with the detector placed at a distance 42.00 mm from the crystal. Rigaku d*trek images were exported to CrysAlisPro[3] and CrystalClear Expert 2.0 r16[4] for processing and corrected for absorption.

Single crystals of ($^{ene}NN^{tBu}$)$FeBr_2$, ($^{propargyl}NN^{tBu}$)$FeBr_2$, ($^{(BBN)2}NN^{tBu}$)$FeBr_2$, and ($^{(BBN)2}NN^{tBu}$)$FeBr2(N_2H_4)$ suitable for X-ray diffraction were coated with poly(isobutylene) oil and quickly transferred to the goniometer head of a Bruker AXS D8 Quest diffractometer with a fixed chi angle, a sealed tube fine focus X-ray tube, single crystal curved graphite incident beam monochromator and a Photon100 CMOS area detector. Examination and data collection were performed with Mo Kα radiation (λ = 0.71073 Å). For all samples, data were collected, reflections were indexed and processed, and the files scaled and corrected for absorption using APEX3.[5] For all samples, the space groups were assigned and the structures were solved by direct methods using XPREP within the SHELXTL suite of programs[6] and refined by full matrix least squares against F^2 with all reflections using Shelxl2017 or Shelxl2018[7] using the graphical interface Shelxle.[8] If not specified otherwise, H atoms attached to carbon atoms were positioned geometrically and constrained to ride on their parent atoms, with carbon hydrogen bond distances of 0.95 Å for and aromatic C-H, 1.00, 0.99 and 0.98 Å for aliphatic C-H, CH_2, and CH_3 moieties, respectively. Methyl H atoms were allowed to rotate but not to tip to best fit the experimental electron density. $U_{iso}(H)$ values were set to a multiple of $U_{eq}(C)$ with 1.5 for CH_3, and 1.2 for CH_2,

and C-H units, respectively. Additional data collection and refinement details, including description of disorder (where present) can be found with the individual structure descriptions, below.

Synthesis of $^{propargyl}NN^{tBu}$ ligand. Inside of a glovebox, a 200 mL Schlenk flask was charged with sodium hydride (0.565 g, 23. 541 mmol), 50 mL THF, and a stirbar. The flask was removed from the glovebox, attached to a Schlenk line, and cooled to -78 °C with a dry ice/acetone bath. Against a flow of N_2, 2-(5-tert-butyl)-1H-pyrazol-3-yl)-6-methylpyridine (3.876 g, 18.003 mmol) was added as a solid. The cold bath was removed and the solution was allowed to gradually warm to room temperature with stirring. Caution! Vigorous H_2 evolution occurs near 0 °C. When H_2 evolution had ceased, propargyl bromide (8.600 g, 72.293 mmol) was added via syringe. The flask was fitted with a reflux condenser and refluxed for 18 hr. The solution was cooled to room temperature and volatiles were removed in vacuo to afford a brown sludge. The material was extracted with 150 mL $CHCl_3$, filtered over Celite, and dried to afford yellow-brown oil. The crude material was purified by column chromatography (silica, R_f = 0.51 in 2:1 hexane:ethyl acetate) to afford light yellow solid (2.385 g, 9.414 mmol, 52%) assigned as 2-(5-tert-butyl)-1-ethynyl-1H-pyrazol-3-yl)-6-methylpyridine. The product was stored at -35 °C between use and was found to degrade to a brown tar if stored at room temperature. High-Res MS for $C_{16}H_{19}N_3$ + H: Calc. 254.1657; Found 254.2002. ^{1}H NMR ($CDCl_3$, 25 °C, 700 MHz) δ = 1.47 (s, 9H, $C(CH_3)_3$), 2.39 (t, *J* = 2.3 Hz, 1H, CCH), 2.60 (s, 3H, CH_3), 5.09 (d, *J* = 2.2 Hz, 2H, N-CH_2), 6.70 (s, 1H, pz-CH), 7.05 (d, *J* = 7.6 Hz, 1H, pyr-CH), 7.58 (t, *J* = 7.7 Hz, 1H, p-pyr-CH), 7.75 (d, *J* = 7.8 Hz, 1H, pyr-CH). ^{13}C NMR ($CDCl_3$, 25 °C, 176 MHz) δ = 24.79 (CH_3), 30.31 ($C(CH_3)_3$), 31.60 ($C(CH_3)_3$), 41.61 (N-CH_2) 73.65 (C≡CH), 78.66 (C≡CH), 103.18 (pz-CH), 117.41 (m-pyr-CH), 122.07 (p-pyr-CH), 150.93, 151.81, 152.96, 158.11. Selected IR data (ATR, neat) v = 2968, 2121 (C≡C), 1594, 1576, 1540, 1491, 1474, 1421, 1400, 1367, 1300, 1257, 1215, 942, 763, 670 cm^{-1}.

Synthesis of ($^{propargyl}NN^{tBu}$)$FeBr_2$. A 20 mL scintillation vial was charged with $FeBr_2$ (0.262 g, 1.21 mmol) and 5 mL DCM. While stirring, ($^{propargyl}NN^{tBu}$) (0.307 g, 1.21 mmol) in 5 mL DCM was added. After 16 hr at RT, the cloudy yellow solution was filtered through Celite and the volatiles were removed in vacuo. The resulting orange solid was washed with 4 x 5 mL of pentane to afford an orange powder assigned as ($^{propargyl}NN^{tBu}$)$FeBr_2$ (0.466 g, 82%). Single, X-ray quality crystals were obtained from slow diffusion of diethyl ether into a DCM solution at room temperature. MALDI-TOF of $C_{32}H_{38}Br_3Fe_2N_6$ (($^{propargyl}NN^{tBu}$)$FeBr_2$)$_2$ – Br: Calc. 856.934; Found 856.623. ^{1}H NMR ($CDCl_3$, 25 °C, 400 MHz) δ = -25.36, -22.29, -16.26, 0.26, 1.04, 2.50, 41.33, 50.68, 54.24. ^{1}H NMR (THF, 25 °C, 400 MHz) δ = -24.00, -22.83, -15.54, -0.49, 2.37, 40.23, 49.29, 53.25. IR (KBr): $\nu_{(C\equiv C)}$ = 2128 cm^{-1}. Elemental analysis: $C_{16}H_{29}Br_2FeN_3$ Calc. C – 42.10, H – 4.78, N – 8.66. Found C – 41.65, H – 4.37, N – 9.05.

Synthesis of ($^{ene}NN^{tBu}$)$FeBr_2$. A 20 mL scintillation vial was charged with ($^{propargyl}NN^{tBu}$)$FeBr_2$ (189 mg, 0.403 mmol) and 5 mL of THF. To this stirring solution was added 9-BBN (149 mg, 1.22 mmol) dissolved in 5 mL of THF. The solution stirred at room temperature for 24 hours before the volatiles were removed in vacuo to afford a yellow powder. The yellow powder was washed with 2 x 20 mL pentane to afford a light yellow powder assigned as ($^{ene}NN^{tBu}$)$FeBr_2$ (0.217 g, 91%). Single, X-ray quality crystals were obtained from layering of a C_6H_6 solution with HMDSO at room temperature. MALDI-TOF of $C_{24}H_{34}Br_2FeN_3$ ($^{ene}NN^{tBu}$)$FeBr_2$: Calc. 591.054; Found 590.891. ^{1}H NMR (THF, 25 °C, 400 MHz) δ = -28.35, -23.98, -16.23, -4.08, -2.76, -1.07, 0.03, 0.39, 2.52, 40.64, 49.25, 54.19. Elemental analysis: $C_{24}H_{34}Br_2BFeN_3$ Calc. C – 48.77, H – 5.80, N – 7.11. $C_{32}H_{38}Br_3Fe_2N_6$•H_2O Calc. C – 47.33, H – 5.96, N – 6.90. Found C – 47.57, H – 5.71, N – 6.87.

Synthesis of $^{(BBN)2}NN^{tBu}$ (1). Inside the glovebox, a 200 mL Schlenk flask was charged with was charged with ($^{propargyl}NN^{tBu}$) (0.712 g, 2.81 mmol) and 10 mL of C_6H_6. While stirring, 9-borabicyclo[3.3.1]nonane (1.03 g, 8.44 mmol) was added as a solution in 5 mL of C_6H_6. The flask was removed from the glovebox and the reaction was heated to 55 °C for 1 hr. The solution was cooled to room temperature and the flask returned to the glovebox. The solvent was removed in vacuo to afford an off-white solid. The off-white solid was rinsed with cold pentane (-35 °C) (3 x 5 mL) to afford a white solid assigned as $^{(BBN)2}NN^{tBu}$ (0.937 g, 67%, purity = 98%). Single, X-ray quality crystals were obtained from a concentrated ether solution at -35 °C. High-Res MS for $C_{16}H_{19}N_3$ + H: Calc. 498.42; Found 498.4194. ^{1}H NMR (C_6D_6, 25 °C, 500 MHz) δ = 1.21 (s, 9H, C(C*H*$_3$)$_3$), 1.29 (m, 4H) 1.67 (m, 4H), 2.00-1.80 (m, 20H), 2.48 (s, 3H, pyr-C*H*$_3$), 2.88-2.72 (m, 3H), 4.19-4.08 (m, 2H, N-C*H*$_2$), 6.60 (d, *J* = 7.5 Hz, 1H, pyr-C*H*) 7.17 (t, *J* = 7.8 Hz, 1H, pyr-C*H*), 7.20 (s, 1H, pz-C*H*), 8.23 (d, *J* = 7.9 Hz, 1H, pyr-C*H*). ^{13}C NMR (C_6D_6, 25 °C, 125 MHz) δ = 23.19, 24.36, 29.89, 30.05, 31.03, 31.65, 33.18, 33.42, 54.04, 102.82, 116.45, 120.99, 136.01, 150.60, 151.42, 152.94, 157.57. ^{11}B NMR (THF, 25 °C) δ = 89.3

Synthesis of $^{(BBN)}NN^{tBu}$ (1-mono). Inside the glovebox, a 200 mL Schlenk flask was charged with was charged with ($^{allyl}NN^{tBu}$) (0.215 g, 0.843 mmol) and 10 mL of C_6H_6. While stirring, 9-borabicyclo[3.3.1]nonane (0.206 g, 1.69 mmol) was added as a solution in 5 mL of C_6H_6. The flask was removed from the glovebox and the reaction was heated to 55 °C for 1 hr. The solution was cooled to room temperature and the flask returned to the glovebox. The solvent was removed in vacuo to afford an off-white solid. The off-white solid was rinsed with cold pentane (-35 °C) (3 x 5 mL) to afford a white solid assigned as $^{(BBN)}NN^{tBu}$ (0.232 mg, 73%, purity = 98%). High-Res MS for $C_{16}H_{19}N_3$ + H: Calc. 378.31; Found 378.3057. ^{1}H NMR (C_6D_6, 25 °C, 500 MHz) δ = 1.09 (s, 9H, C(C*H*$_3$)$_3$), 1.43-1.26 (m, 4H), 1.51 (m, 2H), 1.74-1.57 (m, 5H), 1.86-1.78 (m, 3H), 1.92 (dtt, J = 13.1, 11.2, 5.8 Hz, 2H), 2.10 (p, *J* = 7.3 Hz, 2H), 2.46 (s, 3H, pyr-C*H*$_3$), 4.04 (t, *J* = 7.0 Hz, 2H, N-C*H*$_2$), 6.63 (d, *J* = 7.6 Hz, 1H, pyr-C*H*), 6.88 (s, 1H, pz-C*H*), 7.11 (t, *J* = 7.7 Hz, 1H, pyr-C*H*), 7.87 (d, *J* = 7.7 Hz, 1H, pyr-C*H*). ^{13}C NMR (C_6D_6, 25 °C, 125 MHz) δ = 21.99, 23.67, 24.29, 25.64, 29.49, 30.03, 30.99, 32.17, 103.69, 118.39, 121.56, 135.75, 151.25, 152.20, 152.69, 157.73. ^{11}B NMR (THF, 25 °C) δ = 39.2

Synthesis of [$^{(BBN)2}NN^{tBu}$(OAc)](K-18-crown-6) (1-OAc). A 20 mL scintillation vial was charged with **1** (31.0 mg, 0.062 mmol) and 5 mL of THF. While stirring, potassium acetate (6.11 mg, 0.062 mmol) and 18-crown-6 (16.4 mg, 0.062 mmol) were added as solids. The solution stirred at room temperature for 16 hr, during which the solution became homogenous. After 16 hr, the volatiles were removed in vacuo generating a white solid. The white solid was rinsed with 3 x 5 mL of pentane to afford a white solid assigned as [$^{(BBN)2}NN^{tBu}$(OAc)](K-18-crown-6) (46.6 mg, 87%, purity = 97%). Single, X-ray quality crystals were obtained from slow diffusion of pentane into a THF solution at room temperature. ^{1}H NMR (THF, 25 °C, 400 MHz, some resonances obstructed by proteo-THF after solvent suppression) δ = 0.13 (t, *J* = 4.0 Hz, 1H), 1.03 – 0.86 (m, 4H), 1.34 (s, 9H, C(C*H*$_3$)$_3$), 1.52 – 1.45 (m, 4H), 1.93 (s, 3H, C*H*$_3$COO), 2.10 (dt, *J* = 12.5, 4.3 Hz, 2H), 2.40 (s, 3H, pyr-C*H*$_3$), 4.09 – 4.02 (m, 2H, N-C*H*$_2$), 6.47 (s, 1H, pz-C*H*), 6.83 (d, *J* = 7.5 Hz, 1H, pyr-C*H*), 7.40 (t, *J* = 7.7 Hz, 1H, pyr-C*H*), 7.75 (d, *J* = 7.8 Hz, 1H, pyr-C*H*). ^{11}B NMR (THF, 25 °C) δ = 10.3

Synthesis of [$^{(BBN)2}NN^{tBu}$(NO_2)](Na-18-crown-6) (1-NO_2). A 20 mL scintillation vial was charged with **1** (29.7 mg, 0.060 mmol) and 5 mL of THF. While stirring, sodium nitrite (4.12 mg, 0.060 mmol) and 18-crown-6 (15.8 mg, 0.060 mmol) were added as solids. The solution stirred at room temperature for 16 hr, during which the solution became homogenous accompanied by a color change to yellow. After 16 hr, the volatiles were removed in vacuo generating a yellow solid. The

yellow solid was rinsed with 3 x 5 mL of pentane to afford a yellow solid assigned as [$^{(BBN)2}$NN^{tBu}(NO_2)](Na-18-crown-6) (41.2 mg, 83%, purity = 97%). Single, X-ray quality crystals were obtained from slow diffusion of pentane into a THF solution at room temperature. ^{1}H NMR (C_6D_6, 23 °C, 500 MHz) δ = 1.25 (s, 1H), 1.32 (s, 9H, C(C*H*$_3$)$_3$), 1.37-1.45 (m, 4H), 1.66-2.71 (m, 24 H, BBN-C*H*), 2.50 (s, 3H, pyr-C*H*$_3$), 3.16 (s, 24H, 18-crown-6), 4.47-4.29 (m, 2H, N-C*H*$_2$), 6.65 (d, J = 7.5 Hz, 1H, pyr-C*H*), 7.10 (s, 1H, pyz-C*H*), 7.21 (t, J = 7.7 Hz, 1H, pyr-C*H*), 8.06 (d, J = 7.9 Hz, 1H, pyr-C*H*). ^{1}H NMR (THF, 25 °C, 400 MHz, some resonances obstructed by proteo-THF after solvent suppression) δ = 0.27 (t, *J* = 4.7 Hz, 1H), 0.84 (t, *J* = 7.0 Hz, 1H), 1.16 – 0.93 (m, 6H), 1.35 (s, 9H, C(C*H*$_3$)$_3$), 2.40 (s, 3H, pyr-C*H*$_3$), 4.16 (dd, *J* = 10.8, 6.3 Hz, 2H, N-C*H*$_2$), 6.47 (s, 1H, pz-C*H*), 6.84 (d, J = 7.4 Hz, 1H, pyr-C*H*), 7.42 (t, J = 7.9 Hz, 1H, pyr-C*H*), 7.74 (d, J = 7.9 Hz, 1H, pyr-C*H*). ^{13}C NMR (C_6D_6, 25 °C, 125 MHz) δ = 24.42, 25.45, 29.99, 30.11, 31.20, 33.43, 67.46, 69.01, 101.96, 116.13, 120.53, 135.73, 151.54, 153.59, 157.61. ^{11}B NMR (THF, 25 °C) δ = 12.07, 17.3

Synthesis of [$^{(BBN)2}$NN^{tBu}(H)]K (1-H). A 20 mL scintillation vial was charged with **1** (25.6 mg, 0.051 mmol) and 5 mL of THF and frozen. Upon thawing, KEt_3BH (51 µL, 0.051 mmol) was added cold (-35 °C) as a 1 M solution in THF. The reaction was gradually warmed to room temperature and stirred for 15 minutes. The solvent was removed in vacuo to give a white solid. The white solid was rinsed with 3 x 5 mL of pentane to afford a white solid assigned as [$^{(BBN)2}$NN^{tBu}(H)]K (23.3 mg, 85%, purity = 98%). Single, X-ray quality crystals were obtained from slow diffusion of pentane into a THF solution at room temperature. ^{1}H NMR (C_6D_6, 25 °C, 500 MHz) δ = -0.51 (q, *J* = 5.4 Hz, 1H, B-C*H*-B), -0.35 (s, 1H, B-*H*-B), 0.00 (td, *J* = 7.7, 3.6 Hz, 2H), 0.83 (q, *J* = 3.4 Hz, 2H), 1.16 (s, 9H, C(C*H*$_3$)$_3$), 2.68-1.88 (m, 24H, 9-BBN-C*H*$_2$), 3.32 (td, *J* = 5.3, 4.2, 1.7 Hz, 2H, -C*H*$_2$), 4.48-4.35 (m, 2H, N-C*H*$_2$), 6.09 (s, 1H, pz-C*H*), 6.42 (d, *J* = 7.6 Hz, 1H, pyr-C*H*), 6.87 (d, *J* = 7.8 Hz, 1H, pyr-C*H*), 6.97 (t, *J* = 7.7 Hz, 1H, pyr-C*H*). ^{1}H NMR (THF, 25 °C, 400 MHz, some resonances obstructed by proteo-THF after solvent suppression) δ = -1.11 (q, *J* = 5.5, 5.0 Hz, 1H, B-C*H*-B), -1.02 (s, 1H, B-*H*-B), -0.21 (td, *J* = 7.9, 4.0 Hz, 1H), 0.24 (s, 2H), 0.49 (s, 2H), 0.65 – 0.54 (m, 2H), 1.40 (s, 9H, C(C*H*$_3$)$_3$), 2.06 – 1.78 (m, 24H, 9-BBN-C*H*$_2$), 2.46 (s, 3H, pyr-C*H*$_3$), 4.30 – 4.21 (m, 2H, N-C*H*$_2$), 6.47 (d, *J* = 1.4 Hz, 1H, pyr-C*H*), 7.02 (d, *J* = 7.0 Hz, 1H, pyr-C*H*), 7.64-7.47 (m, 3H, pyr-C*H* and pz-C*H*). ^{13}C NMR (C_6D_6, 25 °C, 125 MHz) δ = 11.53, 15.18, 23.82, 25.34, 26.52, 27.00, 29.54, 31.21, 33.00, 34.20, 34.28, 36.79, 38.29, 58.01, 65.54, 67.50, 101.74, 118.28, 121.37, 137.45, 147.49, 151.81, 152.89, 156.35. ^{11}B NMR (THF, 25 °C) δ = -9.91

Synthesis of $^{(BBN)2}$NN^{tBu}(N_2H_4) (1-N_2H_4). A 20 mL scintillation vial was charged with **1** (27.4 mg, 0.055 mmol) and 5 mL of THF. While stirring, hydrazine (346 µL, 0.055 mmol) was added as a 0.159 M solution in THF and the solution stirred for 15 minutes. Volatiles were removed in vacuo and the resulting solid was washed with cold pentane (-35 °C) to afford a white powder assigned as $^{(BBN)2}$NN^{tBu}(N_2H_4) (23.1 mg, 79%). ^{1}H NMR (THF, 25 °C, 400 MHz, some resonances obstructed by proteo-THF after solvent suppression) δ = 0.13 (t, *J* = 9.6 Hz, 1H), 0.38 (bs, 2H, N-*H*$_2$), 0.80 (s, 2H, N-*H*$_2$), 1.38 (s, 9H, C(C*H*$_3$)$_3$), 2.11 (q, *J* = 6.3 Hz, 2H), 2.51 (s, 3H, pyr-C*H*$_3$), 4.44 (t, *J* = 6.7 Hz, 2H, N-C*H*$_2$), 6.43 (s, 1H, pz-C*H*), 7.01 (d, *J* = 7.3 Hz, 1H, pyr-C*H*), 7.65 – 7.44 (m, 2H, pyr-C*H*). ^{11}B NMR (THF, 25 °C) δ = 4.96

Synthesis of ($^{(BBN)2}$NN^{tBu})$FeBr_2$ (2-Br). A 20 mL scintillation vial was charged with $FeBr_2$ (0.179 g, 0.83 mmol) and 5 mL of THF. While stirring, **1** (0.412 g, 0.83 mmol) was added dropwise as a THF solution (5 mL). The solution stirred at room temperature for 16 hours, resulting in a cloudy yellow solution. Volatiles were removed in vacuo, and the yellow solid was rinsed with 3 x 5 mL pentane and 2 x 5 mL ether to afford a yellow powder assigned as ($^{(BBN)2}$NN^{tBu})$FeBr_2$ (0.538 g,

91%). Single, X-ray quality crystals were obtained from slow diffusion of pentane into a benzene solution at room temperature. MALDI-TOF of $C_{32}H_{49}B_2Br_2FeN_3$ ($^{(BBN)2}NN^{tBu}$)$FeBr_2$: Calc. 713.182; Found 712.835. ^{1}H NMR ($CDCl_3$, 25 °C, 400 MHz) δ = -28.97, -22.38, -17.09, -6.74, -0.46, 0.63, 1.67, 1.98, 2.58, 38.92, 50.39, 55.62. Elemental analysis: $C_{32}H_{49}B_2Br_2FeN_3$ Calc. C – 53.90, H – 6.93, N – 5.89. $C_{32}H_{49}B_2Br_2FeN_3$•$(H_2O)_3$ Calc. C – 50.11, H – 7.23, N – 5.48. Found C – 49.24, H – 6.63, N – 5.22.

Synthesis of ($^{(BBN)2}NN^{tBu}$)$FeCl_2$ (2-Cl). A 20 mL scintillation vial was charged with $FeCl_2$ (0.057 g, 0.45 mmol) and 5 mL of THF. While stirring, **1** (0.223 g, 0.45 mmol) was added dropwise as a THF solution (5 mL). The solution stirred at room temperature for 16 hours, resulting in a cloudy yellow solution. Volatiles were removed in vacuo, and the yellow solid was rinsed with 3 x 5 mL pentane and 2 x 5 mL ether to afford a yellow powder assigned as ($^{(BBN)2}NN^{tBu}$)$FeCl_2$ (0.249 g, 89%). Single, X-ray quality crystals were obtained from slow diffusion of pentane into a THF solution at room temperature. ^{1}H NMR (C_6D_6, 25 °C, 400 MHz) δ = -25.88, -21.21, -18.01, -6.87, -0.55, 0.65, 1.19, 1.60, 1.81, 2.15, 4.63, 38.04, 47.49, 52.96.

Synthesis of ($^{(BBN)2}NN^{tBu}$)$NiBr_2$ (3). A 20 mL scintillation vial was charged with (DME)$NiBr_2$ (0.189 g, 0.61 mmol) and 5 mL of THF. While stirring, **1** (0.305 g, 0.61 mmol) was added dropwise as a THF solution (5 mL). The solution stirred at room temperature for 16 hours, resulting in a cloudy purple solution. Volatiles were removed in vacuo, and the purple solid was rinsed with 3 x 5 mL pentane and 2 x 5 mL ether to afford a purple powder assigned as ($^{(BBN)2}NN^{tBu}$)$NiBr_2$ (0.403 g, 92%). Single, X-ray quality crystals were obtained from slow diffusion of pentane into a THF solution at room temperature. MALDI-TOF of $C_{32}H_{49}B_2NiN_3$ ($^{(BBN)2}NN^{tBu}$)$NiBr_2$ – 2 Br: Calc. 555.335; Found 554.828. ^{1}H NMR (THF, 25 °C, 400 MHz) δ = 2.20, 2.94, 4.09, 4.37, 6.25, 11.77, 11.79, 17.30, 19.18, 25.11, 48.87, 54.73, 79.78. Elemental analysis: $C_{32}H_{49}B_2NiN_3$ Calc. C – 53.69, H – 6.90, N – 5.87. Found C – 53.84, H – 7.03, N – 5.78.

Synthesis of ($^{(BBN)2}NN^{tBu}$)$ZnBr_2$ (4-Br). A 20 mL scintillation vial was charged with $ZnBr_2$ (0.094 g, 0.42 mmol) and 5 mL of THF. While stirring, **1** (0.207 g, 0.42 mmol) was added dropwise as a THF solution (5 mL). The solution stirred at room temperature for 16 hours, resulting in a cloudy colorless solution. Volatiles were removed in vacuo, and the white solid was rinsed with 3 x 5 mL pentane and 2 x 5 mL ether to afford a white powder assigned as ($^{(BBN)2}NN^{tBu}$)$ZnBr_2$ (0.283 g, 94%, purity = 98%). ^{1}H NMR (500 MHz, C_6D_6) δ = 6.73 (t, *J* = 7.8 Hz, 1H, pyr-C*H*), 6.51 (d, *J* = 7.7 Hz, 1H, pyr-C*H*), 6.18 (d, *J* = 7.8 Hz, 1H, pyr-C*H*), 5.90 (s, 1H, pz-C*H*), 4.54 – 4.47 (m, 2H, N-CH_2), 3.67 – 3.47 (m, 2H, -CH_2), 3.21 (t, *J* = 6.6 Hz, 1H, B-C*H*-B) 2.67 (s, 3H, pyr-CH_3), 2.27 – 1.79 (m, 24H, 9-BBN-CH_2), 1.41 (tt, *J* = 5.4, 3.2 Hz, 4H, 9-BBN-C*H*), 1.05 (s, 9H, pz-(CH_3)$_3$). ^{13}C NMR (C_6D_6, 25 °C, 125 MHz) δ = 15.24, 23.26, 23.79, 25.45, 29.20, 30.76, 31.31, 33.36, 33.68, 54.87, 65.56, 67.46, 101.15, 117.07, 124.79, 139.41, 145.29, 145.87, 155.38, 159.16.

Synthesis of ($^{(BBN)2}NN^{tBu}$)$ZnCl_2$ (4-Cl). A 20 mL scintillation vial was charged with $ZnCl_2$ (0.030 g, 0.22 mmol) and 5 mL of THF. While stirring, **1** (0.110 g, 0.22 mmol) was added dropwise as a THF solution (5 mL). The solution stirred at room temperature for 16 hours, resulting in a cloudy colorless solution. Volatiles were removed in vacuo, and the white solid was rinsed with 3 x 5 mL pentane and 2 x 5 mL ether to afford a white powder assigned as ($^{(BBN)2}NN^{tBu}$)$ZnCl_2$ (0.129 g, 92%). Single, X-ray quality crystals were obtained from slow diffusion of pentane into a THF solution at room temperature. ^{1}H NMR (C_6D_6, 25 °C, 400 MHz) δ = 1.01 (s, 9H, (CH_3)$_3$), 1.44-1.29 (m, 4H), 2.20-1.76 (m, 24H, 9-BBN-CH_2), 2.57 (s, 3H, pyr-CH_3), 3.09 (d, *J* = 13.6 Hz, 2H), 4.39 (dd, *J* = 11.5, 5.4 Hz, 2H, N-CH_2) 5.86 (d, *J* = 1.8 Hz, 1H, pz-C*H*), 6.14 (d, *J* = 7.8 Hz, 1H, pyr-C*H*), 6.47 (d, *J* = 7.8 Hz, 1H, pyr-C*H*), 6.69 (t, *J* = 7.8 Hz, 1H, pyr-C*H*). ^{1}H NMR (THF, 25 °C, 400

MHz, some resonances obstructed by proteo-THF after solvent suppression) δ = 1.36 – 1.24 (m, 4H), 1.45 (s, 9H, (CH_3)$_3$), 2.85 – 2.72 (m, 5H, pyr-CH_3 and -CH_2), 4.35 – 4.28 (m, 2H, N-CH_2), 6.85 (s, 1H, pz-C*H*), 7.41 (d, *J* = 7.8 Hz, 1H, pyr-C*H*), 7.81 (d, *J* = 7.8 Hz, 1H, pyr-C*H*), 7.95 (t, *J* = 7.8 Hz, 1H, pyr-C*H*). ^{13}C NMR (C_6D_6, 25 °C, 125 MHz) δ = 15.32, 23.27, 23.65, 25.44, 29.20, 30.65, 31.29, 31.87, 33.19, 33.34, 33.65, 54.96, 65.56, 67.49, 100.99, 117.02, 124.63, 139.40, 145.37, 146.01, 155.32, 159.11.

Synthesis of ($^{(BBN)2}$NN^{tBu})FeBr$_2$(N_2H_4) (2-N_2H_4). A 20 mL scintillation vial was charged with **2-Br** (34.6 mg, 0.049 mmol) and 5 mL THF. While stirring, hydrazine (305 µL, 0.049 mmol) was added as a 0.159 M solution in THF and the solution was stirred at room temperature for 15 minutes. Volatiles were removed in vacuo, and the yellow solid was rinsed with 3 x 5 mL pentane to afford a yellow powder assigned as ($^{(BBN)2}$NN^{tBu})FeBr$_2$(N_2H_4) (31.8 mg, 88%). Single, X-ray quality crystals were obtained from slow diffusion of pentane into a THF solution at room temperature. MALDI-TOF of $C_{32}H_{49}B_2Br_2FeN_3$ ($^{(BBN)2}$NN^{tBu})FeBr$_2$(N_2H_4) – N_2H_4 : Calc. 713.182; Found 712.871. ^{1}H NMR (THF, 25 °C, 400 MHz) δ = -33.01, -25.52, -18.53, -12.95, -4.88, -1.57, -1.22, 0.64, 0.48, 1.38, 2.30, 2.42, 3.02, 7.81, 10.11, 10.49, 34.17, 52.46, 55.84. IR (KB_r): $\nu_{(N-H)}$ = 3296, 3204 cm^{-1}. Elemental analysis: $C_{32}H_{53}B_2Br_2FeN_5$ Calc. C – 51.59, H – 7.17, N – 9.40. $C_{32}H_{53}B_2Br_2FeN_5$•(H_2O)$_2$ Calc. C – 49.21, H – 7.36, N – 8.97. Found C – 49.50, H – 7.02, N – 8.70.

Synthesis of ($^{(BBN)2}$NN^{tBu})NiBr$_2$(N_2H_4) (3-N_2H_4). A 20 mL scintillation vial was charged with **3-Br** (0.052 mg, 0.073 mmol) and 5 mL THF. While stirring, hydrazine (457 µL, 0.073 mmol) was added as a 0.159 M solution in THF and the solution was stirred at room temperature for 15 minutes. Volatiles were removed in vacuo, and the purple/red solid was rinsed with 3 x 5 mL pentane to afford a light red powder assigned as ($^{(BBN)2}$NN^{tBu})NiBr$_2$(N_2H_4) (44.0 mg, 81%). Single, X-ray quality crystals were obtained from slow diffusion of pentane into a THF solution at room temperature. MALDI-TOF of $C_{32}H_{53}B_2NiN_5$ ($^{(BBN)2}$NN^{tBu})NiBr$_2$(N_2H_4) – 2 Br: Calc. 587.367; Found 587.737. ^{1}H NMR (THF, 25 °C, 400 MHz) δ = 2.96, 4.11, 4.42, 4.59, 5.75, 6.77, 8.05, 11.10, 13.36, 17.43, 21.46, 26.69, 41.16, 47.11, 57.05, 82.23. IR (KB_r): $\nu_{(N-H)}$ = 3312, 3248 cm^{-1}. Elemental analysis: $C_{32}H_{53}B_2NiBr_2N_5$ Calc. C – 51.39, H – 7.14, N – 9.36. Found C – 51.97, H – 7.42, N – 9.02.

Synthesis of ($^{(BBN)2}$NN^{tBu})ZnBr$_2$(N_2H_4) (4-Br-N_2H_4). A 20 mL scintillation vial was charged with **4-Br** (34.1 mg, 0.047 mmol) and 5 mL THF. While stirring, hydrazine (297 µL, 0.047 mmol) was added as a 0.159 M solution in THF and the solution was stirred at room temperature for 15 minutes. Volatiles were removed in vacuo, and the white solid was rinsed with 3 x 5 mL pentane to afford a white powder assigned as ($^{(BBN)2}$NN^{tBu})ZnBr$_2$(N_2H_4) (32.1 mg, 90%). ^{1}H NMR (C_6D_6, 25 °C, 400 MHz) δ = 1.01 (s, 9H, (CH_3)$_3$), 1.63-2.25 (m, 24H, 9-BBN-CH_2), 3.10 (m, 2H), 4.49-4.42 (m, 2H, N-CH_2), 5.02 (s, 1H), 5.86 (s, 1H, pz-C*H*), 6.15 (d, *J* = 7.7 Hz, 1H), 6.48 (d, *J* = 7.9 Hz, 1h, pyr-C*H*), 6.70 (t, *J* = 7.8 Hz, 1H, pyr-C*H*).

Synthesis of ($^{(BBN)2}$NN^{tBu})ZnCl$_2$(N_2H_4) (4-Cl-N_2H_4). A 20 mL scintillation vial was charged with **4-Cl** (25.4 mg, 0.04 mmol) and 5 mL THF. While stirring, hydrazine (252 µL, 0.04 mmol) was added as a 0.159 M solution in THF and the solution was stirred at room temperature for 15 minutes. Volatiles were removed in vacuo, and the white solid was rinsed with 3 x 5 mL pentane to afford a white powder assigned as ($^{(BBN)2}$NN^{tBu})ZnCl$_2$(N_2H_4) (23.7 mg, 89%). Single, X-ray quality crystals were obtained from slow diffusion of pentane into a THF solution at room temperature. ^{1}H NMR (THF, 25 °C, 400 MHz, some resonances obstructed by proteo-THF after solvent suppression) δ = -0.04 (t, *J* = 7.1 Hz, 1H), 1.00 – 0.89 (m, 4H), 1.45 (s, 9H, (CH_3)$_3$), 2.11 – 2.01 (m, 2H), 2.76 (s, 3H, pyr-CH_3), 4.54 – 4.47 (m, 2H, N-CH_2), 6.44 (s, 4H, N_2H_4), 6.79 (s, 1H, pz-C*H*), 7.36 (d, *J* =

7.8 Hz, 1H, pyr-C*H*), 7.78 (d, *J* = 7.8 Hz, 1H, pyr-C*H*), 7.93 (t, *J* = 7.8 Hz, 1H, pyr-C*H*). IR (KB_r): $\nu_{(N-H)}$ = 3291, 3224 cm^{-1}

Synthesis of ($^{(BBN)2}NN^{tBu}$)ZnBr(N_2H_3) (5-Br). A 20 mL scintillation vial was charged with **4-Br-N_2H_4** (28.7 mg, 0.038 mmol) and 5 mL of THF. A separate scintillation vial was charged with potassium bis(trimethylsilylamide) (7.6 mg, 0.038 mmol) and 3 mL of THF. Both solutions were frozen, and upon thawing, the KHMDS solution was added dropwise to the stirring solution of **4-Br-N_2H_4.** The solution gradually warmed to room temperature and stirred for 15 minutes before filtration through Celite. Volatiles were removed in vacuo to afford a light yellow powder which was rinsed with 3 x 5 mL pentane. The yellow powder was redissolved in 2 mL ether and filtered through Celite. Volatiles again removed in vacuo to afford a light yellow powder assigned as ($^{(BBN)2}NN^{tBu}$)ZnBr(N_2H_3) (18.7 mg, 73%, purity = 98%). Single, X-ray quality crystals were obtained from slow diffusion of pentane into a THF solution at -35 °C. ^{1}H NMR (C_6D_6, 25 °C, 400 MHz) δ = -0.65 (s, 1H), 0.96 (s, 9H, (C*H*$_3$)$_3$), 1.01-2.46 (m, 24H, BBN-C*H*$_2$), 2.51 (s, 3H, pyr-C*H*$_3$) 2.84 (dt, *J* = 16.1, 8.3 Hz, 1H), 4.28 (d, *J* = 8.3 Hz, 1H), 4.40 (dd, *J* = 15.1, 8.9 Hz, 1H), 4.89 (dd, *J* = 15.3, 8.3 Hz, 1H), 5.75 (d, *J* = 9.5 Hz, 1H), 5.87 (s, 1H, pz-C*H*), 6.26 (d, *J* = 7.8 Hz, 1H, pyr-C*H*), 6.45 (d, *J* = 7.8 Hz, 1*H*), 6.73 (t, *J* = 7.8 Hz, 1H, pyr-C*H*). ^{1}H NMR (THF, 25 °C, 400 MHz, some resonances obstructed by proteo-THF after solvent suppression) δ = -0.84 (s, 1H), 0.25 (d, *J* = 7.3 Hz, 1H), 0.54 (s, 1H), 0.62 (s, 1H), 0.71 (q, *J* = 7.4, 6.3 Hz, 1H), 0.83 (t, *J* = 6.9 Hz, 1H), 0.94 (d, *J* = 13.5 Hz, 1H), 1.17 – 1.07 (m, 2H), 1.33 – 1.22 (m, 2H), 1.43 (s, 9H, (C*H*$_3$)$_3$), 2.62 (dd, *J* = 15.5, 8.6 Hz, 1H), 2.79 (s, 3H, pyr-C*H*$_3$), 4.46 (d, *J* = 7.0 Hz, 1H), 4.70 (t, *J* = 4.9 Hz, 2H), 5.66 (t, *J* = 8.8 Hz, 1H), 6.14 (d, *J* = 10.5 Hz, 1H), 6.86 (s, 1H, pz-C*H*), 7.45 (d, *J* = 7.8 Hz, 1H, pyr-C*H*), 7.82 (d, *J* = 7.9 Hz, 1H, pyr-C*H*), 8.01 (t, *J* = 7.7 Hz, 1H, pyr-C*H*). ^{13}C NMR (C_6D_6, 25 °C, 125 MHz) δ = 11.86, 20.30, 22.05, 22.59, 22.66, 23.38, 23.52, 27.60, 29.69, 29.82, 30.00, 30.29, 20.51, 30.82, 31.70, 31.98, 32.01, 32.75, 53.26, 100.48, 115.57, 122.39, 138.00, 141.20, 144.47, 153.96, 155.46.

Synthesis of ($^{(BBN)2}NN^{tBu}$)ZnCl(N_2H_3) (5-Cl). Followed the same synthetic procedure as **(5-Br)**, using **4-Cl-N_2H_4** (32.9 mg, 0.049 mmol) as the zinc starting material. Using this procedure, a light yellow powder was obtained assigned as ($^{(BBN)2}NN^{tBu}$)ZnCl(N_2H_3) (21.7 mg, 79%). Single, X-ray quality crystals were obtained from slow diffusion of pentane into a THF solution at -35 °C. ^{1}H NMR (THF, 25 °C, 400 MHz, some resonances obstructed by proteo-THF after solvent suppression) δ = -0.88 (s, 1H), 0.24 (d, *J* = 7.2 Hz, 1H), 0.53 (s, 1H), 0.60 (s, 1H), 0.68 (p, *J* = 6.2, 5.2 Hz, 1H), 0.84 (t, *J* = 6.9 Hz, 1H), 1.02 – 0.89 (m, 1H), 1.17 – 1.10 (m, 2H), 1.27 (tt, *J* = 13.0, 11.2, 4.3 Hz, 2H), 1.44 (s, 9H, (C*H*$_3$)$_3$), 2.18 – 2.01 (m, 2H), 2.63 (q, *J* = 8.7, 8.0 Hz, 1H), 2.78 (s, 3H, pyr-C*H*$_3$), 4.46 (d, *J* = 6.9 Hz, 1H), 4.70 (t, *J* = 4.6 Hz, 2H), 5.59 (dd, *J* = 10.5, 7.2 Hz, 1H) 6.20 (d, *J* = 10.5 Hz, 1H), 6.86 (s, 1H, pz-C*H*), 7.45 (d, *J* = 7.8 Hz, 1H, pyr-C*H*), 7.81 (d, *J* = 7.8 Hz, 1H, pyr-C*H*), 8.01 (t, *J* = 7.8 Hz, 1H, pyr-C*H*).). ^{11}B NMR (THF, 25 °C) δ = 1.39. IR (KB_r): $\nu_{(N-H)}$ = 3292, 3288, 3228 cm^{-1}

Synthesis of ($^{(BBN)2}NN^{tBu}$)FeBr(N_2H_2) (6). A 20 mL scintillation vial was charged with **2-N_2H_4** (62.4 mg, 0.084 mmol) and 5 mL of THF. A separate scintillation vial was charged with potassium bis(trimethylsilylamide) (16.7 mg, 0.084 mmol) and 3 mL of THF. Both solutions were frozen, and upon thawing, the KHMDS solution was added dropwise to the stirring solution of **2-N_2H_4.** The solution gradually warmed to room temperature and stirred for 15 minutes before filtration through Celite. Volatiles were removed in vacuo to afford a yellow powder which was rinsed with 3 x 5 mL pentane. The yellow powder was redissolved in 5 mL ether and filtered through Celite. Volatiles again removed in vacuo to afford a light yellow powder assigned as ($^{(BBN)2}NN^{tBu}$)FeBr(N_2H_2) (38.8

mg, 68%). Single, X-ray quality crystals were obtained from slow diffusion of pentane into a THF solution at -35 °C. MALDI-TOF of $C_{32}H_{49}B_2BrFeN_3$ ($^{(BBN)2}NN^{tBu}$)FeBr(N_2H_2) – N_2H_3 : Calc. 633.253; Found 633.074. ^{1}H NMR (THF, 25 °C, 400 MHz) δ = -30.31, -16.89, -15.47, -11.27, -8.79, -6.88, -2.73, 1.07, 1.42, 1.79, 3.59, 3.66, 4.07, 5.02, 5.62, 7.16, 8.54, 9.06, 9.87, 14.27, 15.06, 16.94, 24.06, 39.91, 41.28, 50.27, 55.95. IR (KB_r): $\nu_{(N-H)}$ = 3291, 3224 cm^{-1}. The sensitivity of **6** even in the solid state precluded elemental analysis collection.

Hydride competition experiment. A 20 mL scintillation vial was charged with **1** (11.1 mg, 0.022 mmol), **1-mono** (8.4 mg, 0.022 mmol) and 3 mL of THF and frozen. Upon thawing, KEt_3BH (22.3 µL, 1M THF solution, 0.022 mmol) was added to the stirring solution. The solution gradually warmed to room temperature and stirred for 15 minutes. The sample was concentrated to 1 mL in vacuo for ^{1}H NMR spectroscopy analysis.

Hydride transfer experiment. A 20 mL scintillation vial was charged with **1-mono** (12.1 mg, 0.032 mmol) and 3 mL of THF and frozen. Upon thawing, KEt_3BH (32.2 µL, 1M THF solution, 0.032 mmol) was added to the stirring solution. The solution gradually warmed to room temperature and stirred for 15 minutes. Volatiles were removed in vacuo to afford a white powder which was rinsed with 3 x 5 mL of pentane. The white solid was redissolved in 1 mL of THF, and to this stirring solution was added **1** (16.0 mg, 0.032 mmol) as a solution in 1 mL of THF. The reaction stirred for 30 minutes at room temperature before an aliquot was taken for ^{1}H NMR spectroscopy analysis.

Nitrite competition experiment. A 20 mL scintillation vial was charged with **1** (13.4 mg, 0.027 mmol), **1-mono** (10.1 mg, 0.027 mmol) and 3 mL of THF. To this stirring solution was added $NaNO_2$ (1.9 mg, 0.027 mmol) and 18-crown-6 (7.1 mg, 0.027 mmol) both as solids. The solution stirred at room temperature for 2 hours, upon which there was a color change from colorless to yellow. The solution was concentrated to 1 mL in vacuo for ^{1}H NMR spectroscopy analysis.

Hydrazine competition experiments. A 20 mL scintillation vial was charged with **1** (10.5 mg, 0.021 mmol), **1-mono** (7.9 mg, 0.021 mmol) and 1 mL of THF. 20 µL of HMDSO were added as an internal standard. To this stirring solution was added N_2H_4 (66.3 µL, 0.159M THF solution, 0.01 mmol) and the reaction stirred for 15 minutes at room temperature. The sample was transferred to a J-Young tube for ^{1}H NMR spectroscopy analysis. The J-Young tube was returned to the glovebox, and 0.5 equiv. of N_2H_4 (66.3 µL, 0.159M THF solution, 0.01 mmol) was added directly to the J-Young tube.

The same procedure was followed for hydrazine competition experiments with **4** and **4-mono.**

Selective nitrite capture experiments

1) A 20 mL scintillation vial was charged with **1** (11.7 mg, 0.024 mmol) and 1 mL of THF. A separate scintillation vial was charged with TBAF (6.2 mg, 0.024 mmol) and 1 mL of THF. The TBAF solution was added dropwise to the stirring solution of **1**, and the resulting solution stirred at room temperature for 2 hours before removal of the solvent in vacuo to afford a white solid. The solid was washed with 2 x 5 mL of pentane and redissolved in 0.500 mL of THF for NMR spectroscopy analysis.
2) A 20 mL scintillation vial was charged with **1** (13.4 mg, 0.027 mmol) and 1 mL of THF. A separate scintillation vial was charged with $TBANO_2$ (7.8 mg, 0.027 mmol) and 1 mL of THF. The $TBANO_2$ solution was added dropwise to the stirring solution of **1**, resulting in an immediate color change to yellow. The resulting solution stirred at room temperature

for 2 hours before removal of the solvent in vacuo to afford a yellow solid. The solid was washed with 2 x 5 mL of pentane and redissolved in 0.500 mL of THF for NMR spectroscopy analysis.

3) A 20 mL scintillation vial was charged with **1** (16.0 mg, 0.032 mmol) and 1 mL of THF. A separate scintillation vial was charged with $TBANO_2$ (9.3 mg, 0.032 mmol), TBAF (8.4 mg, 0.032 mmol) and 1 mL of THF. The $TBANO_2$/TBAF solution was added dropwise to the stirring solution of **1**, resulting in an immediate color change to yellow. The resulting solution stirred at room temperature for 2 hours before removal of the solvent in vacuo to afford a yellow solid. The solid was washed with 2 x 5 mL of pentane and redissolved in 0.500 mL of THF for NMR spectroscopy analysis.

4) A 20 mL scintillation vial was charged with **1** (7.6 mg, 0.015 mmol) and 1 mL of THF. A separate scintillation vial was charged with $TBANO_2$ (4.4 mg, 0.015 mmol), TBAF (39.9 mg, 0.15 mmol) and 2 mL of THF. The $TBANO_2$/TBAF solution was added dropwise to the stirring solution of **1**, resulting in an immediate color change to yellow. The resulting solution stirred at room temperature for 2 hours before removal of the solvent in vacuo to afford a yellow solid. The solid was washed with 2 x 5 mL of pentane and redissolved in 0.500 mL of THF for NMR spectroscopy analysis.

5) A 20 mL scintillation vial was charged with **1** (9.0 mg, 0.018 mmol) and 1 mL of THF. A separate scintillation vial was charged with $TBANO_2$ (5.2 mg, 0.018 mmol), TBAF (94.0 mg, 0.360 mmol), $TBANO_3$ (109.1 mg, 0.360 mmol) and 2 mL of THF. The $TBANO_2$/$TBANO_3$/TBAF solution was added dropwise to the stirring solution of **1**, resulting in an immediate color change to yellow. The resulting solution stirred at room temperature for 2 hours before removal of the solvent in vacuo to afford a yellow solid. The solid was washed with 2 x 5 mL of pentane and redissolved in 0.500 mL of THF for NMR spectroscopy analysis.

For the above selective nitrite capture experiments, a THF solution of the anion mixture (containing 20 equiv. F^-, 20 equiv. NO_3^-, 1 equiv. NO_2^- for Trial 5) was added to **1** in THF evaluate the anion selectivity of the ditopic receptor independent of kinetic factors such as solubility or order of addition.

Hydroboration of $^{propargyl}NN^{tBu}$. To assess the effect of solvent and temperature on single vs. double hydroboration, we reacted $^{propargyl}NN^{tBu}$ with 2 equiv. 9-BBN in THF. A 20 mL scintillation vial was charged with $^{propargyl}NN^{tBu}$ (33.4 mg, 0.12 mmol) and 3 mL of THF. To this stirring solution was added 9-BBN (30.3 mg, 0.25 mmol) dissolved in 1 mL of THF. The solution stirred at room temperature for 12 hours. The THF solvent was concentrated in vacuo, and a ^{1}H NMR spectrum was collected on the light-yellow solution. The ^{1}H NMR spectrum showed partial conversion (~67% as judged by pyz-C*H*) to the ditopic ligand **1**. The ^{1}H NMR spectrum also showed olefinic resonances, indicating that the other species (~33%) corresponds to the monoborylated "ene" ligand. This data clearly indicates that double hydroboration with 9-BBN is accessible at room temperature in THF solvent. Therefore, the selectivity observed for the generation of Fe and Zn "ene" complexes using the same reaction conditions is unique to coordinated $^{(propargyl)}NN^{tBu}$.

Hydroboration of ($^{propargyl}NN^{tBu}$)$ZnBr_2$. To assess the generality of post-metalation hydroboration only hydroborating a single time, we targeted synthesis of ($^{propargyl}NN^{tBu}$)$ZnBr_2$ followed by hydroboration. A 20 mL scintillation vial was charged with $^{propargyl}NN^{tBu}$ (220.0 mg, 0.82 mmol) and 3 mL of THF. A separate scintillation vial was charged with $ZnBr_2$ (184.0 mg, 0.82 mmol) and 2 mL of THF. To the stirring $ZnBr_2$ slurry was added $^{propargyl}NN^{tBu}$ dropwise, and the

solution stirred at room temperature for 16 hours before the THF solvent was removed in vacuo to afford a white solid. The white solid was rinsed with 3 x 5 mL of pentane and assayed for purity by ^{1}H NMR spectroscopy. A 20 mL scintillation vial was then charged with (^{propargyl}NN^{tBu})ZnBr$_2$ (50.2 mg, 0.10 mmol), 9-BBN (31.0 mg, 0.25 mmol), and 5 mL of THF. The solution stirred at room temperature for 16 hours before the THF solvent was removed in vacuo to afford an off-white solid. The solid was rinsed with 2 x 3 mL of pentane and 2 x 3 mL of ether to afford a white solid assigned as (^{ene}NN^{tBu})ZnBr$_2$. The ^{1}H NMR spectrum of the product exhibited clear olefinic resonances, indicating *single* hydroboration instead of double hydroboration.

Hydrolysis of 1. A J-Young tube was charged with **1** (25.2 mg, 0.05 mmol) and 600 µL of THF. To this J-Young tube was added H_2O (101 µL of 0.2 M solution in THF, 0.10 mmol) and the sample was monitored by ^{1}H NMR spectroscopy. After 10 minutes, a new species is evident in the ^{1}H NMR spectrum. After 1 hour, **1** was completely converted into a new species.

Synthesis of 1-D. A scintillation vial was charged with **1** (21.3 mg, 0.04 mmol), $NaBD_4$ (5.4 mg, 0.13 mmol) and 3 mL of THF. This slurry stirred at room temperature for 16 hours before the solution was filtered through filter paper. The THF solvent was removed in vacuo to afford a white solid, which was rinsed with 3 x 3 mL of pentane. ^{1}H NMR and IR spectroscopy data were collected on the isolated solid.

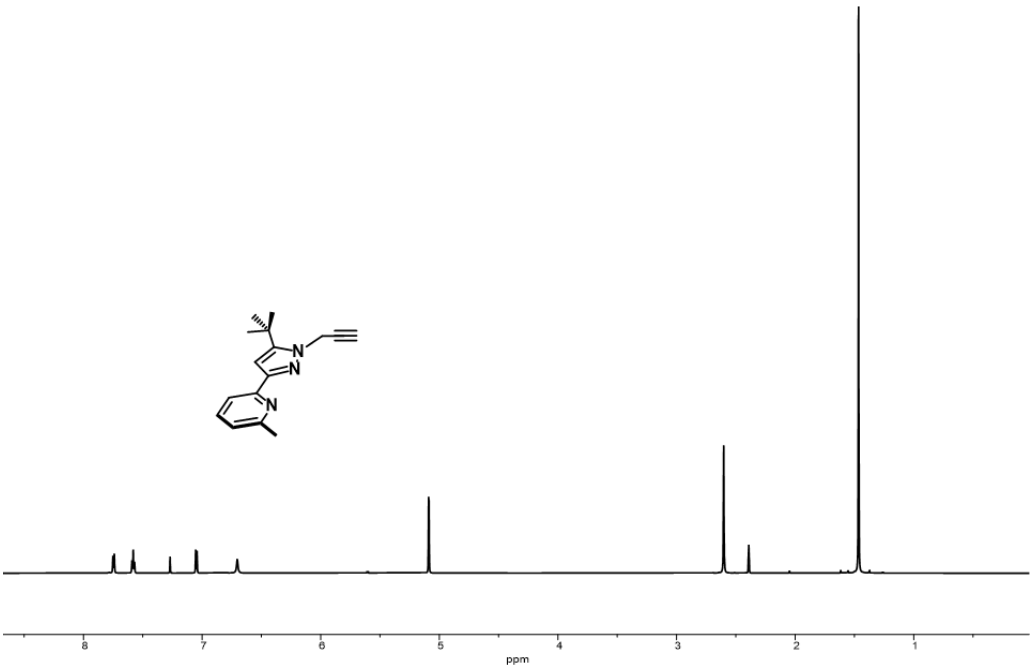

Figure S1. ^{1}H NMR spectrum ($CDCl_3$, 23 °C) of $^{propargyl}NN^{tBu}$.

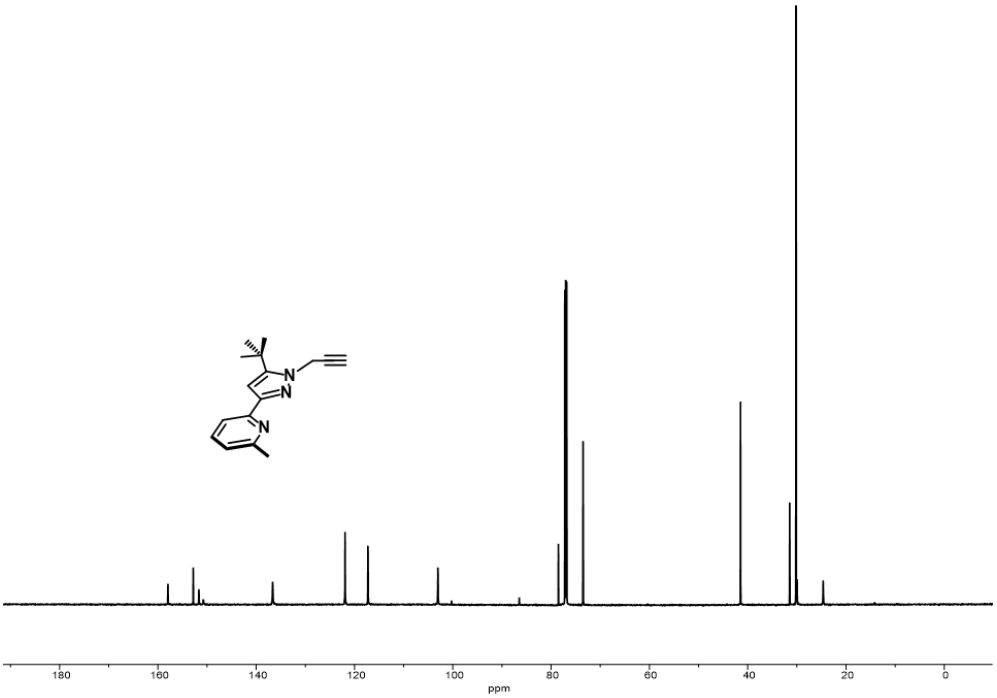

Figure S2. ^{13}C NMR spectrum ($CDCl_3$, 23 °C) of $^{propargyl}NN^{tBu}$.

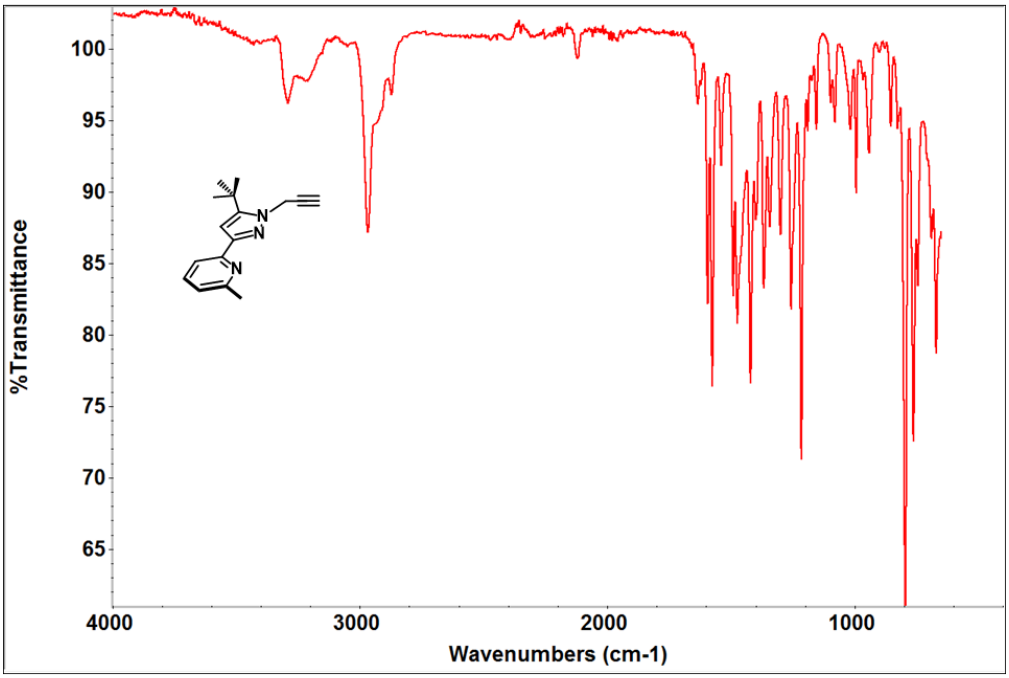

Figure S3. Infrared spectrum (ATIR) of $^{propargyl}NN^{tBu}$.

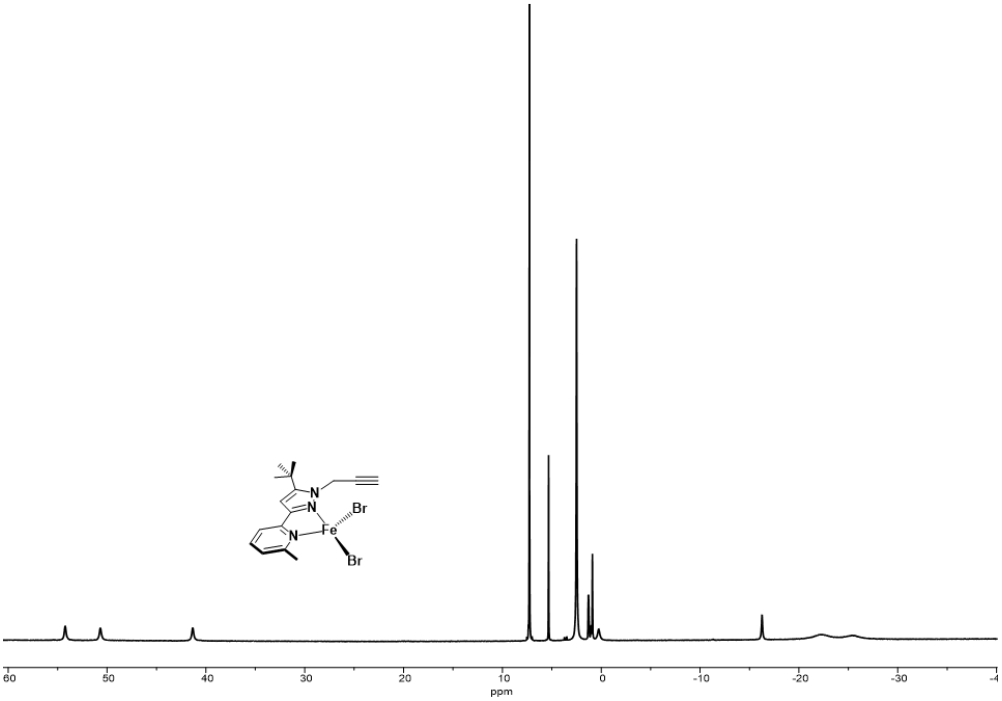

Figure S4. ^{1}H NMR spectrum ($CDCl_3$, 23 °C) of ($^{propargyl}NN^{tBu}$)$FeBr_2$.

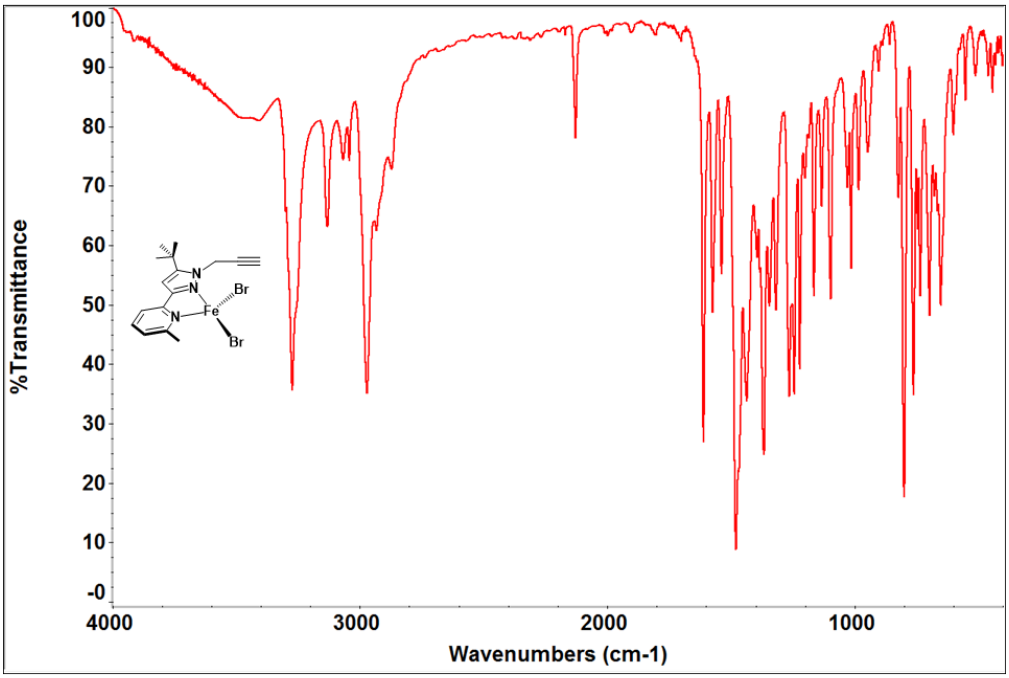

Figure S5. Infrared spectrum (KBr) of (^{propargyl}NN^{tBu})FeBr$_2$.

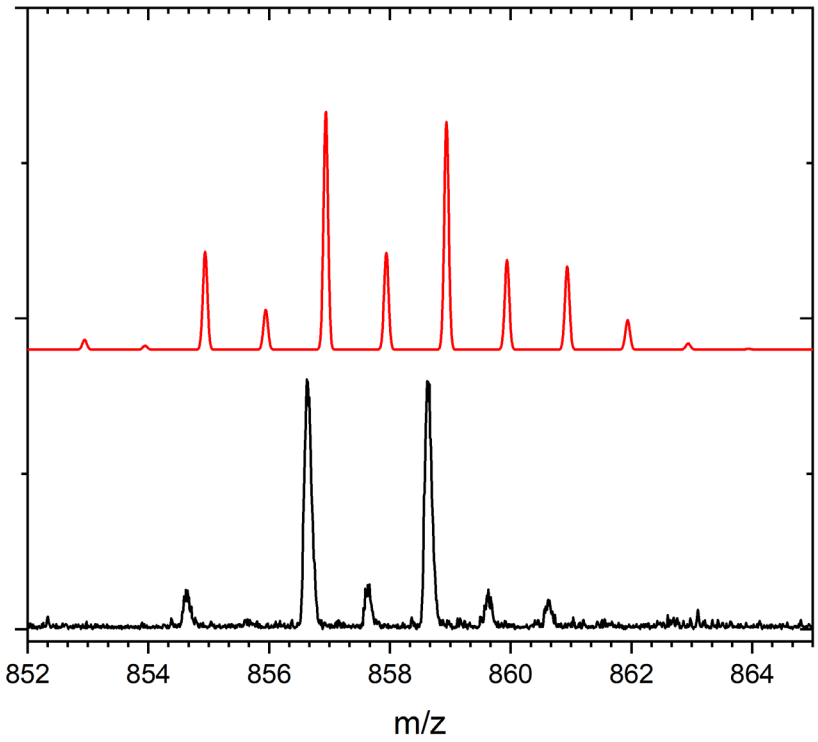

Figure S6. MALDI-TOF spectrum of (^{propargyl}NN^{tBu})FeBr$_2$ (bottom, black) and simulation (top, red).

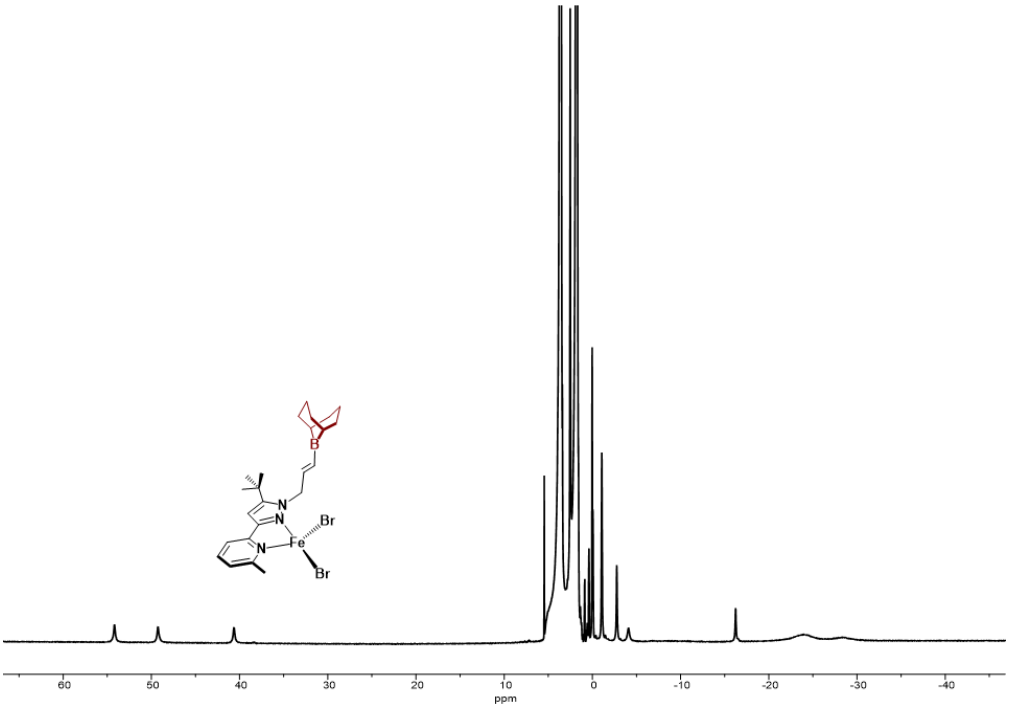

Figure S7. ^{1}H NMR spectrum ($CDCl_3$, 23 °C) of ($^{ene}NN^{tBu}$)$FeBr_2$.

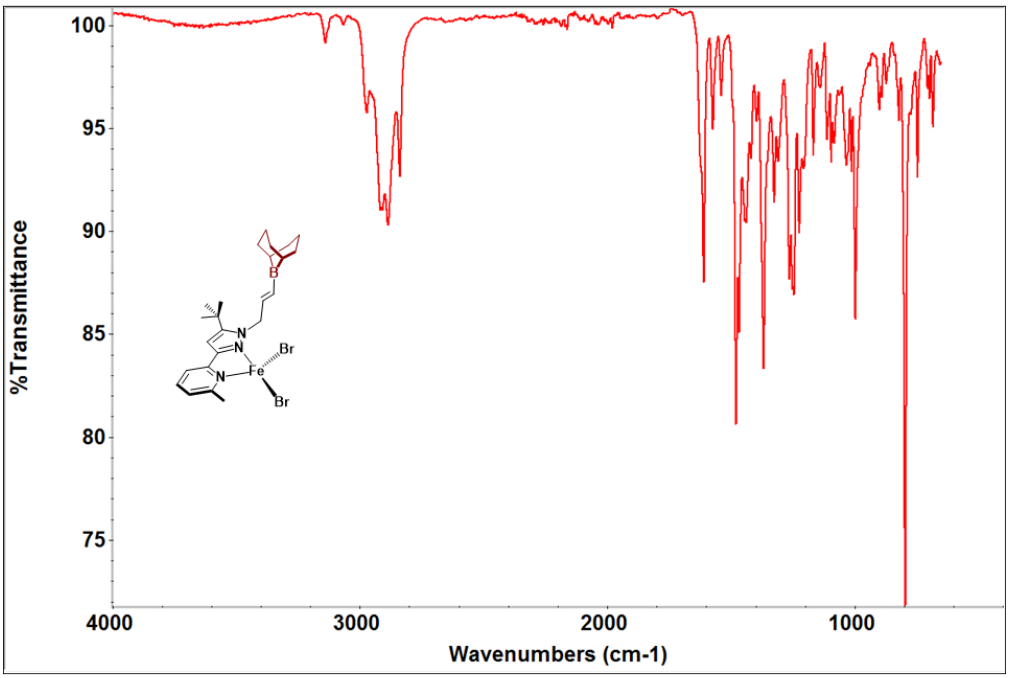

Figure S8. Infrared spectrum (ATIR) of ($^{ene}NN^{tBu}$)$FeBr_2$.

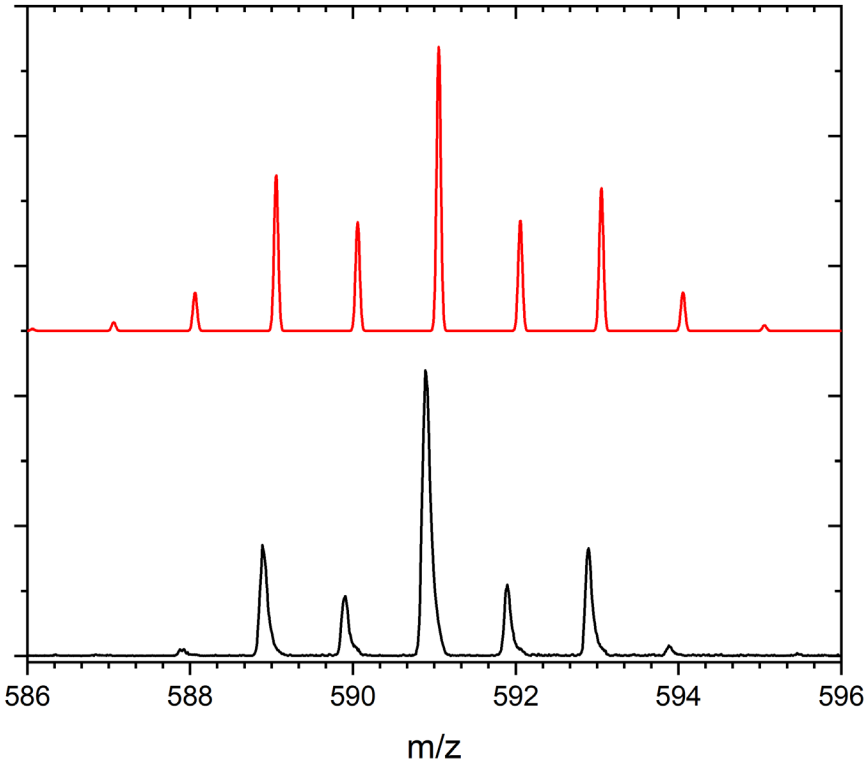

Figure S9. MALDI-TOF spectrum of (^{ene}NN^{tBu})FeBr$_2$ (bottom, black) and simulation (top, red).

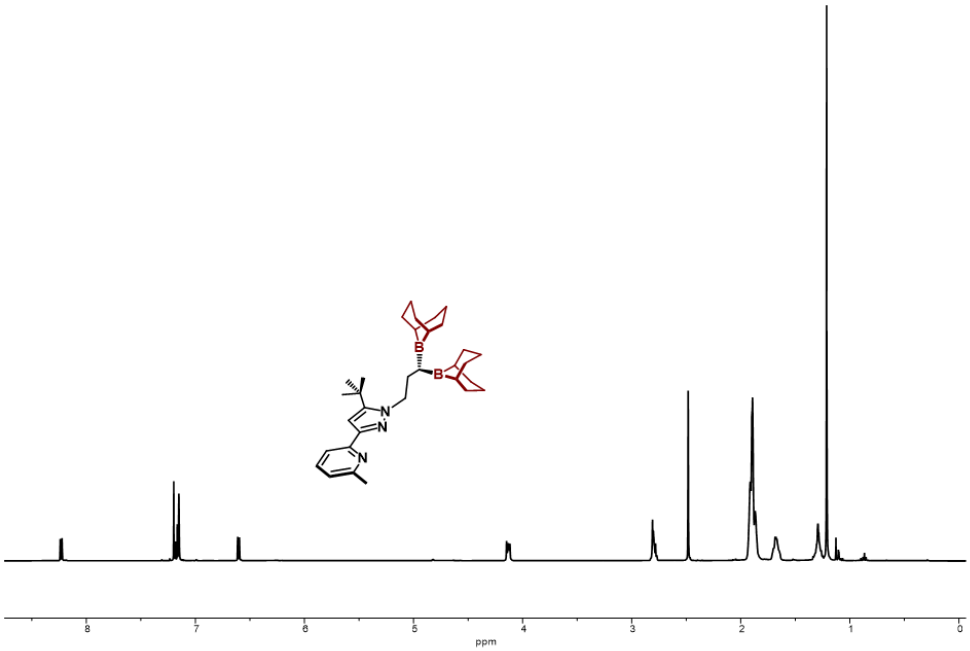

Figure S10. ^{1}H NMR spectrum (C_6D_6, 23 °C) of $^{(BBN)2}$NN^{tBu}.

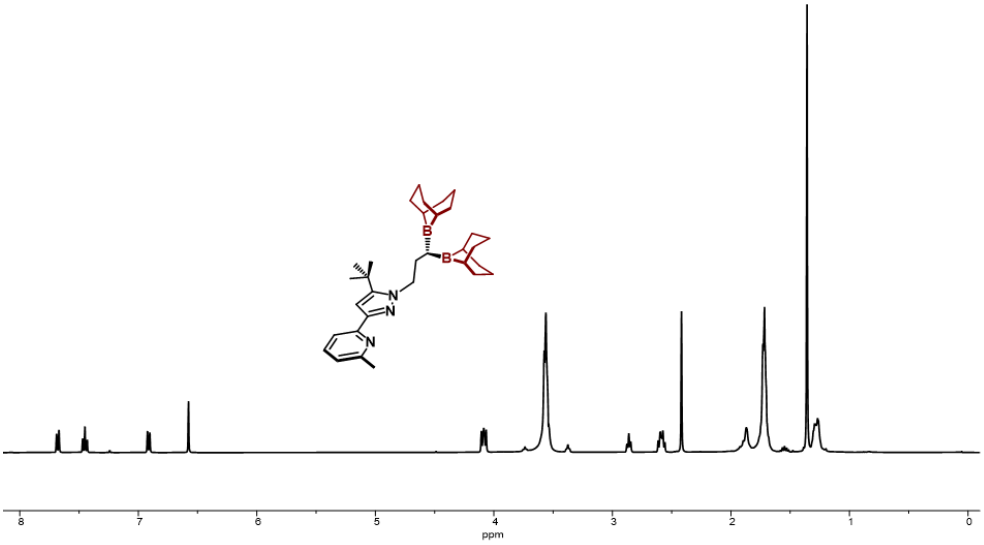

Figure S11. ^{1}H NMR spectrum (THF, 23 °C) of $^{(BBN)2}NN^{tBu}$.

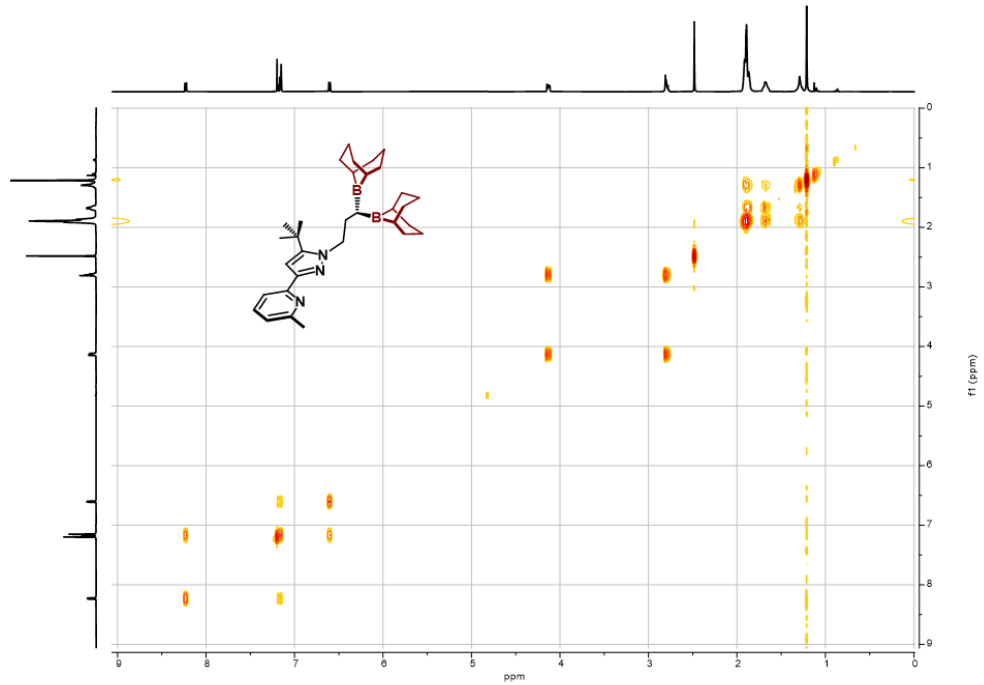

Figure S12. ^{1}H-^{1}H COSY spectrum (C_6D_6, 23 °C) of $^{(BBN)2}NN^{tBu}$.

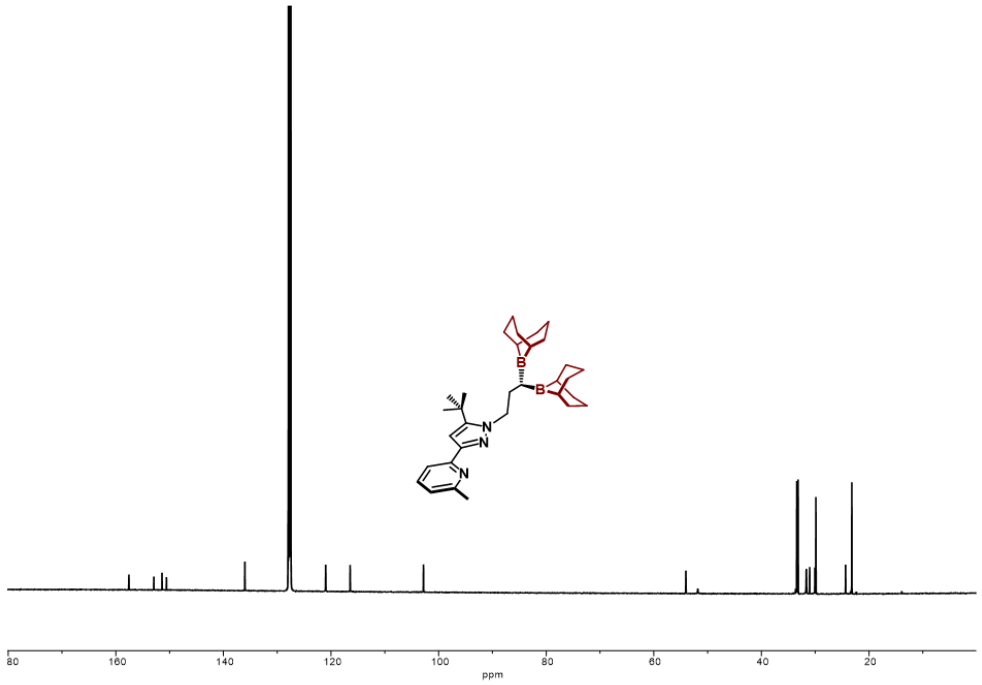

Figure S13. ^{13}C NMR spectrum (C_6D_6, 23 °C) of $^{(BBN)2}NN^{tBu}$.

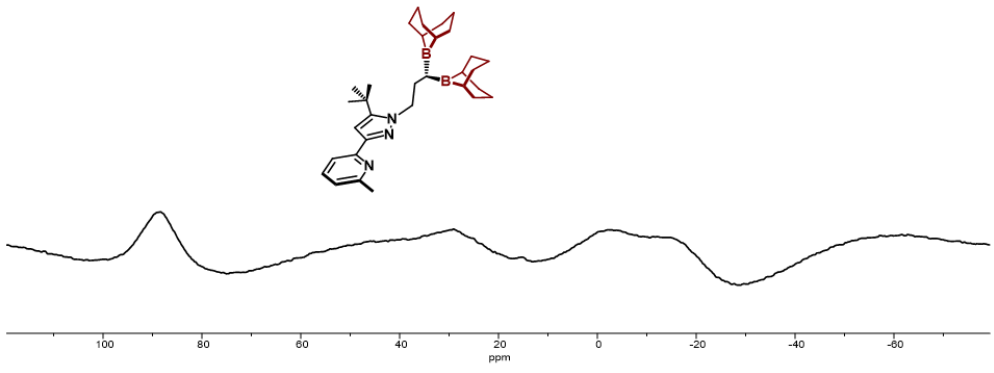

Figure S14. ^{11}B NMR spectrum (THF, 23 °C) of $^{(BBN)2}NN^{tBu}$.

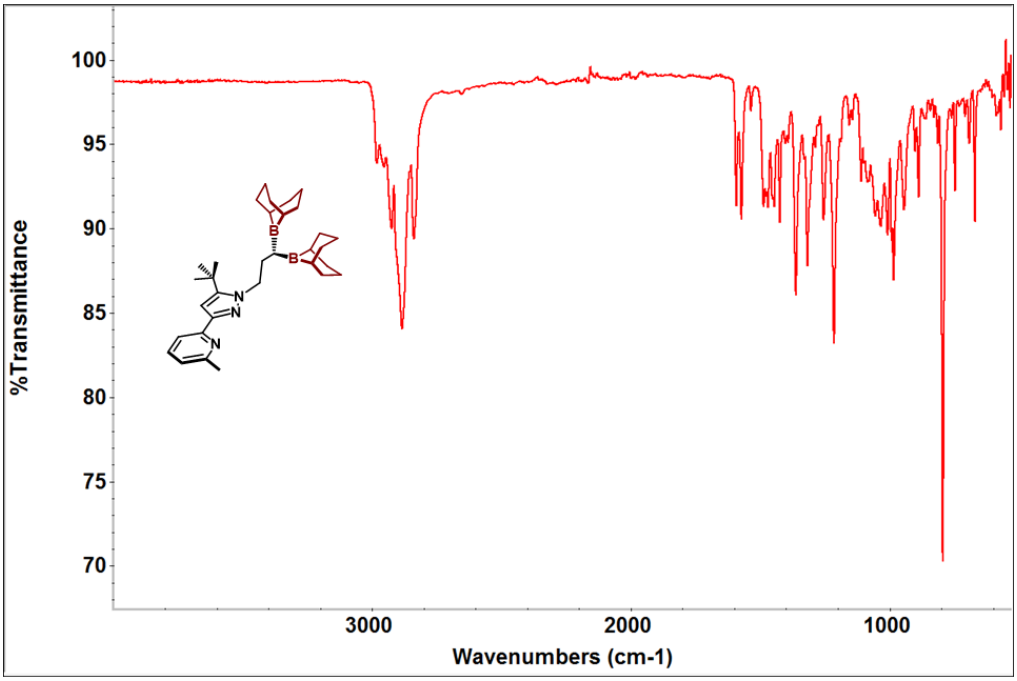

Figure S15. Infrared spectrum (ATIR) of $^{(BBN)2}NN^{tBu}$.

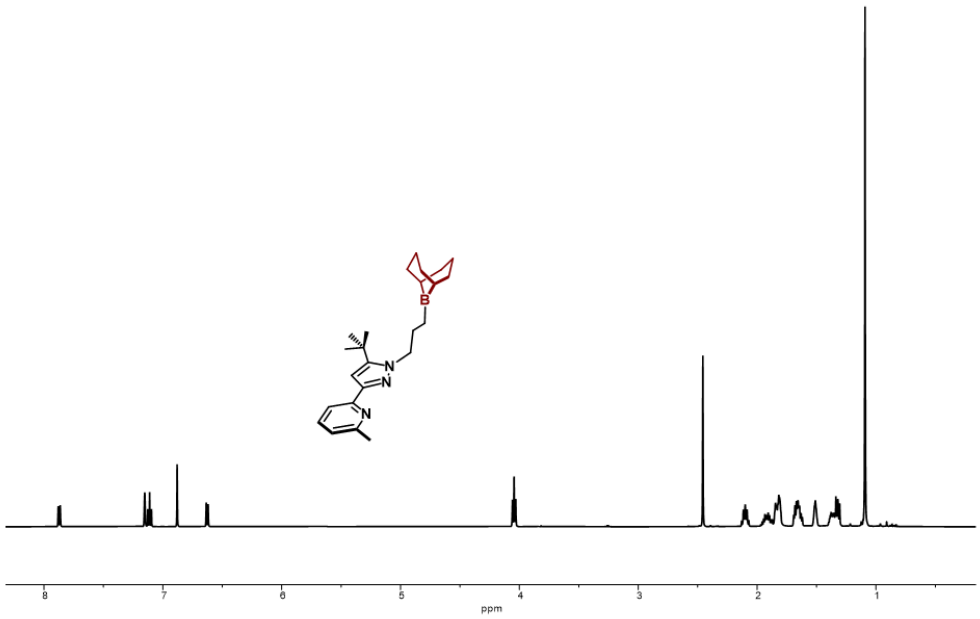

Figure S16. ^{1}H NMR spectrum (C_6D_6, 23 °C) of $^{(BBN)}NN^{tBu}$.

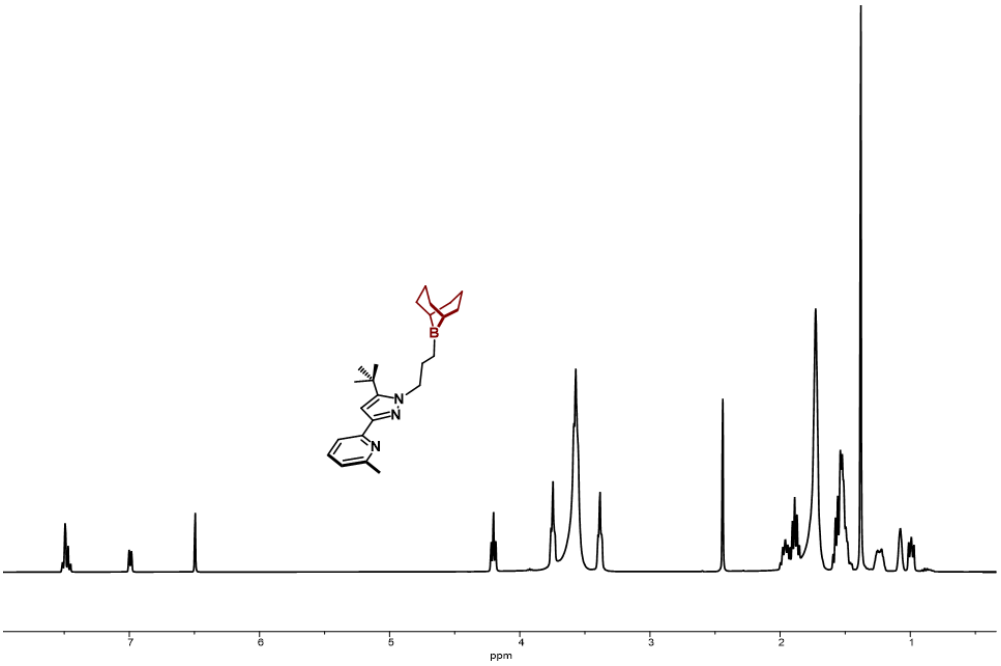

Figure S17. ^{1}H NMR spectrum (THF, 23 °C) of $^{(BBN)}NN^{tBu}$.

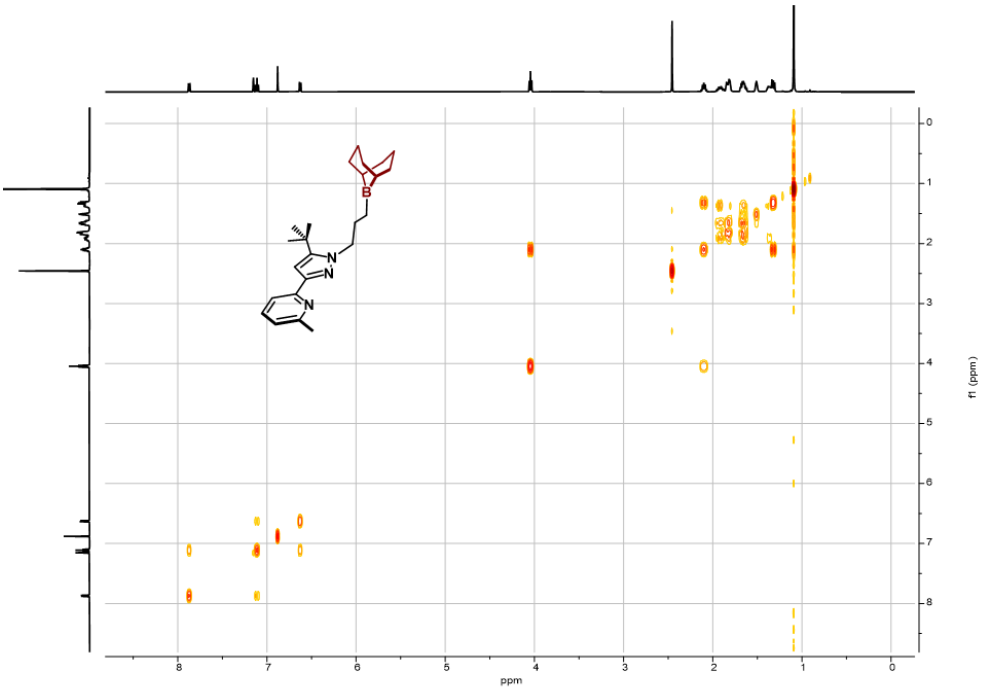

Figure S18. ^{1}H-^{1}H COSY spectrum (C_6D_6, 23 °C) of $^{(BBN)}NN^{tBu}$.

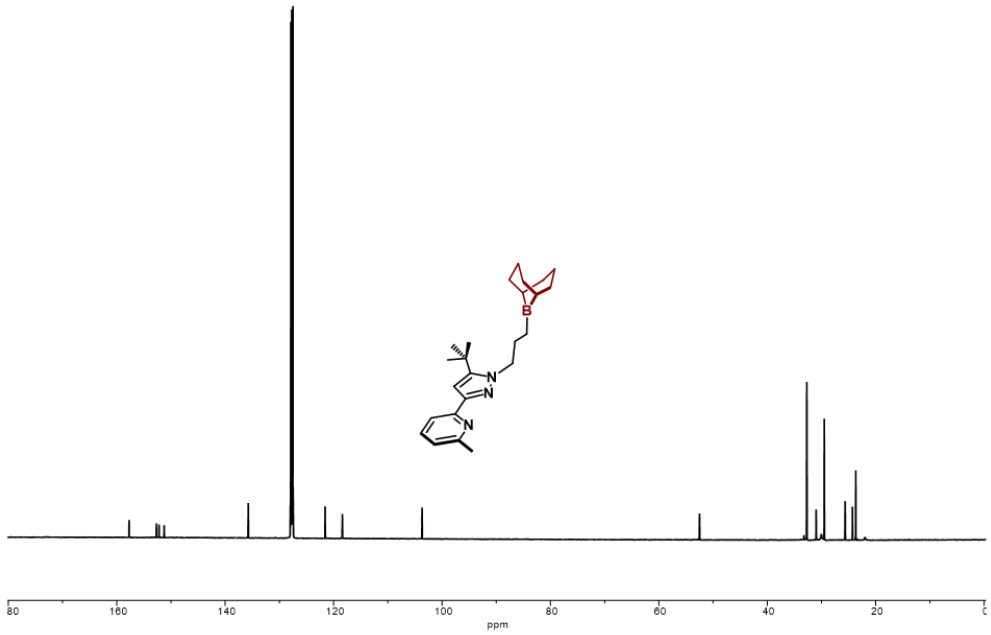

Figure S19. ^{13}C NMR spectrum (C_6D_6, 23 °C) of $^{(BBN)}NN^{tBu}$.

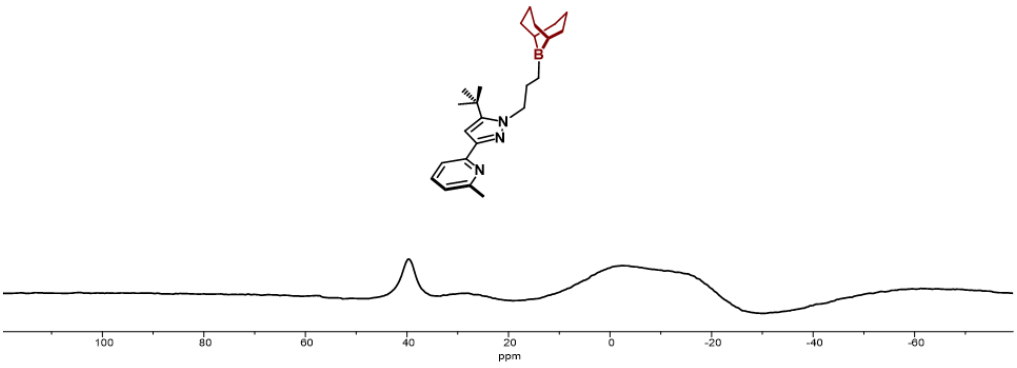

Figure S20. ^{11}B NMR spectrum (THF, 23 °C) of $^{(BBN)}NN^{tBu}$.

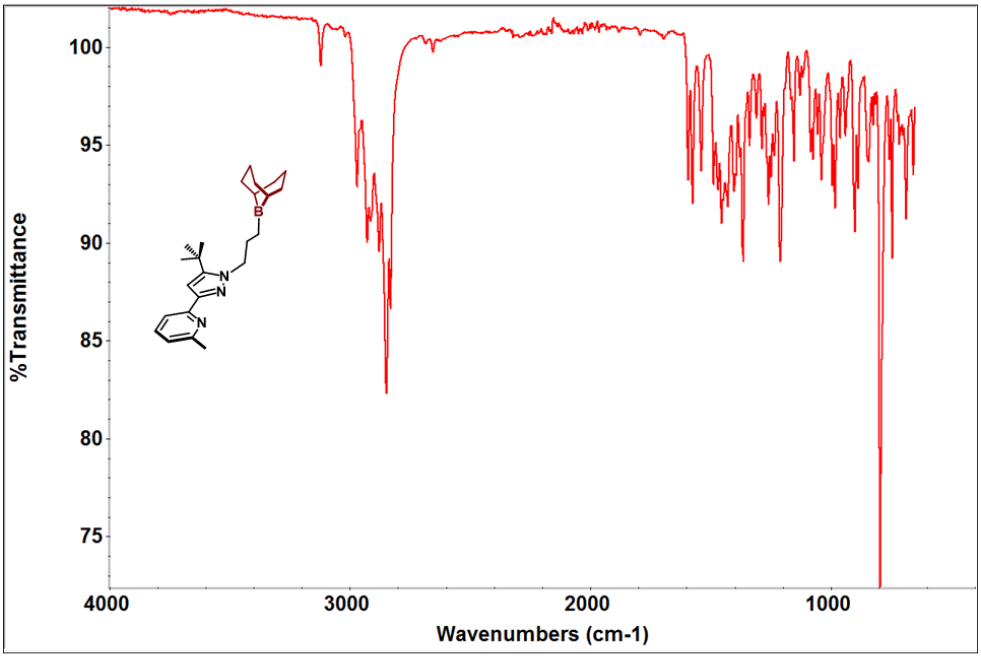

Figure S21. Infrared spectrum (ATIR) of $^{(BBN)}NN^{tBu}$.

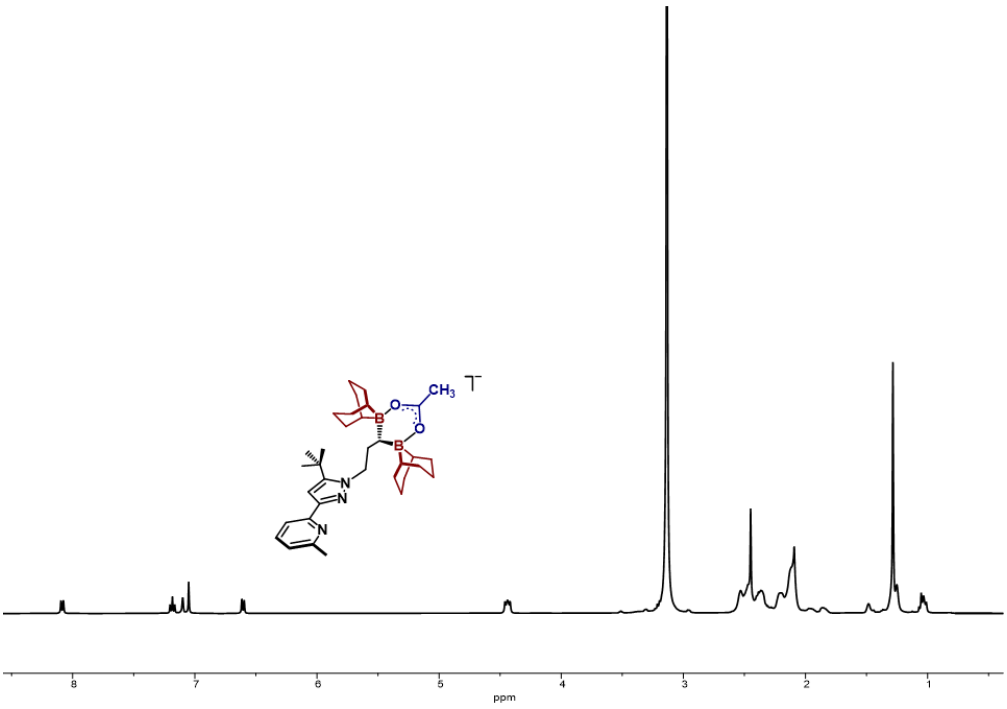

Figure S22. ^{1}H NMR spectrum (C_6D_6, 23 °C) of $[^{(BBN)2}NN^{tBu}(OAc)](K\text{-}18\text{-}crown\text{-}6)$.

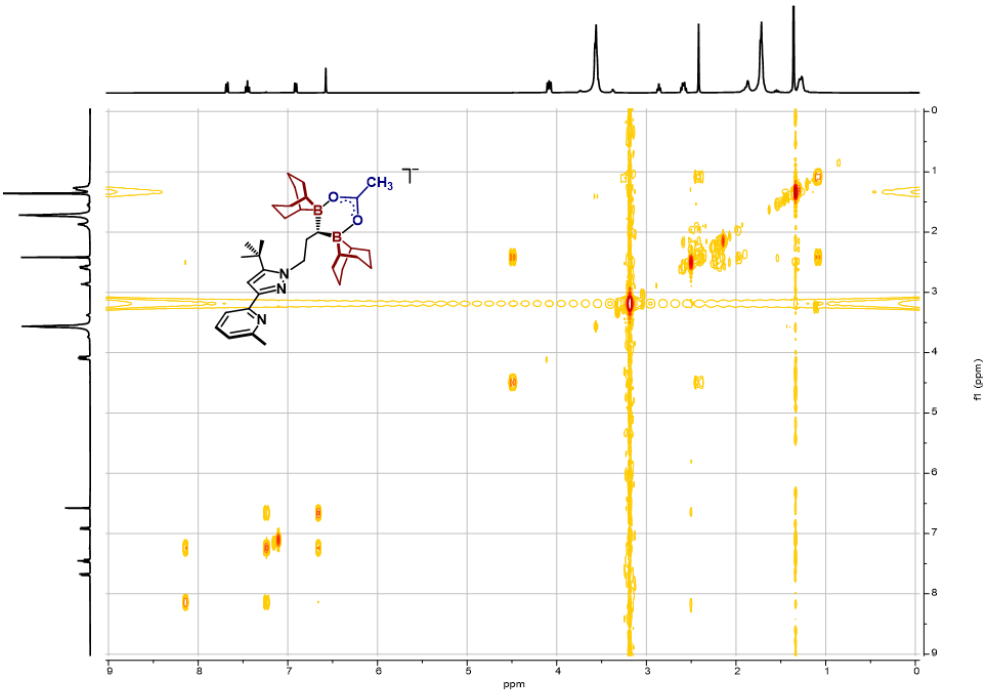

Figure S23. ^{1}H-^{1}H COSY spectrum (C_6D_6, 23 °C) of [$^{(BBN)2}$NN^{tBu}(OAc)](K-18-crown-6).

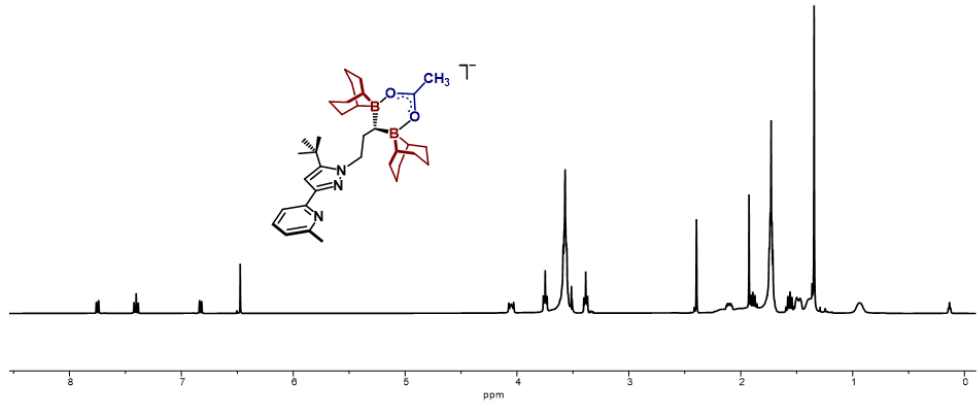

Figure S24. ^{1}H NMR spectrum (THF, 23 °C) of [$^{(BBN)2}$NN^{tBu}(OAc)](K-18-crown-6).

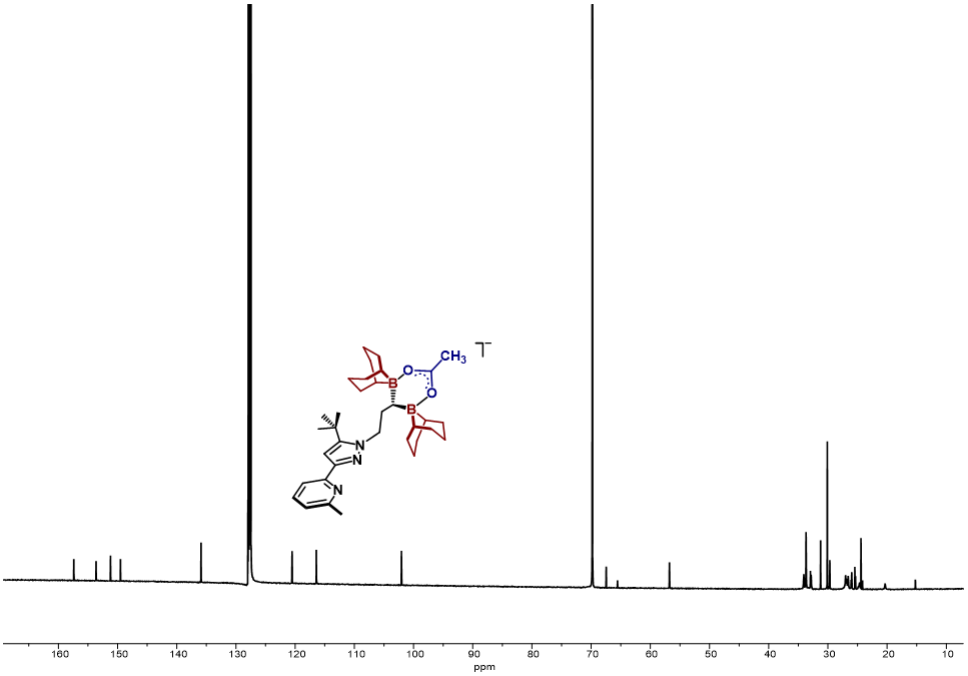

Figure S25. ^{13}C NMR spectrum (C_6D_6, 23 °C) of [$^{(BBN)2}NN^{tBu}$(OAc)](K-18-crown-6).

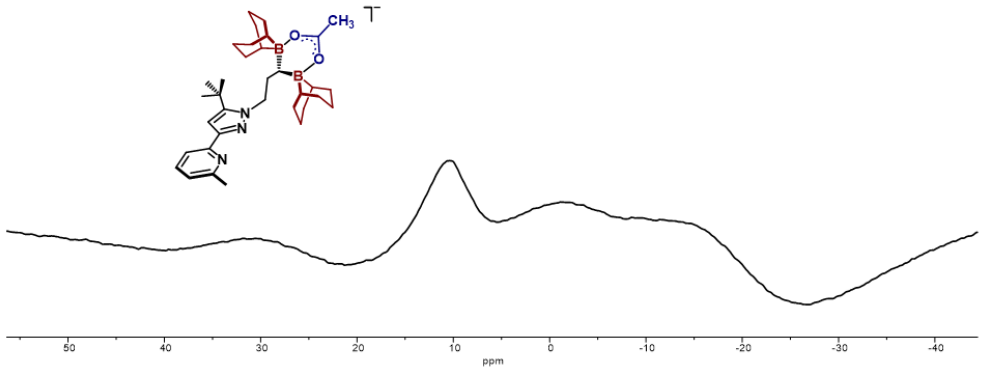

Figure S26. ^{11}B NMR spectrum (THF, 23 °C) of [$^{(BBN)2}NN^{tBu}$(OAc)](K-18-crown-6).

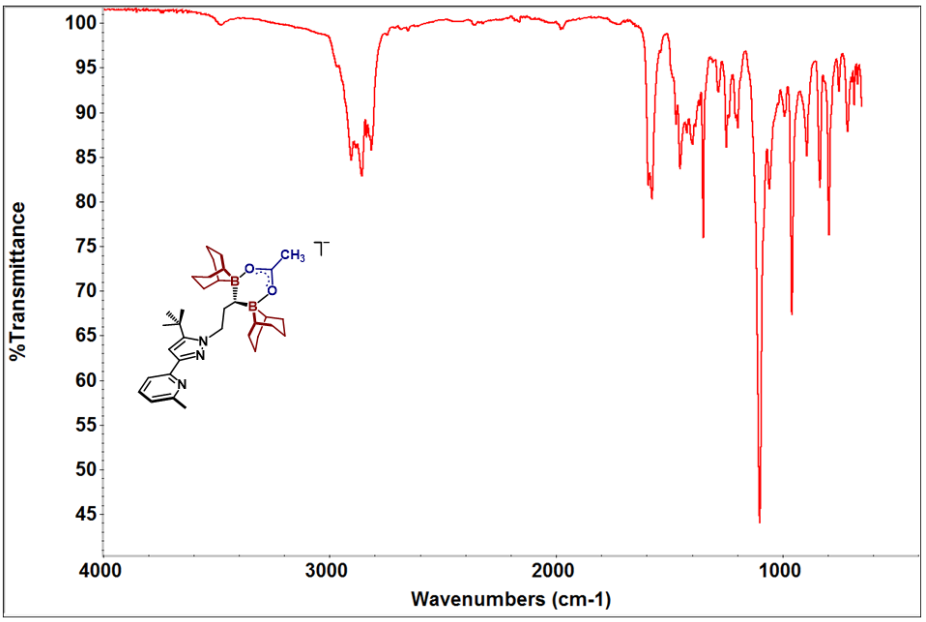

Figure S27. Infrared spectrum (KBr) of [$^{(BBN)2}$NN^{tBu}(OAc)](K-18-crown-6).

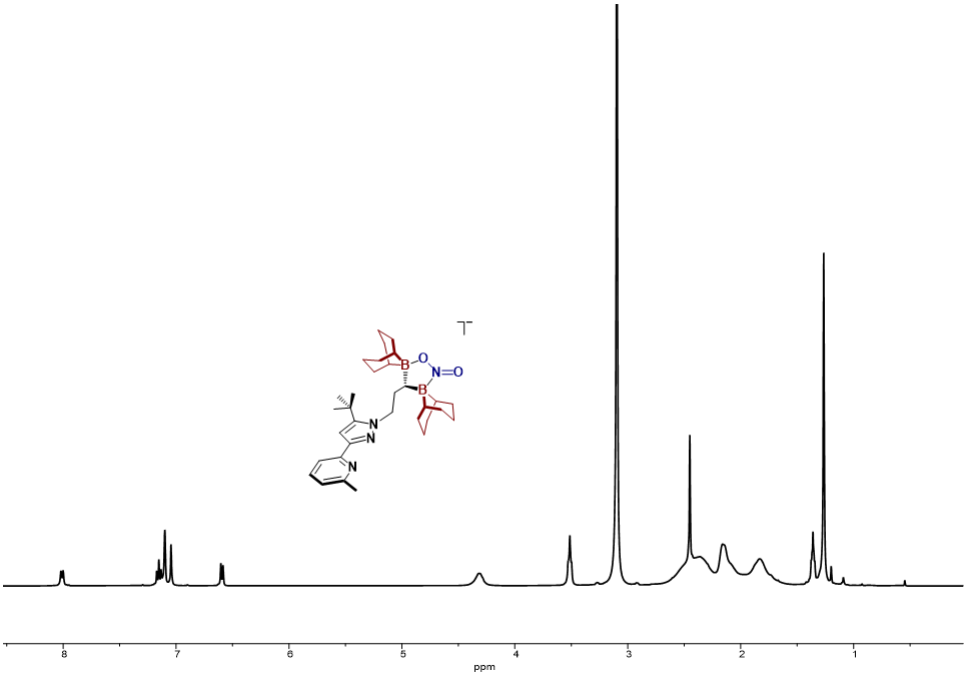

Figure S28. ^{1}H NMR spectrum (C_6D_6, 23 °C) of [$^{(BBN)2}$NN^{tBu}(NO_2)](Na-18-crown-6).

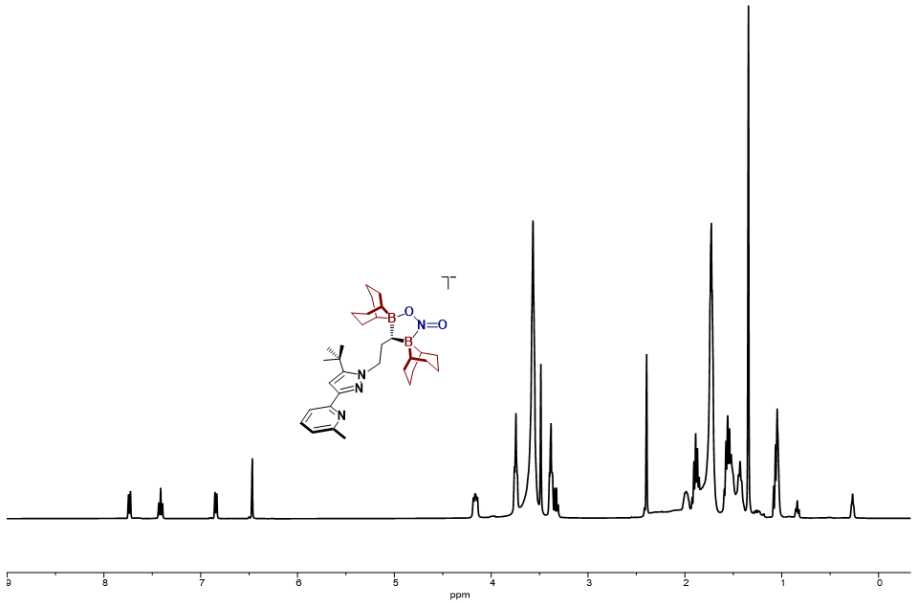

Figure S29. ^{1}H NMR spectrum (THF, 23 °C) of [$^{(BBN)2}$NN^{tBu}(NO_2)](Na-18-crown-6).

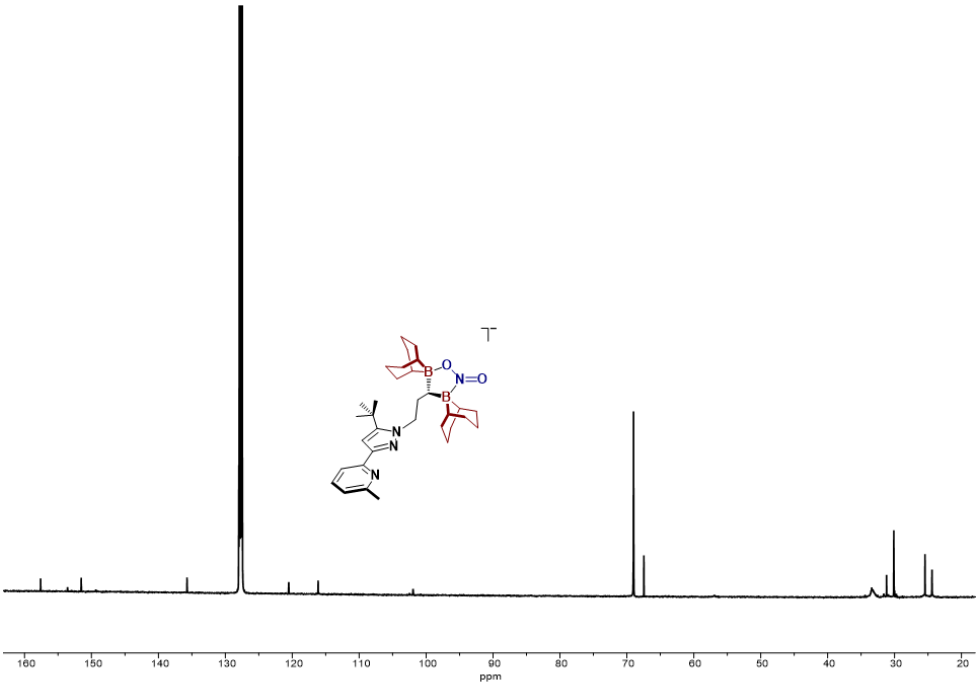

Figure S30. ^{13}C NMR spectrum (C_6D_6, 23 °C) of [$^{(BBN)2}$NN^{tBu}(NO_2)](Na-18-crown-6).

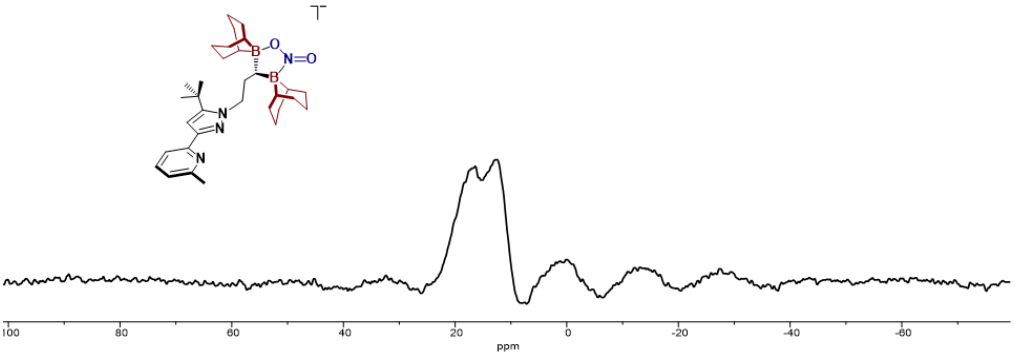

Figure S31. ^{11}B NMR spectrum (THF, 23 °C) of [$^{(BBN)2}$NN^{tBu}(NO_2)](Na-18-crown-6)(1-NO_2).

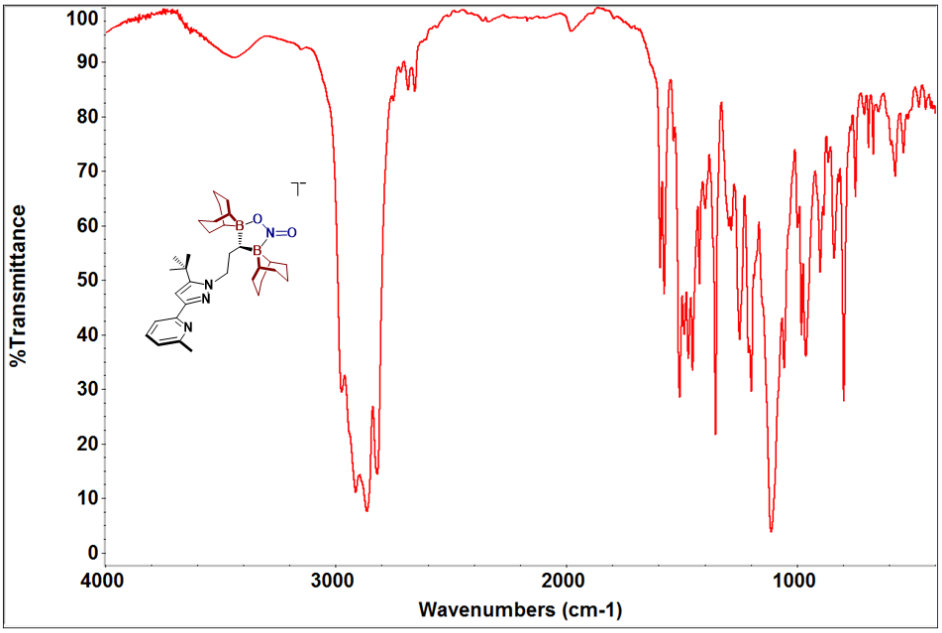

Figure S32. Infrared spectrum (KBr) of [$^{(BBN)2}$NN^{tBu}(NO_2)](Na-18-crown-6)(1-NO_2).

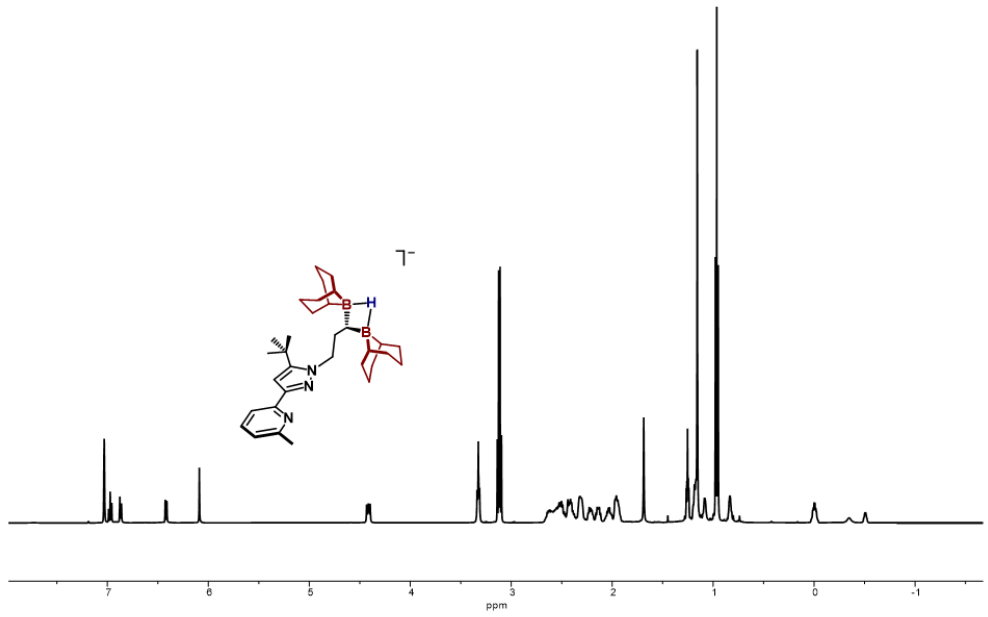

Figure S33. ^{1}H NMR spectrum (C_6D_6, 23 °C) of [$^{(BBN)2}$NN^{tBu}(H)]K.

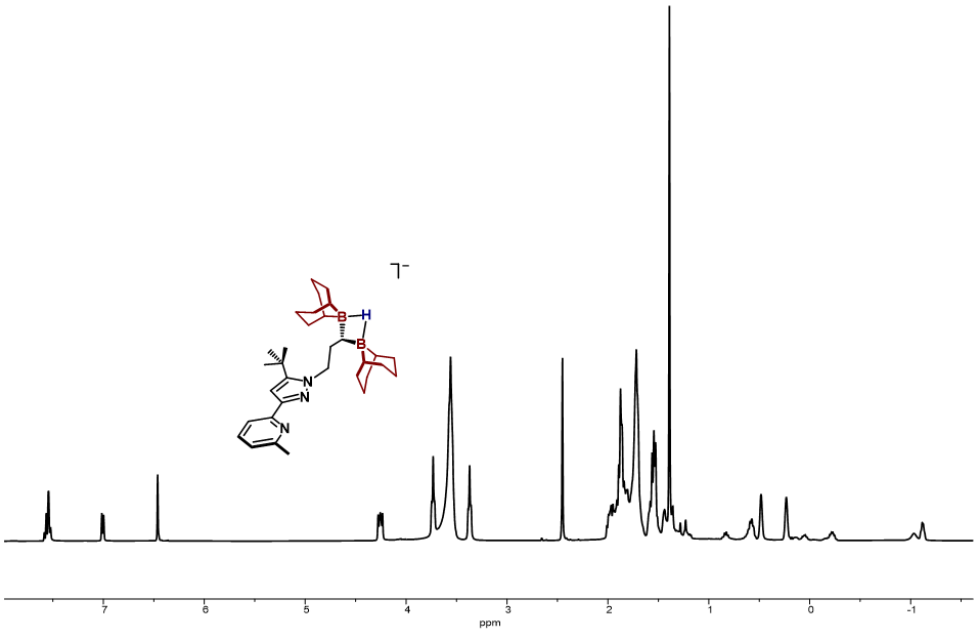

Figure S34. ^{1}H NMR spectrum (THF, 23 °C) of [$^{(BBN)2}$NN^{tBu}(H)]K.

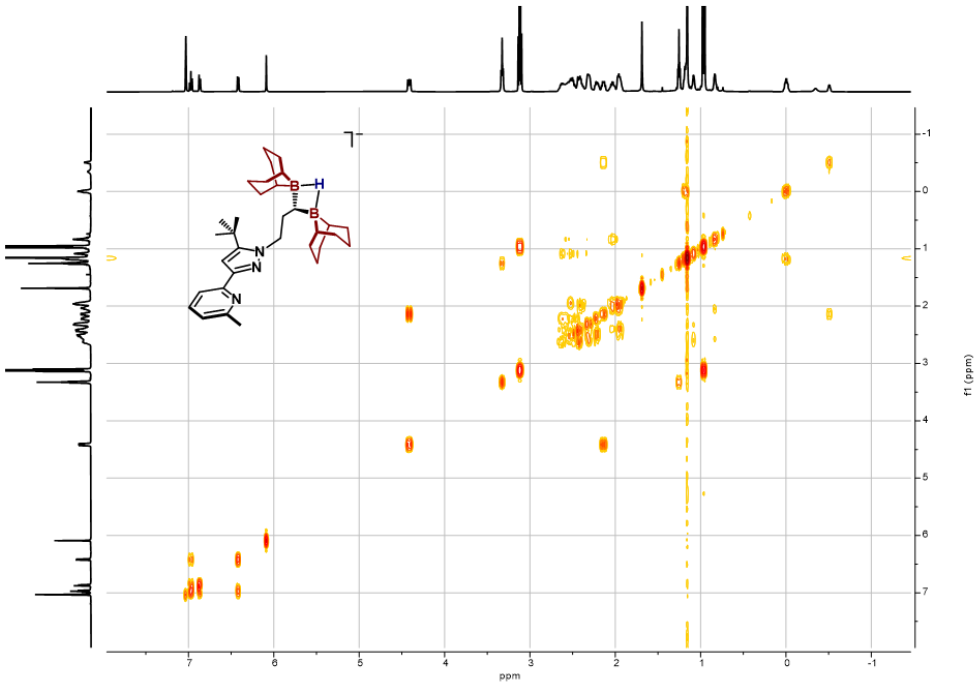

Figure S35. ^{1}H-^{1}H COSY spectrum (C_6D_6, 23 °C) of [$^{(BBN)2}$NN^{tBu}(H)]K.

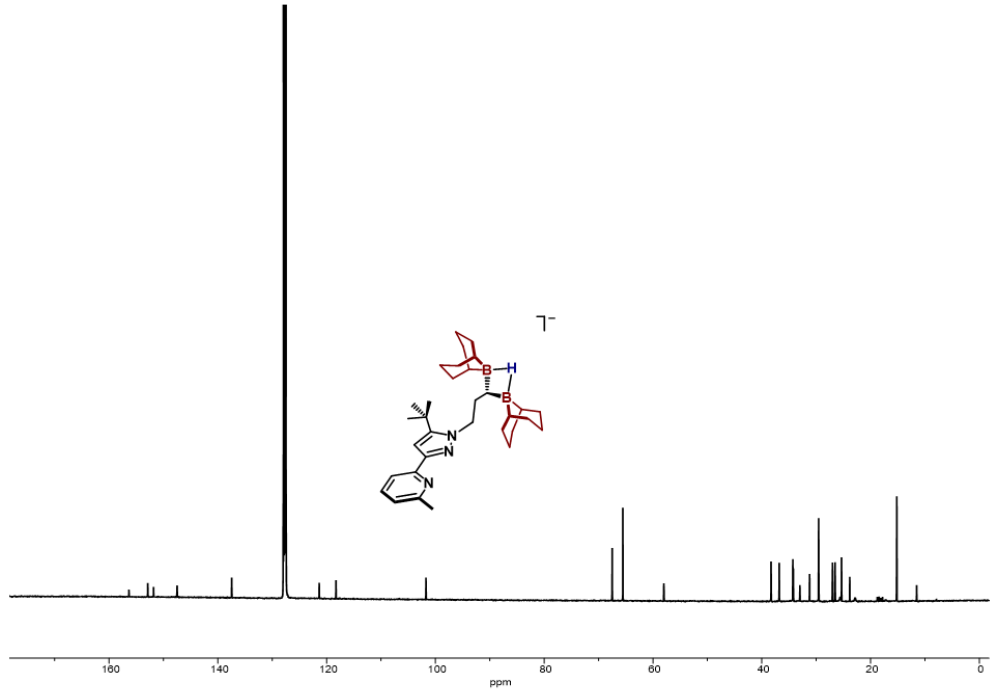

Figure S36. ^{13}C NMR spectrum (C_6D_6, 23 °C) of [$^{(BBN)2}$NN^{tBu}(H)]K**.**

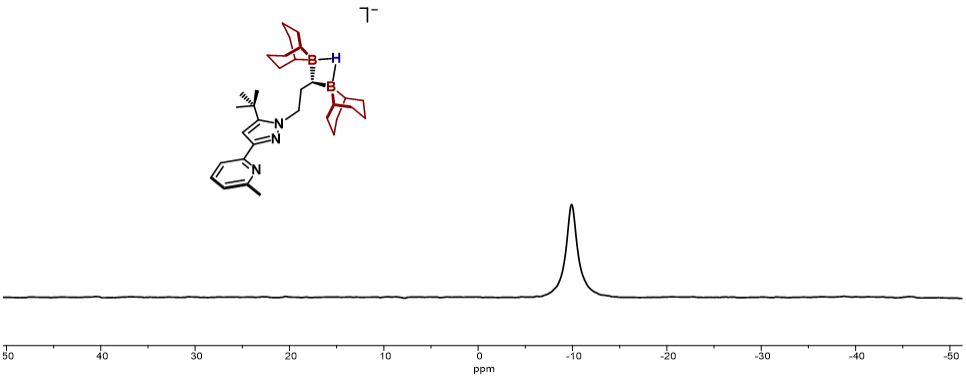

Figure S37. ^{11}B NMR spectrum (C_6D_6, 23 °C) of [$^{(BBN)2}$NN^{tBu}(H)]K**.**

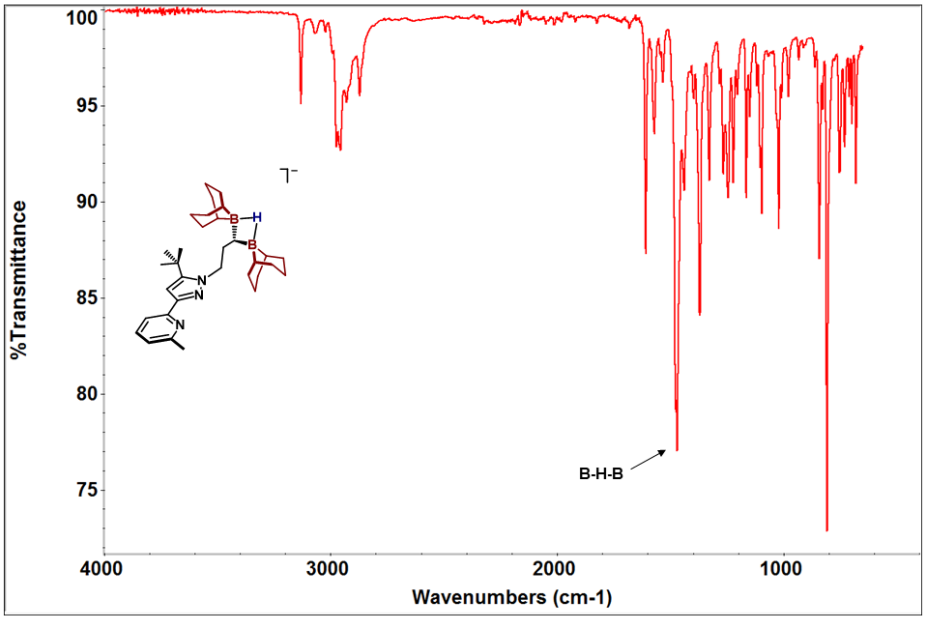

Figure S38. Infrared spectrum (ATIR) of [$^{(BBN)2}$NN^{tBu}(H)]K**.** The bridging B-H-B vibrational mode (1477 cm^{-1}) is shifted to lower energy and consistent with predicted DFT stretching frequency (1557 cm^{-1}). For reference, the DFT predicted B-H stretch of the monotopic analogue (2092 cm^{-1}) is consistent with typical borohydrides.

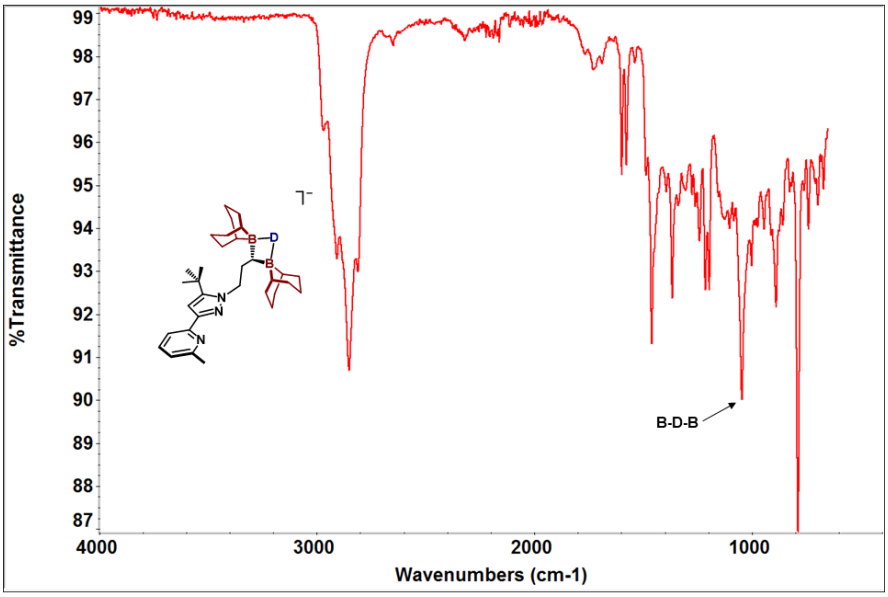

Figure S39. Infrared spectrum (ATIR) of [$^{(BBN)2}$NN^{tBu}(D)]Na**.** The identified bridging B-D-B vibrational mode (1046 cm^{-1}) is in good agreement with the expected reduced mass shift (calc: 1044 cm^{-1}).

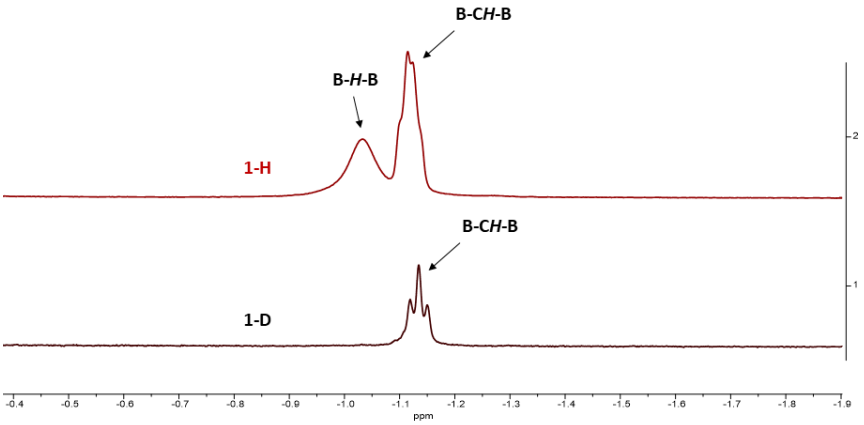

Figure S40. ^{1}H NMR spectrum (THF, 23 °C) of the hydride region for **1-H** vs. **1-D**. The overlaid ^{1}H NMR spectrum of **1-H** compared to **1-D** shows loss of the broad singlet resonance at -1.05 ppm in THF. The slightly upfield resonance at -1.13 ppm corresponds to the B-C*H*-B proton, which is validated by the crosspeak with a tether arm -CH_2 in the ^{1}H-^{1}H COSY spectrum (**Figure S35**).

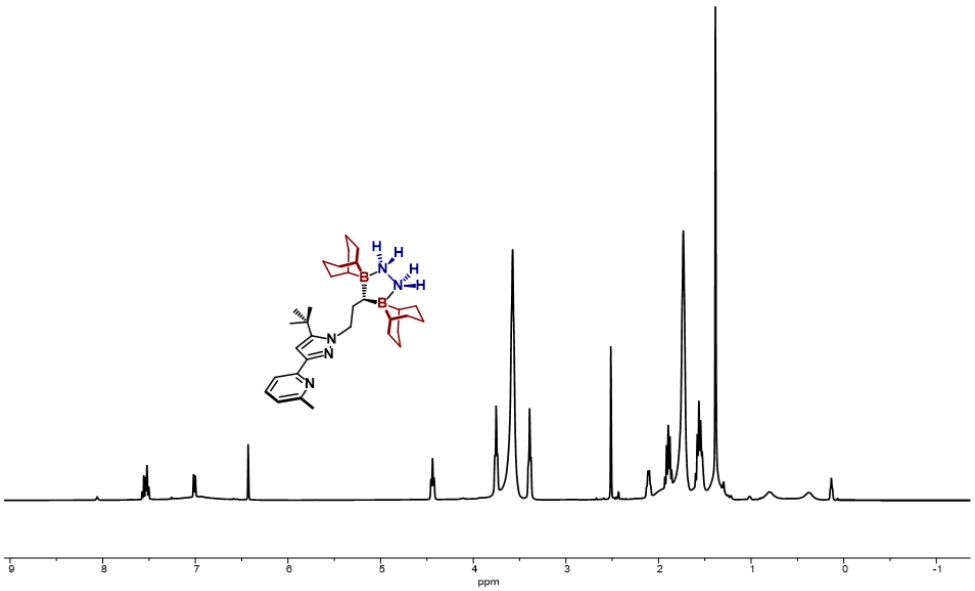

Figure S41. ^{1}H NMR spectrum (THF, 23 °C) of $^{(BBN)2}NN^{tBu}(N_2H_4)$.

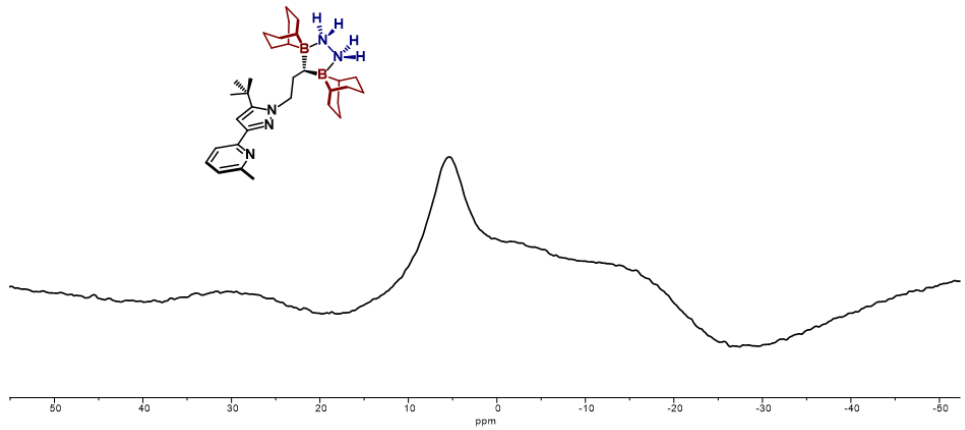

Figure S42. ^{11}B NMR spectrum (THF, 23 °C) of $^{(BBN)2}NN^{tBu}(N_2H_4)$.

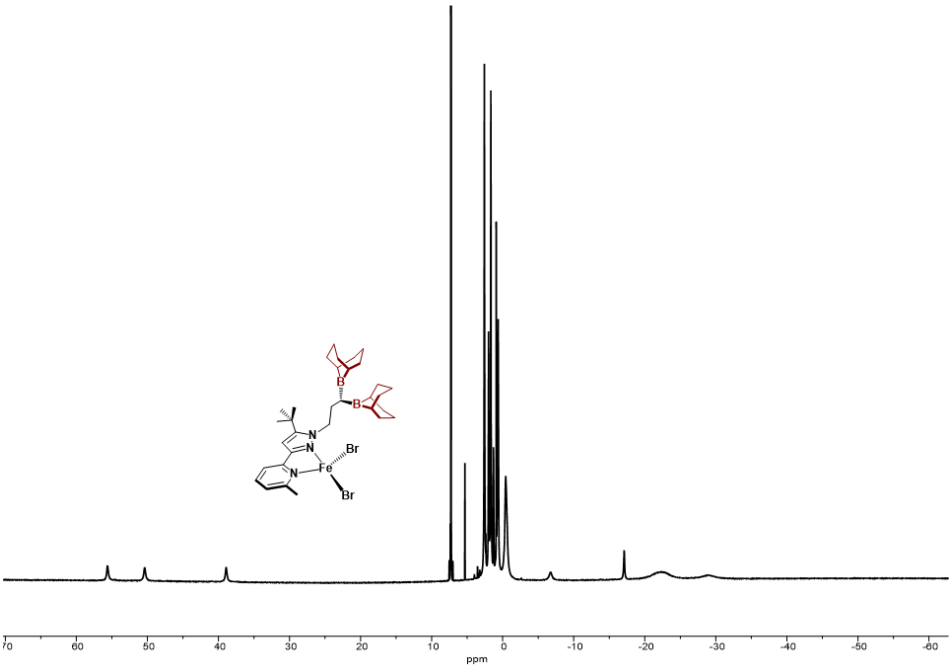

Figure S43. ^{1}H NMR spectrum ($CDCl_3$, 23 °C) of ($^{(BBN)2}NN^{tBu}$)$FeBr_2$.

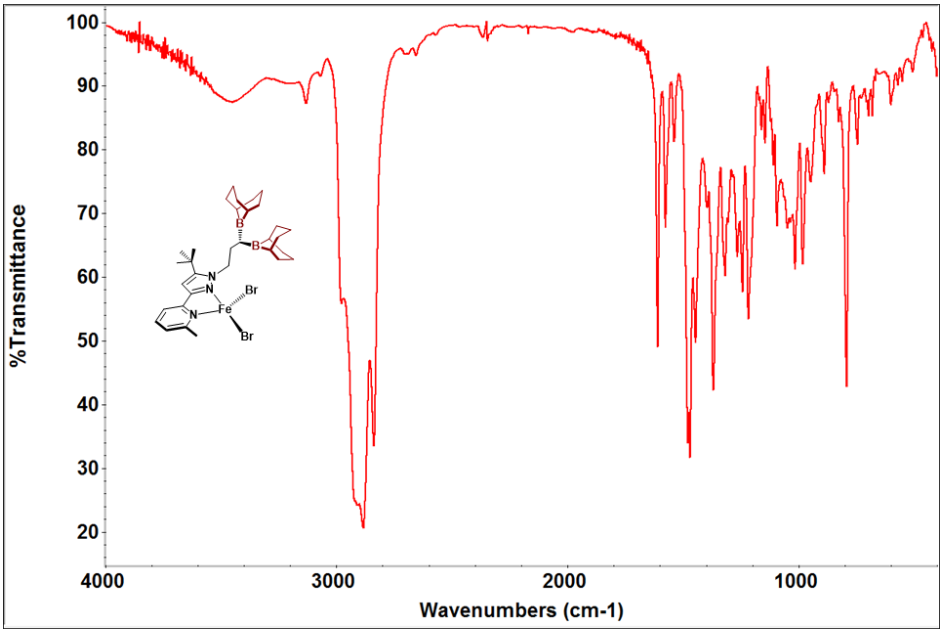

Figure S44. Infrared spectrum (KBr) of ($^{(BBN)2}NN^{tBu}$)$FeBr_2$.

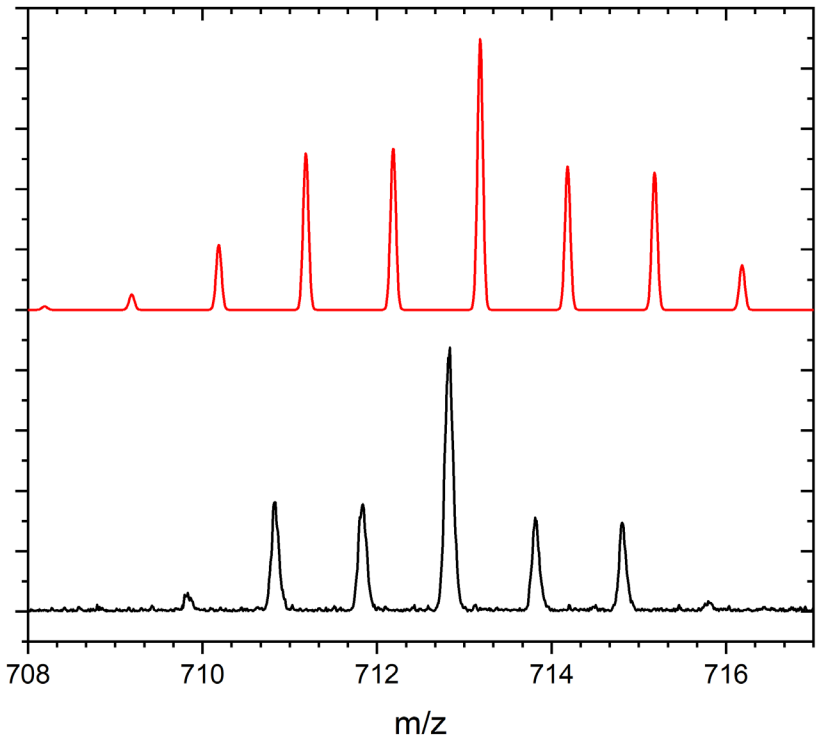

Figure S45. MALDI-TOF spectrum of ($^{(BBN)2}$NN^{tBu})FeBr$_2$ (bottom, black) and simulation (top, red).

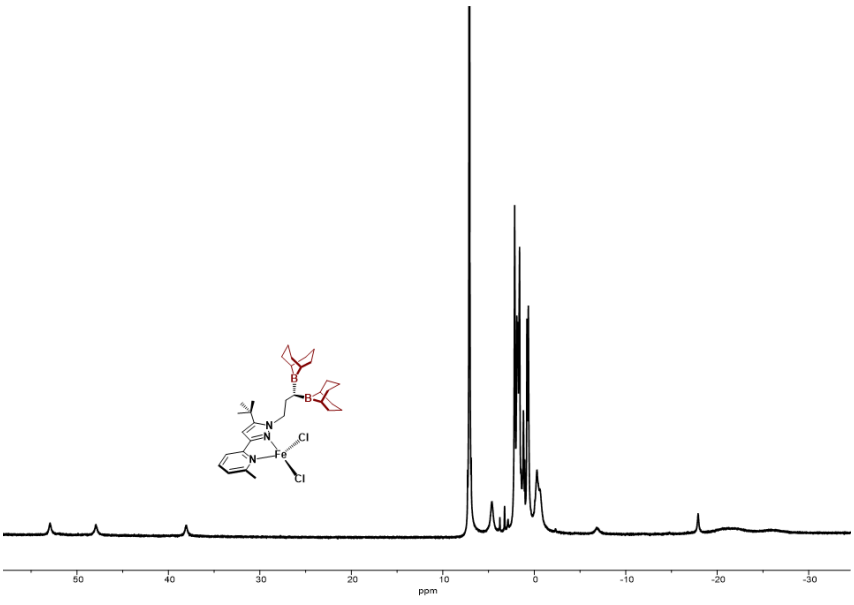

Figure S46. ^{1}H NMR spectrum (C_6H_6, 23 °C) of ($^{(BBN)2}$NN^{tBu})FeCl$_2$.

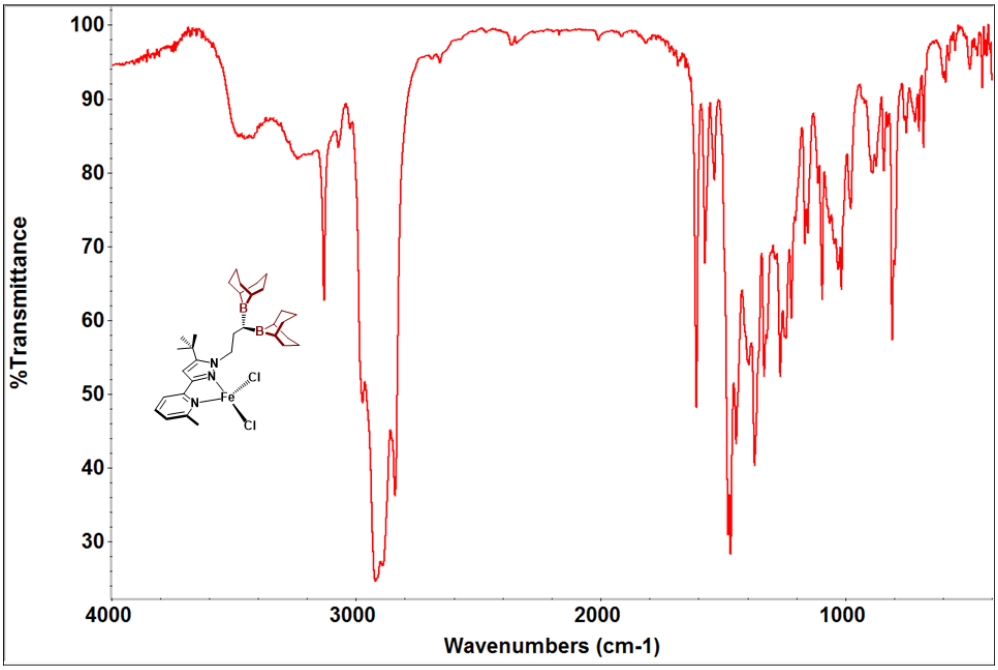

Figure S47. Infrared spectrum (KBr) of ($^{(BBN)2}$NN^{tBu})$FeCl_2$.

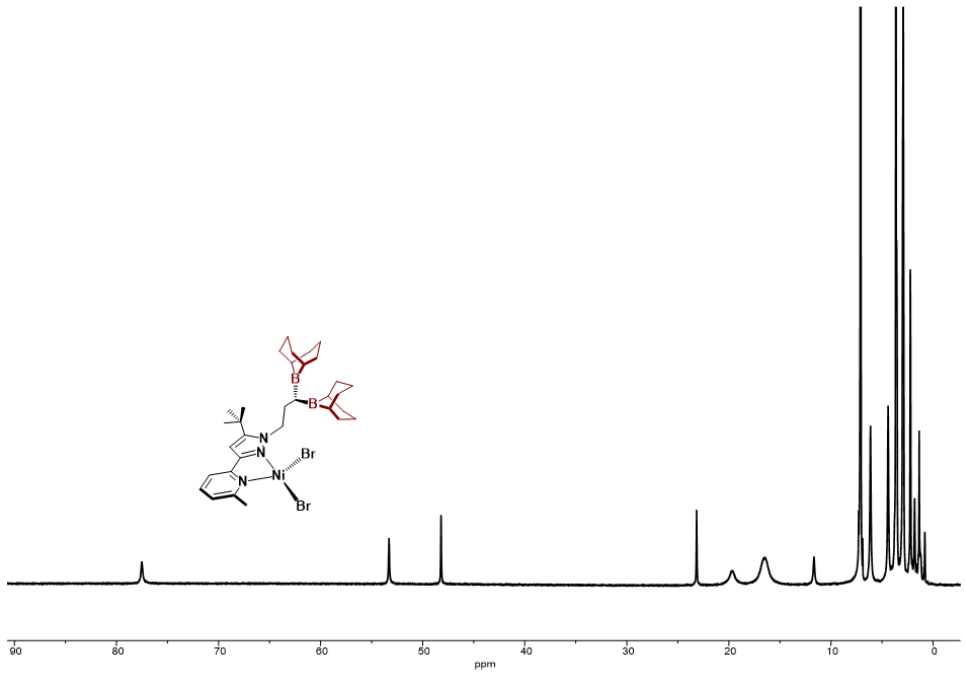

Figure S48. ^{1}H NMR spectrum (THF, 23 °C) of ($^{(BBN)2}$NN^{tBu})$NiBr_2$.

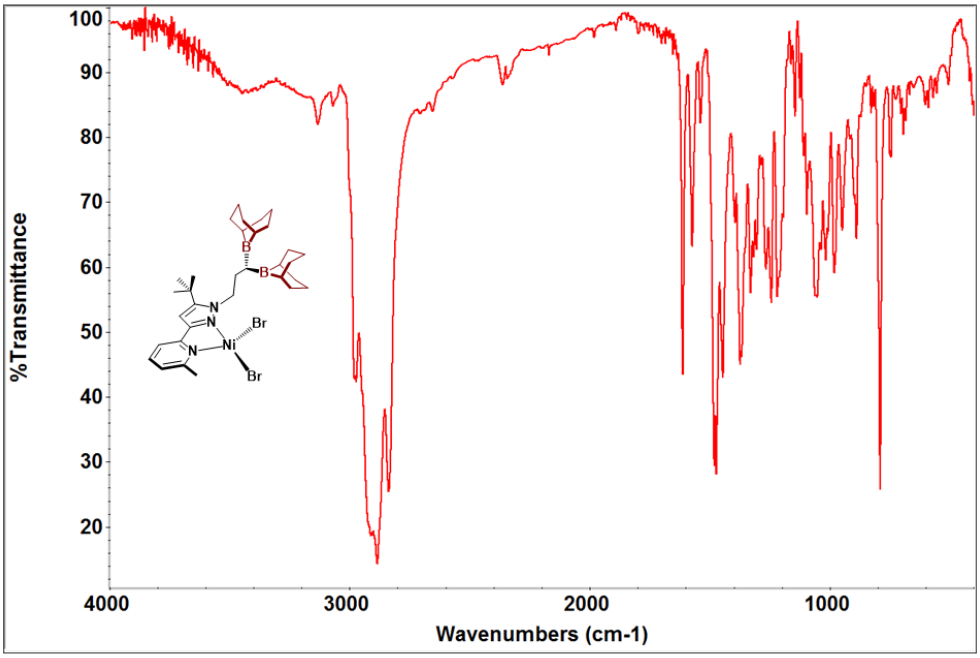

Figure S49. Infrared spectrum (KBr) of ($^{(BBN)2}$NN^{tBu})NiBr$_2$.

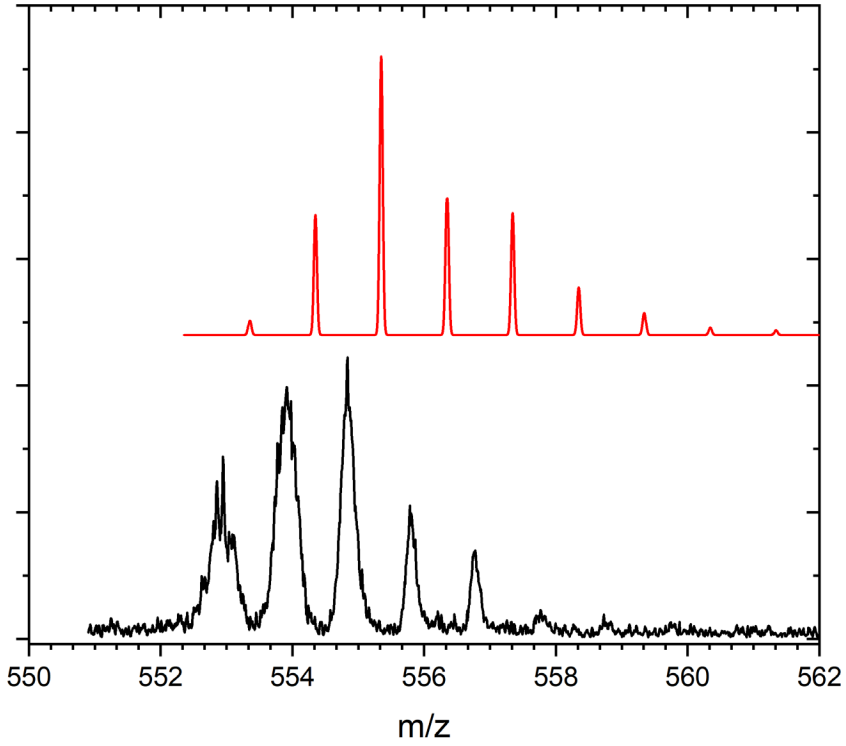

Figure S50. MALDI-TOF spectrum of ($^{(BBN)2}$NN^{tBu})NiBr$_2$ (bottom, black) and simulation (top, red).

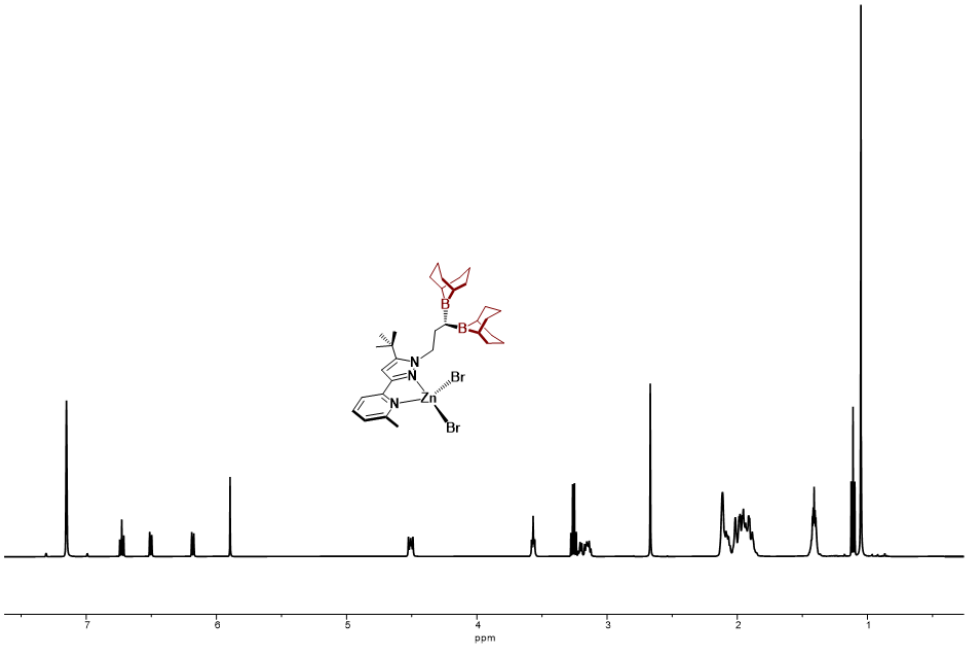

Figure S51. ^{1}H NMR spectrum (C_6D_6, 23 °C) of ($^{(BBN)2}NN^{tBu}$)$ZnBr_2$.

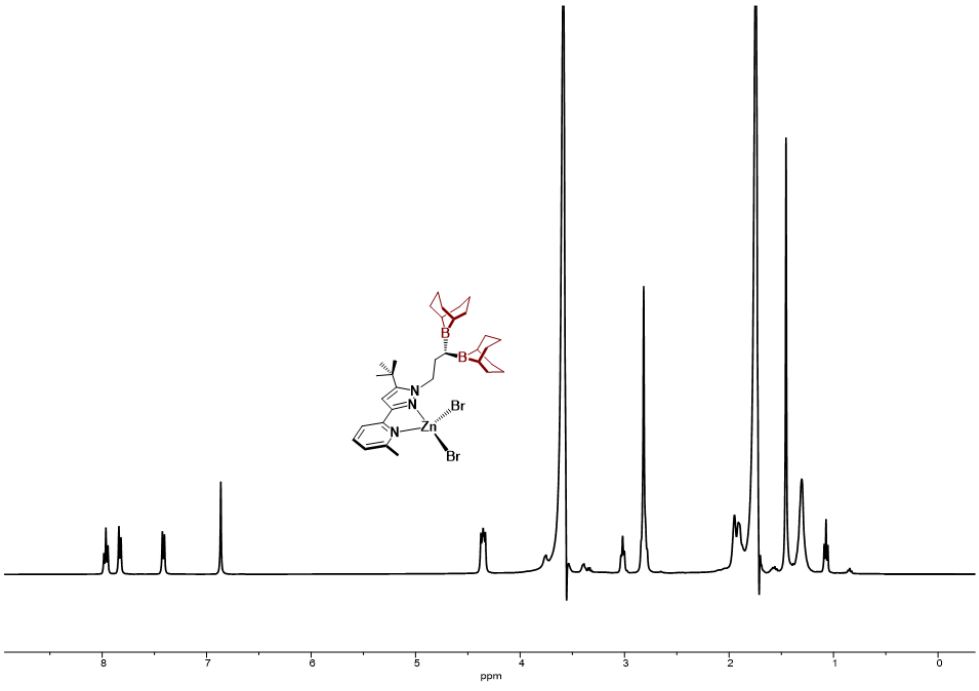

Figure S52. ^{1}H NMR spectrum (THF, 23 °C) of ($^{(BBN)2}NN^{tBu}$)$ZnBr_2$.

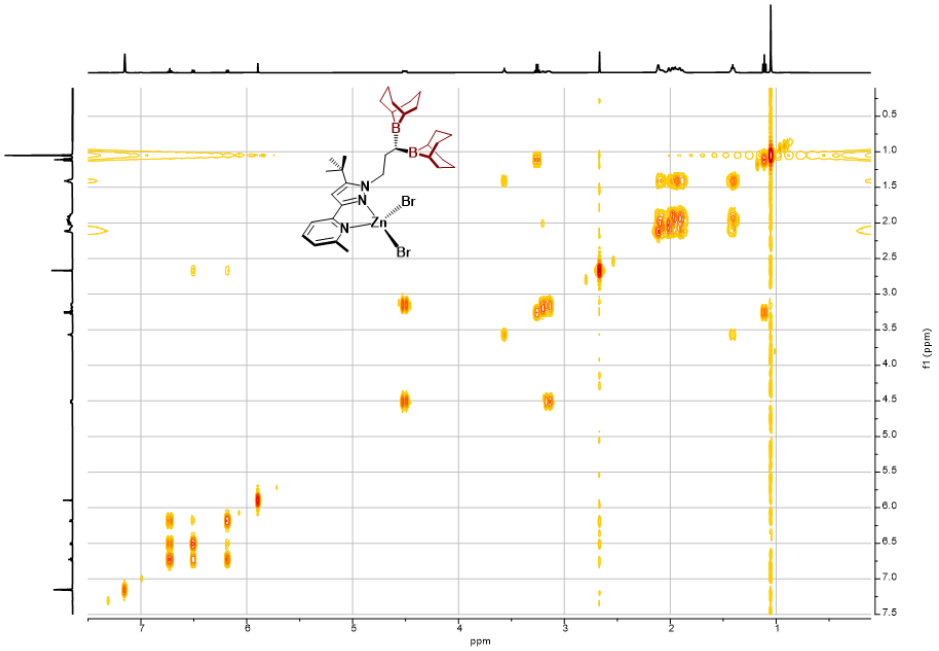

Figure S53. ^{1}H-^{1}H COSY spectrum (C_6D_6, 23 °C) of ($^{(BBN)2}$NN^{tBu})ZnBr$_2$.

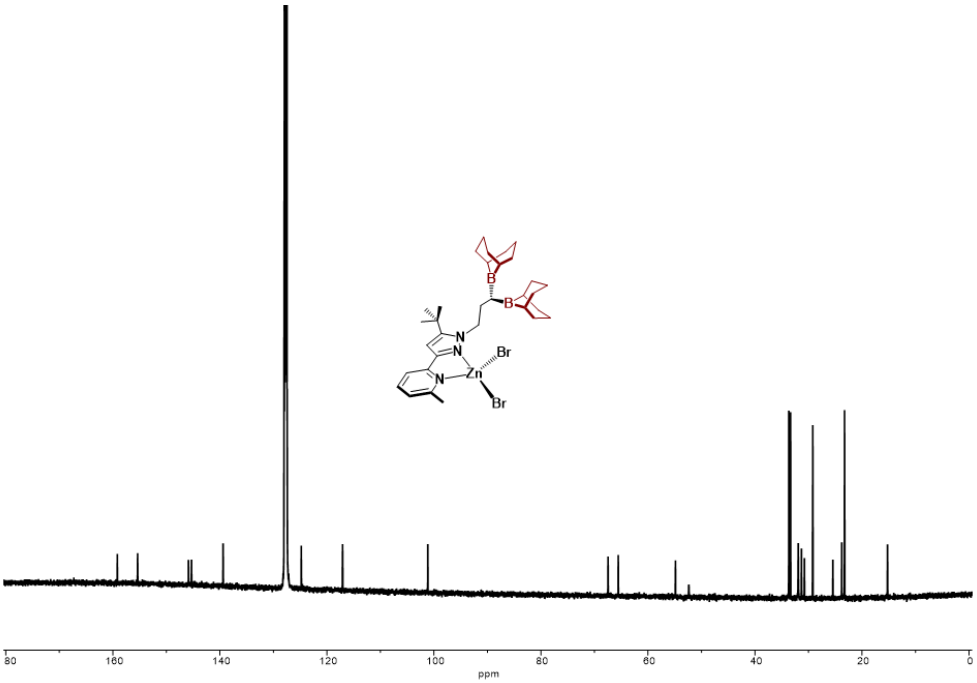

Figure S54. ^{13}C NMR spectrum (C_6D_6, 23 °C) of ($^{(BBN)2}$NN^{tBu})ZnBr$_2$.

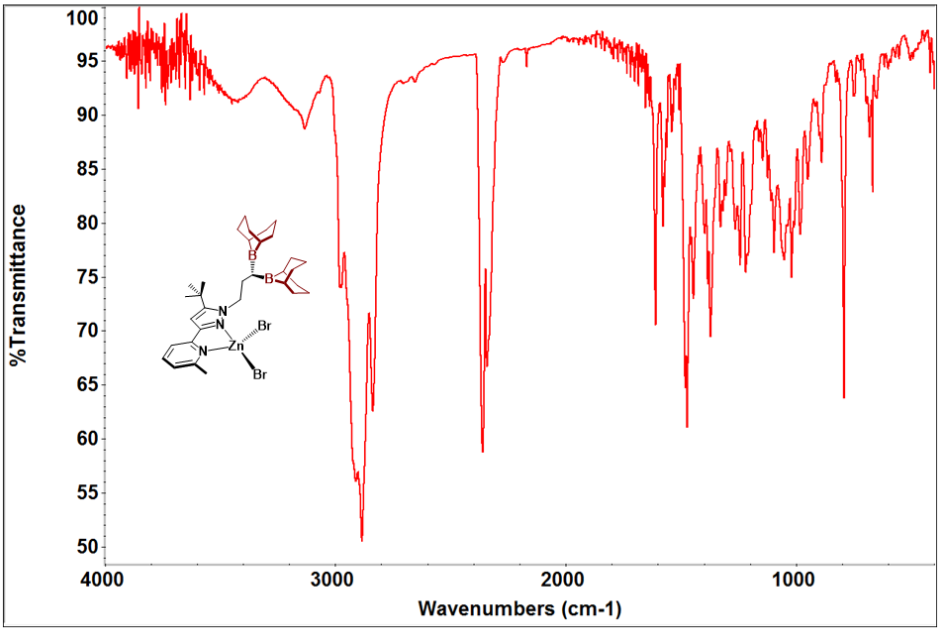

Figure S55. Infrared spectrum (KBr) of ($^{(BBN)2}NN^{tBu}$)$ZnBr_2$. Absorption band at 2350 cm^{-1} corresponds to atmospheric CO_2.

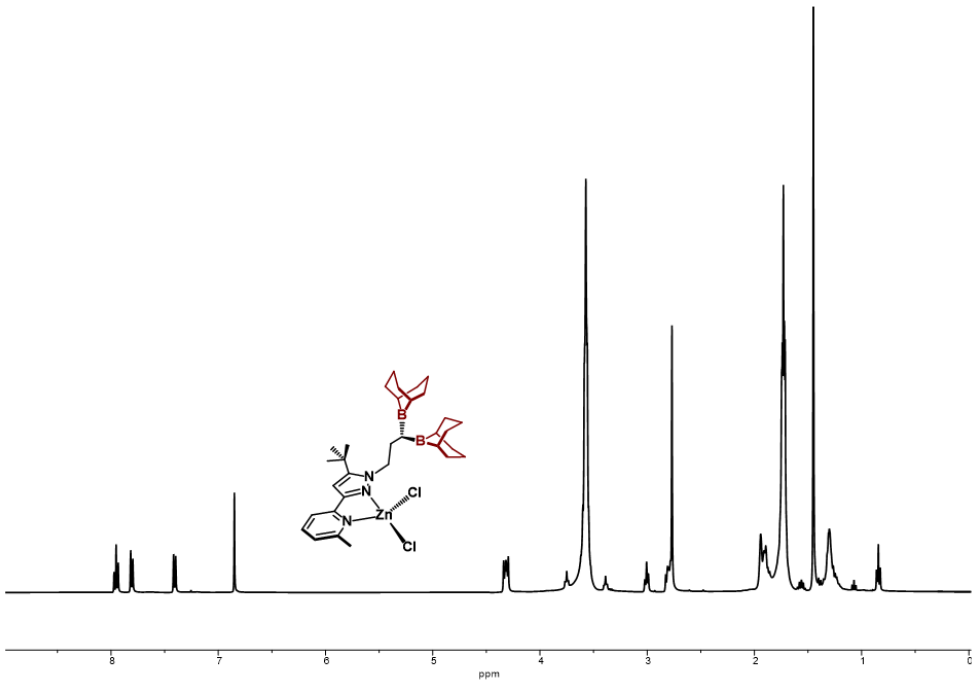

Figure S56. ^1H NMR spectrum (THF, 23 °C) of ($^{(BBN)2}NN^{tBu}$)$ZnCl_2$.

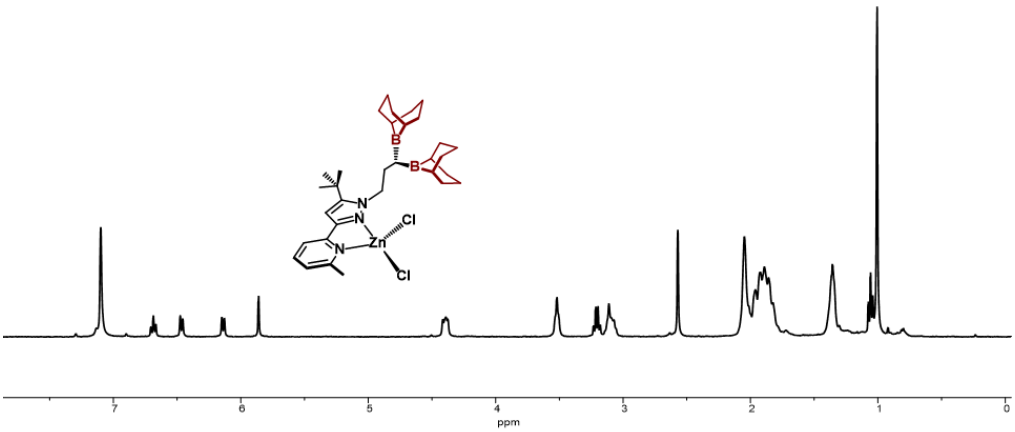

Figure S57. ^{1}H NMR spectrum (C_6D_6, 23 °C) of ($^{(BBN)2}NN^{tBu}$)$ZnCl_2$.

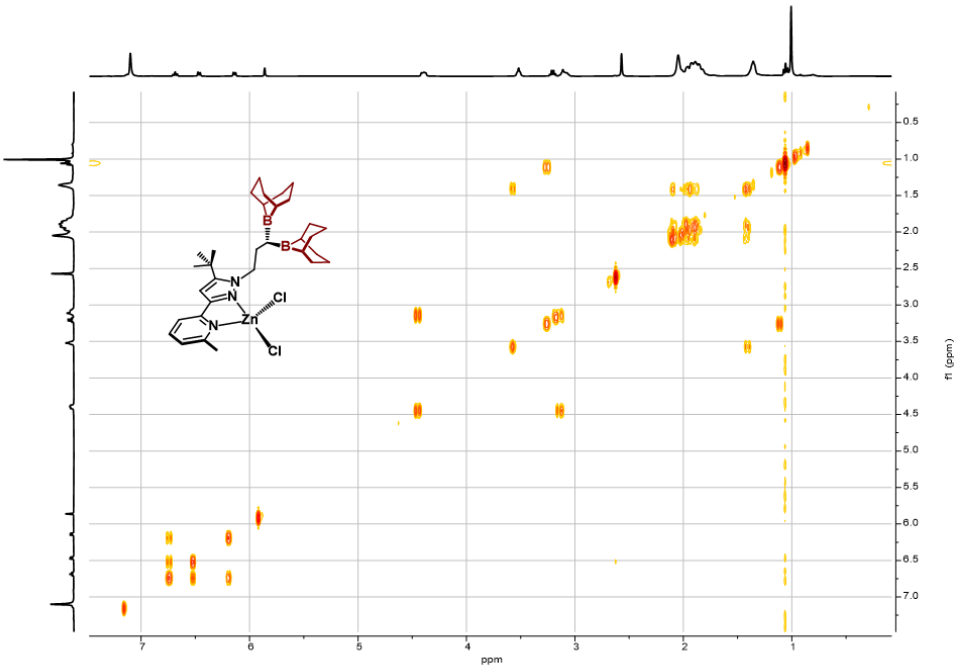

Figure S58. ^{1}H-^{1}H COSY spectrum (C_6D_6, 23 °C) of ($^{(BBN)2}NN^{tBu}$)$ZnCl_2$.

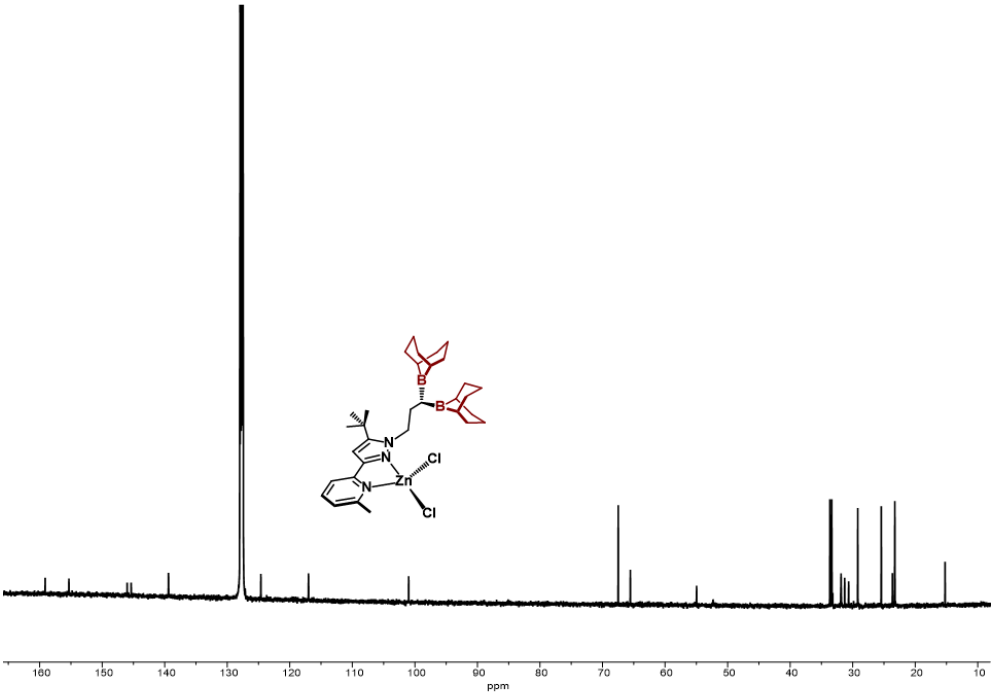

Figure S59. ^{13}C NMR spectrum (C_6D_6, 23 °C) of ($^{(BBN)2}NN^{tBu}$)$ZnCl_2$.

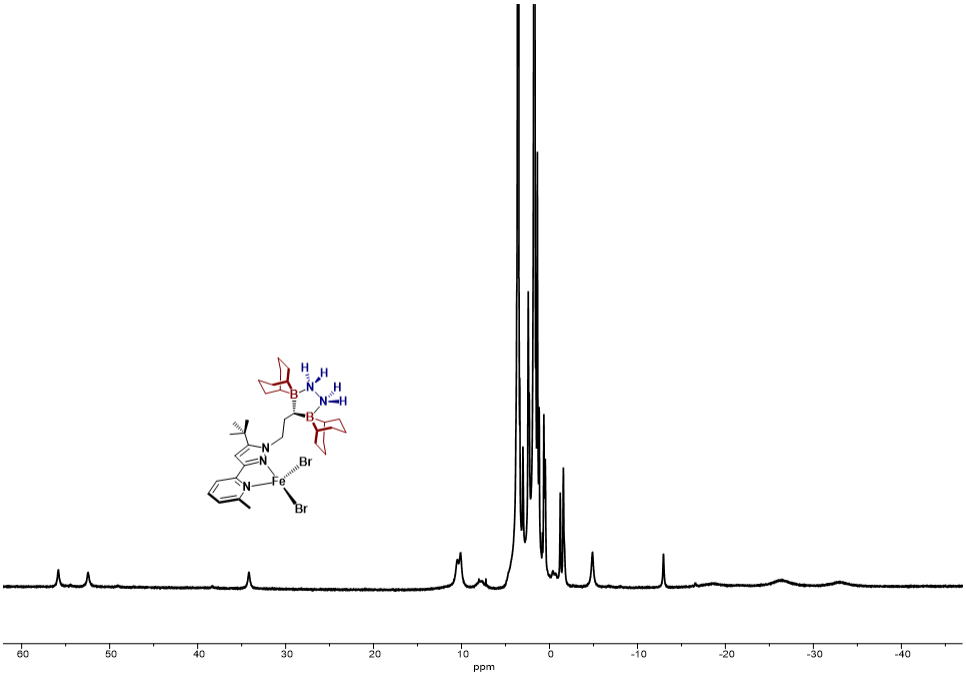

Figure S60. ^{1}H NMR spectrum (THF, 23 °C) of ($^{(BBN)2}NN^{tBu}$)$FeBr_2(N_2H_4)$.

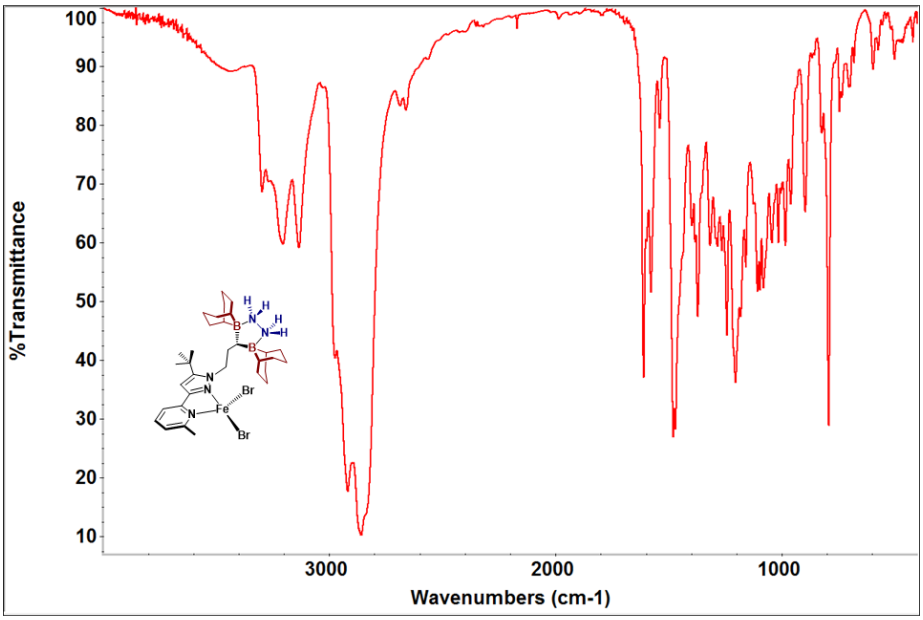

Figure S61. Infrared spectrum (KBr) of ($^{(BBN)2}NN^{tBu}$)$FeBr_2(N_2H_4)$.

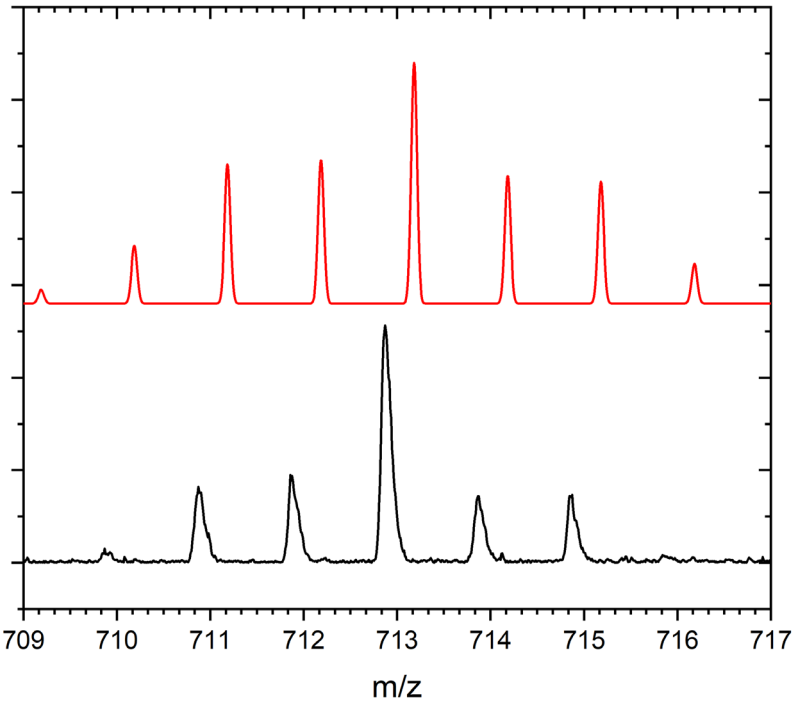

Figure S62. MALDI-TOF spectrum of ($^{(BBN)2}NN^{tBu}$)$FeBr_2(N_2H_4)$ (bottom, black) and simulation(top, red).

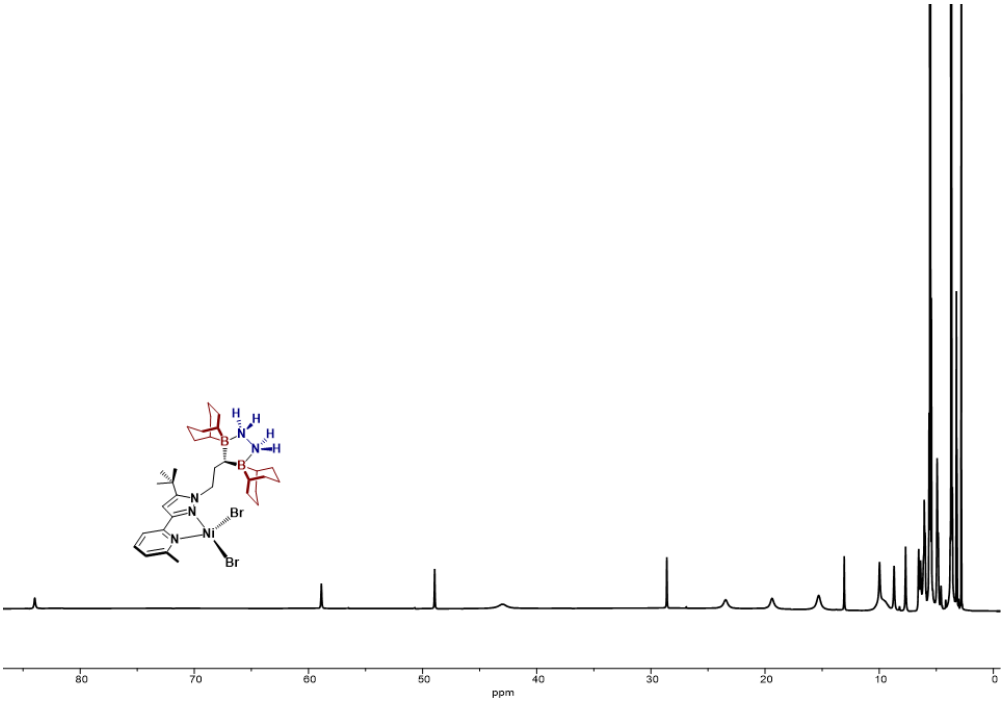

Figure S63. ^{1}H NMR spectrum (THF, 23 °C) of ($^{(BBN)2}$NN^{tBu})NiBr$_2$(N$_2$H$_4$).

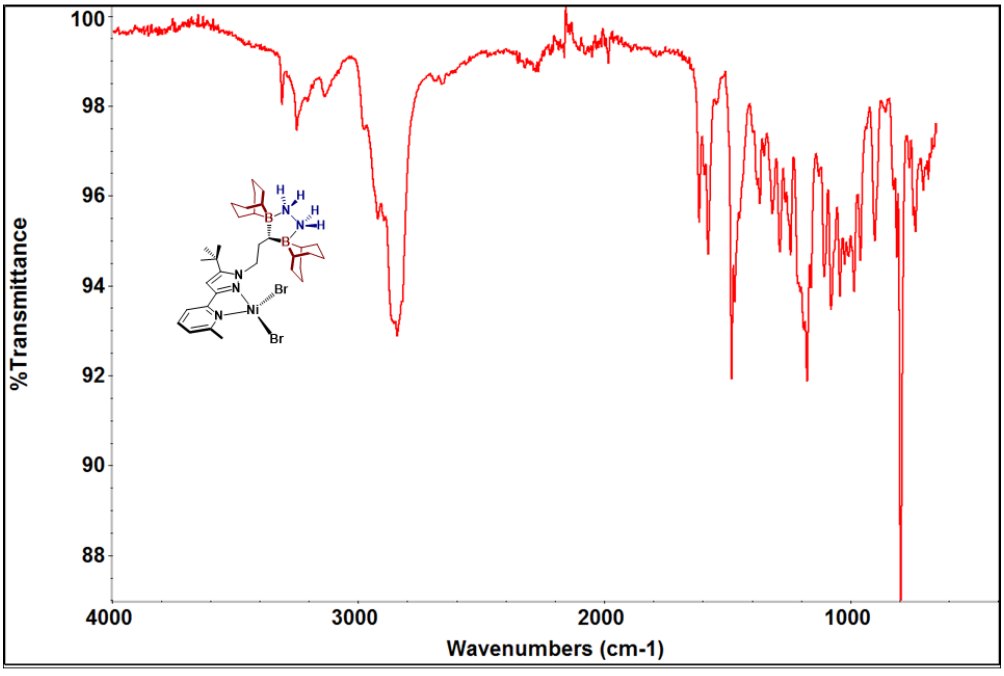

Figure S64. Infrared spectrum (KBr) of ($^{(BBN)2}$NN^{tBu})NiBr$_2$(N$_2$H$_4$).

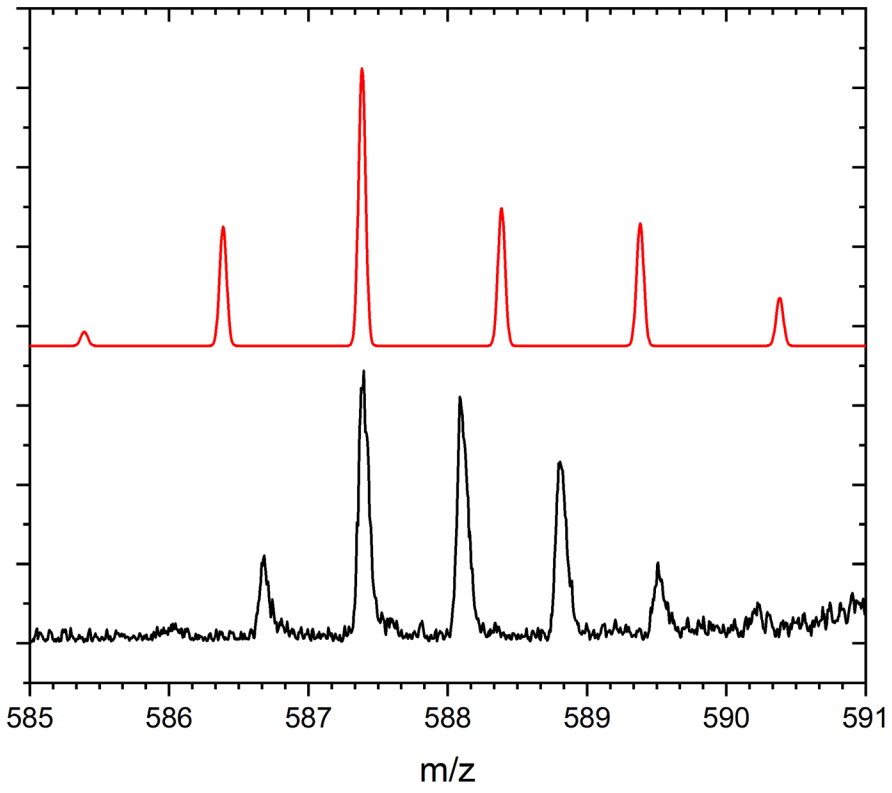

Figure S65. MALDI-TOF spectrum of ($^{(BBN)2}NN^{tBu}$)$NiBr_2(N_2H_4)$ (bottom, black) and simulation (top, red).

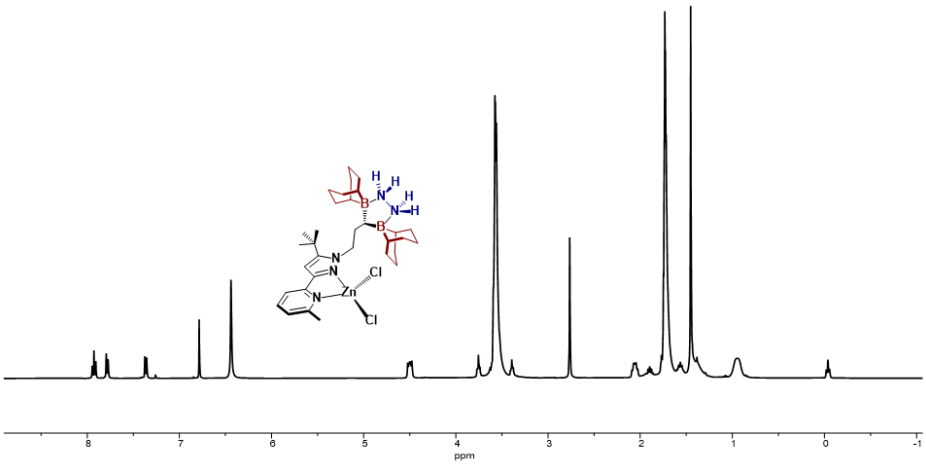

Figure S66. ^{1}H NMR spectrum (THF, 23 °C) of ($^{(BBN)2}NN^{tBu}$)$ZnCl_2(N_2H_4)$. (top, red).

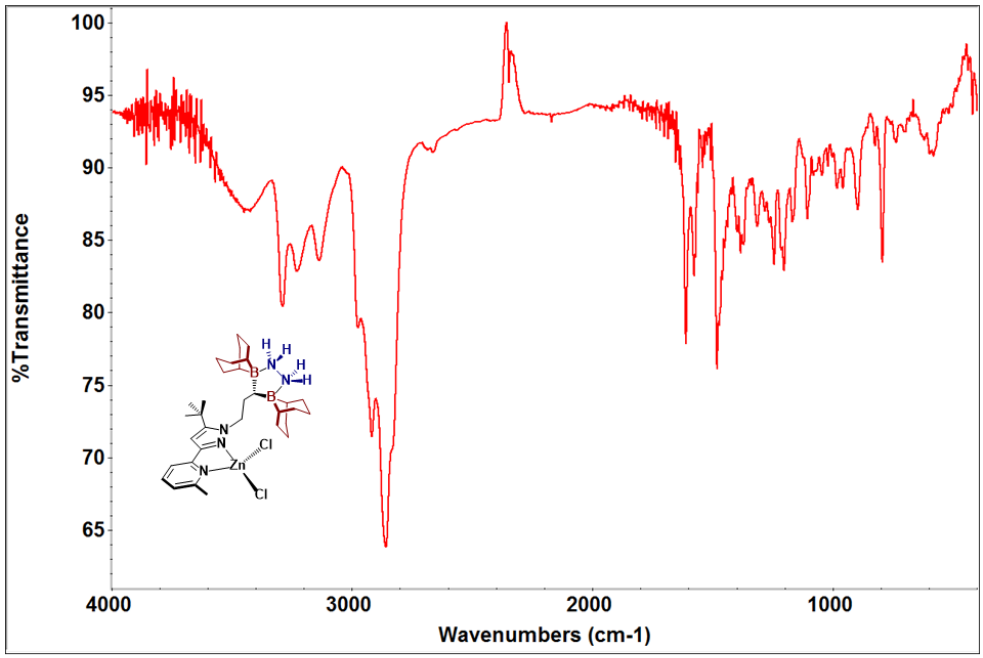

Figure S67. Infrared spectrum (KBr) of ($^{(BBN)2}NN^{tBu}$)$ZnBr_2(N_2H_4)$.

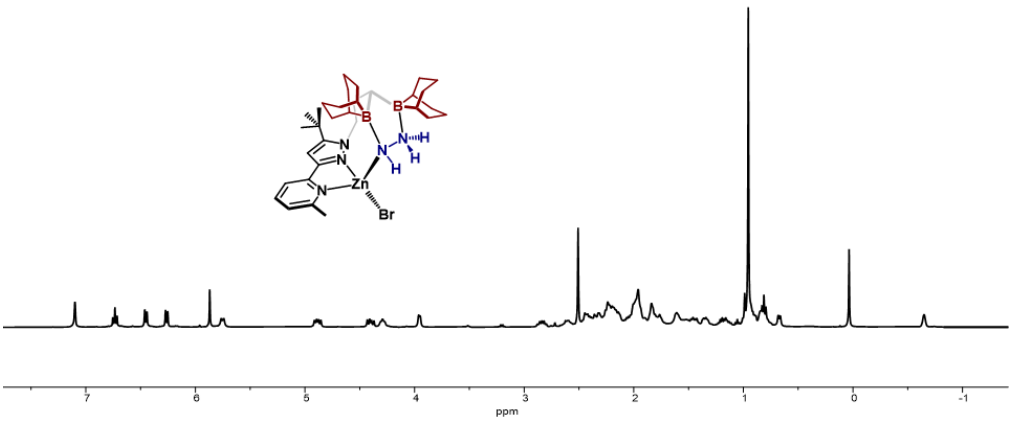

Figure S68. ^1H NMR spectrum (C_6D_6, 23 °C) of ($^{(BBN)2}NN^{tBu}$)$ZnBr(N_2H_3)$.

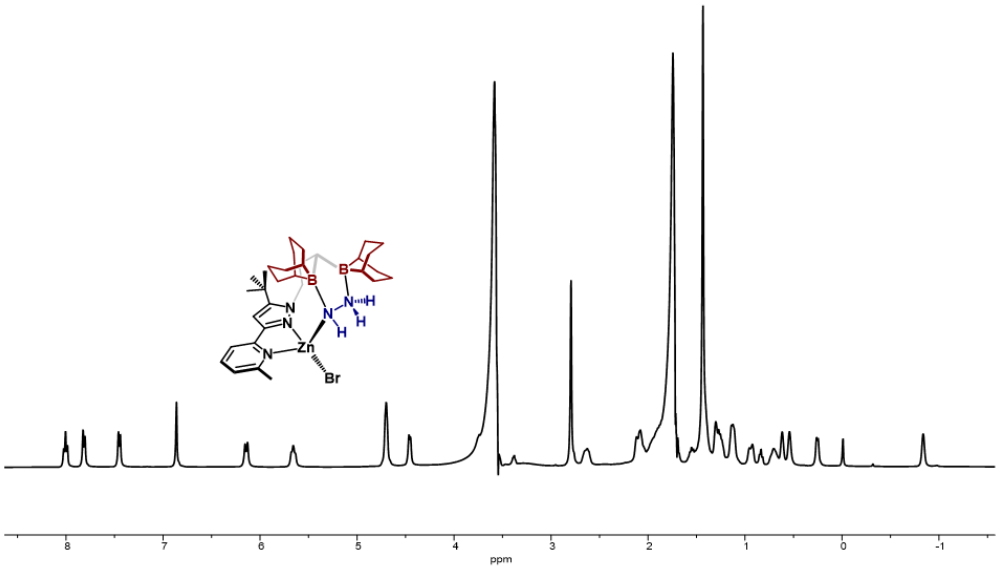

Figure S69. ^{1}H NMR spectrum (THF, 23 °C) of ($^{(BBN)2}$NN^{tBu})ZnBr(N_2H_3).

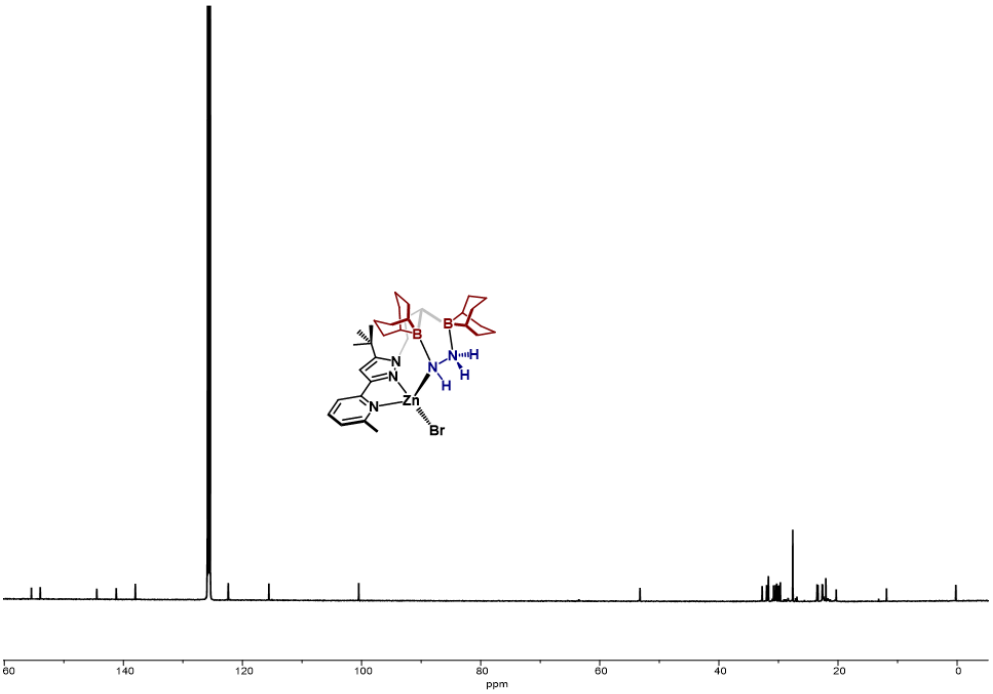

Figure S70. ^{13}C NMR spectrum (C_6D_6, 23 °C) of ($^{(BBN)2}$NN^{tBu})ZnBr(N_2H_3).

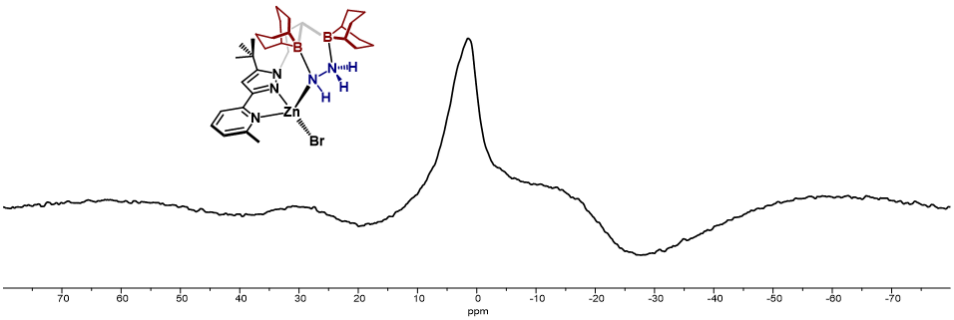

Figure S71. ^{11}B NMR spectrum (THF, 23 °C) of ($^{(BBN)2}$NN^{tBu})ZnBr(N_2H_3).

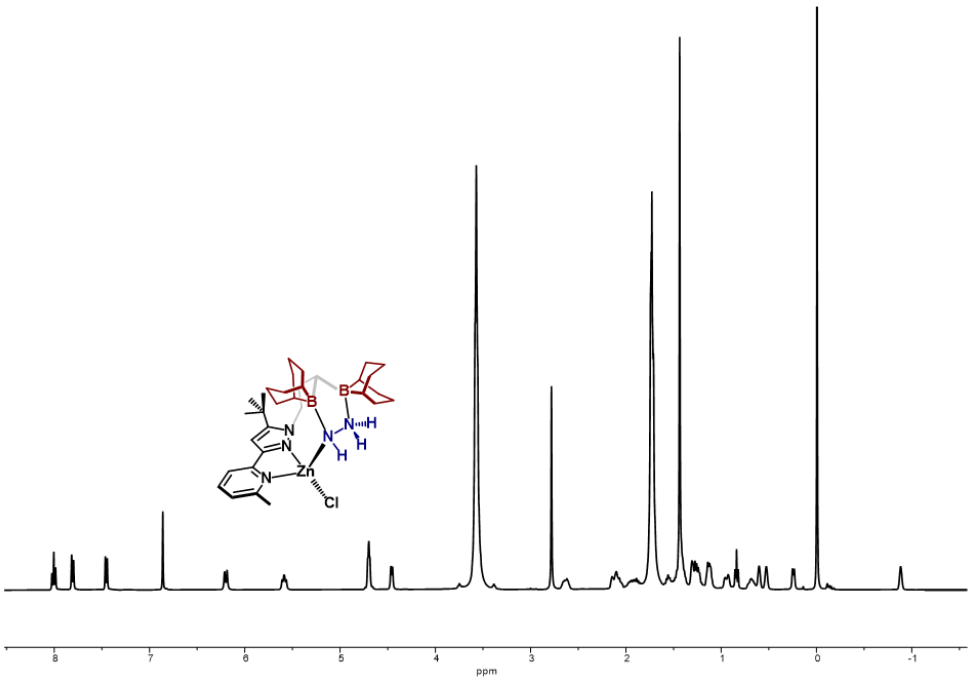

Figure S72. ^{1}H NMR spectrum (THF, 23 °C) of ($^{(BBN)2}$NN^{tBu})ZnCl(N_2H_3).

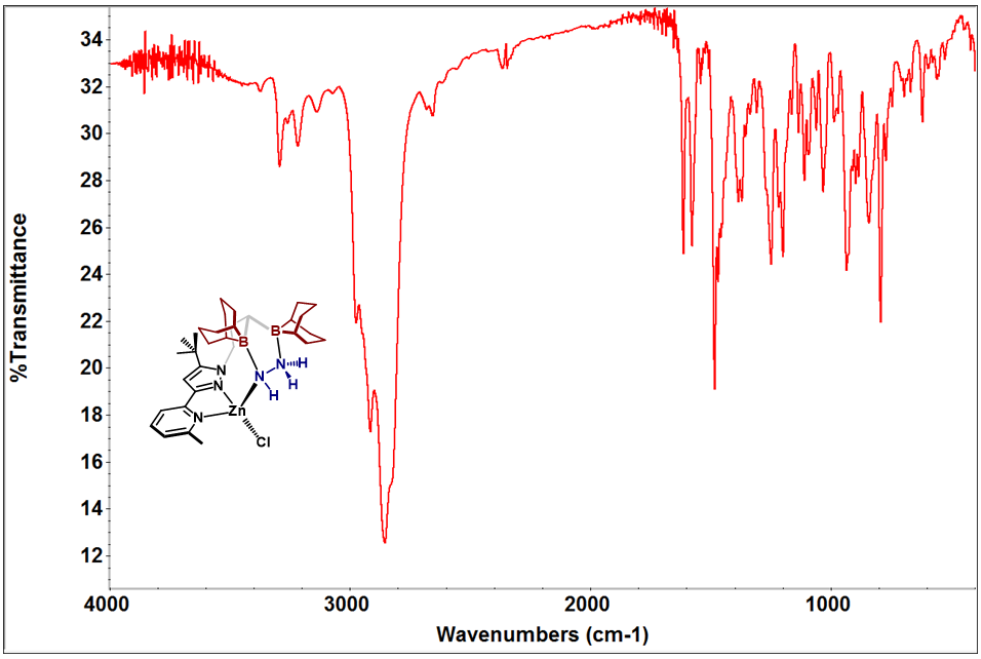

Figure S73. Infrared spectrum (KBr) of ($^{(BBN)2}$NN^{tBu})ZnCl(N_2H_3).

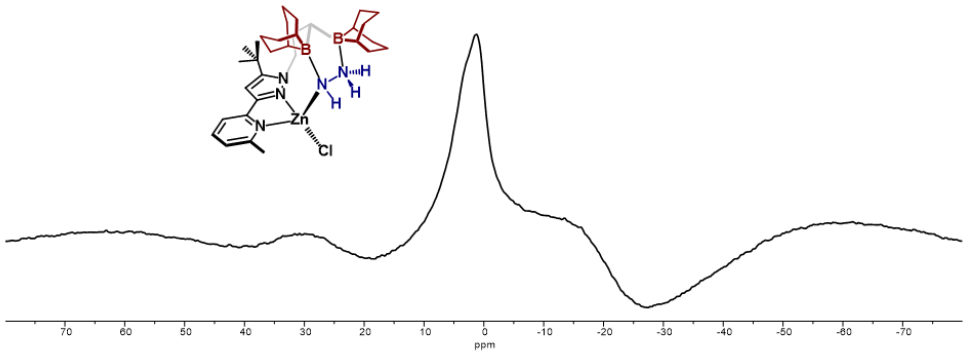

Figure S74. ^{11}B NMR spectrum (THF, 23 °C) of ($^{(BBN)2}$NN^{tBu})ZnCl(N_2H_3).

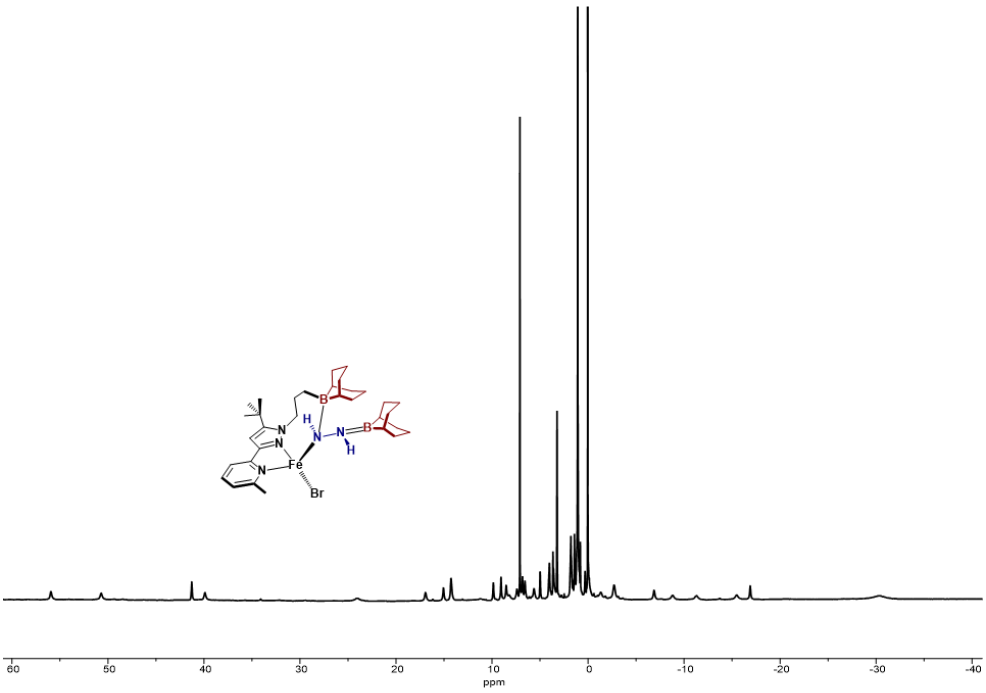

Figure S75. ^{1}H NMR spectrum (C_6D_6, 23 °C) of ($^{(BBN)2}NN^{tBu}$)FeBr(N_2H_2).

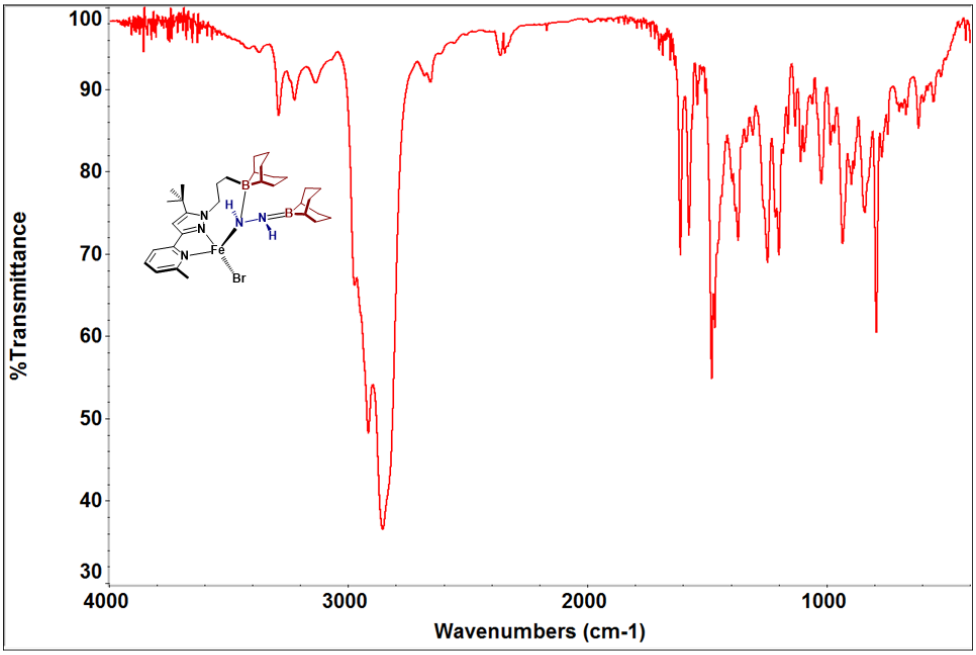

Figure S76. Infrared spectrum (KBr) of ($^{(BBN)2}NN^{tBu}$)FeBr(N_2H_2).

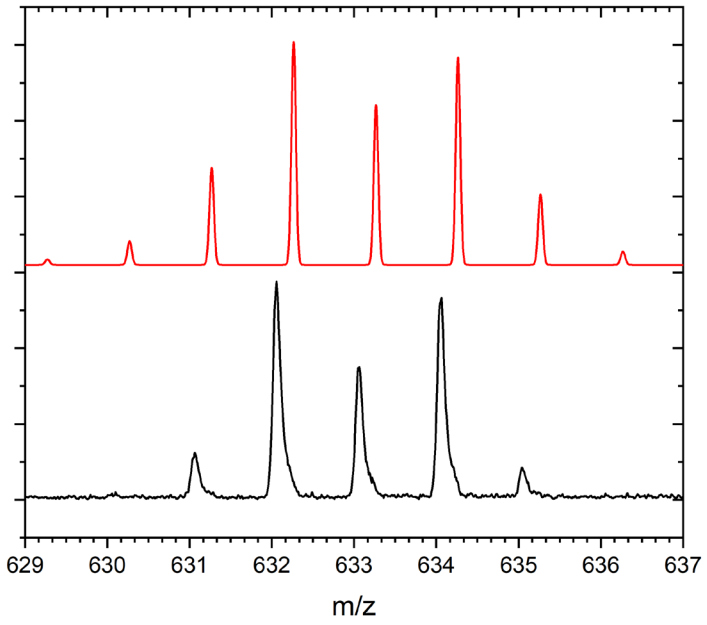

Figure S77. MALDI-TOF spectrum of ($^{(BBN)2}$NN^{tBu})FeBr(N_2H_2) (bottom, black) and simulation (top, red).

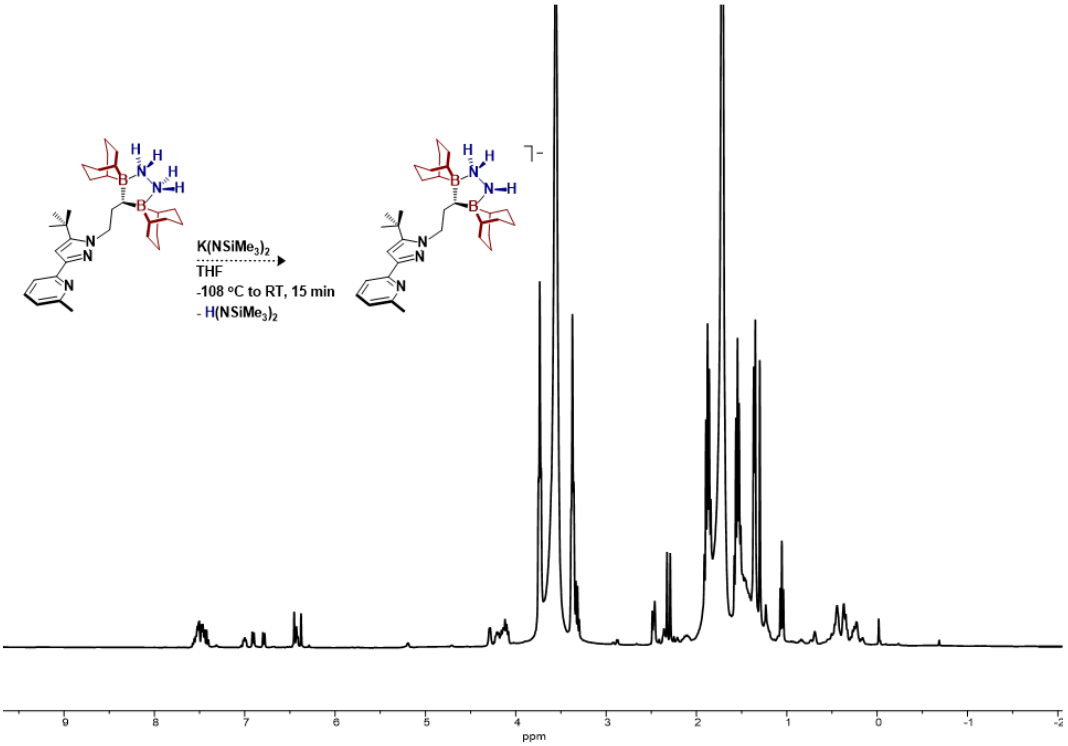

Figure S78. ^{1}H NMR spectrum (THF, 23 °C) of reaction between ($^{(BBN)2}$NN^{tBu})(N_2H_4) and KHMDS showing a mixture of products.

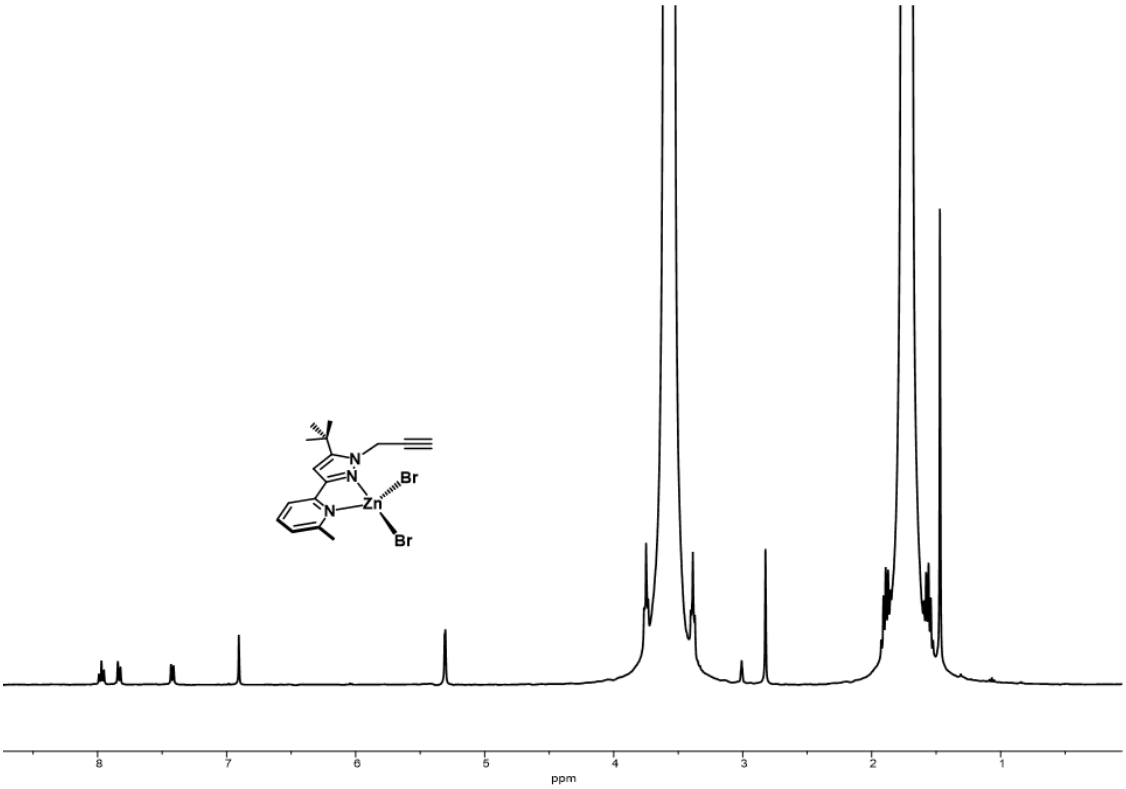

Figure S79. ^{1}H NMR spectrum (THF, 23 °C) of (^{propargyl}NN^{tBu})ZnBr$_2$.

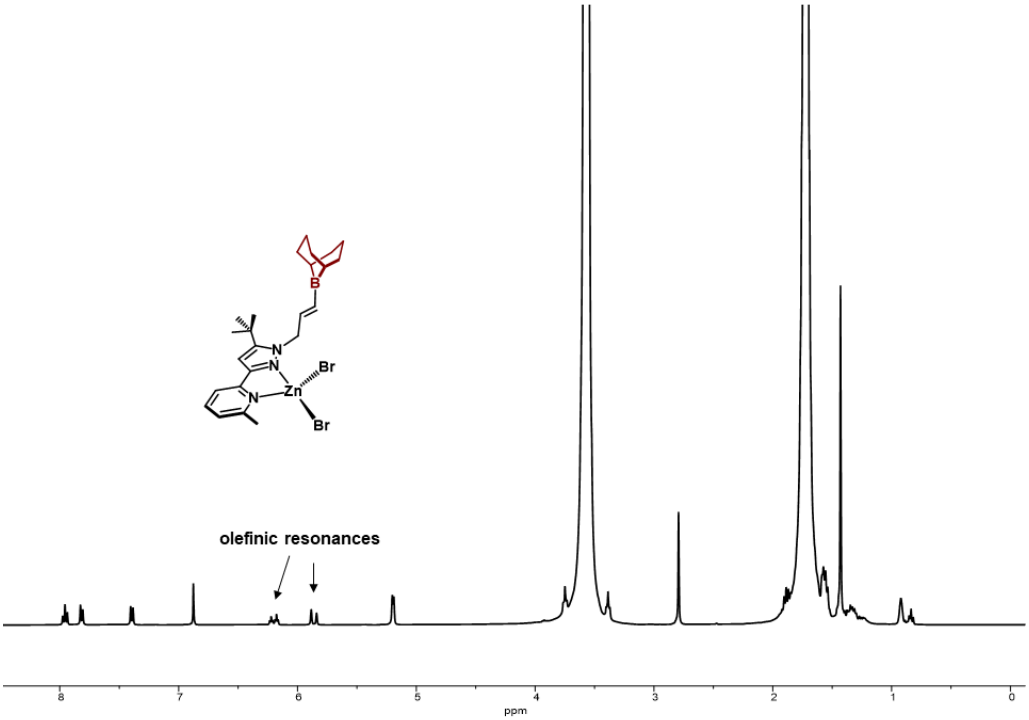

Figure S80. ^{1}H NMR spectrum (THF, 23 °C) of (^{ene}NN^{tBu})ZnBr$_2$.

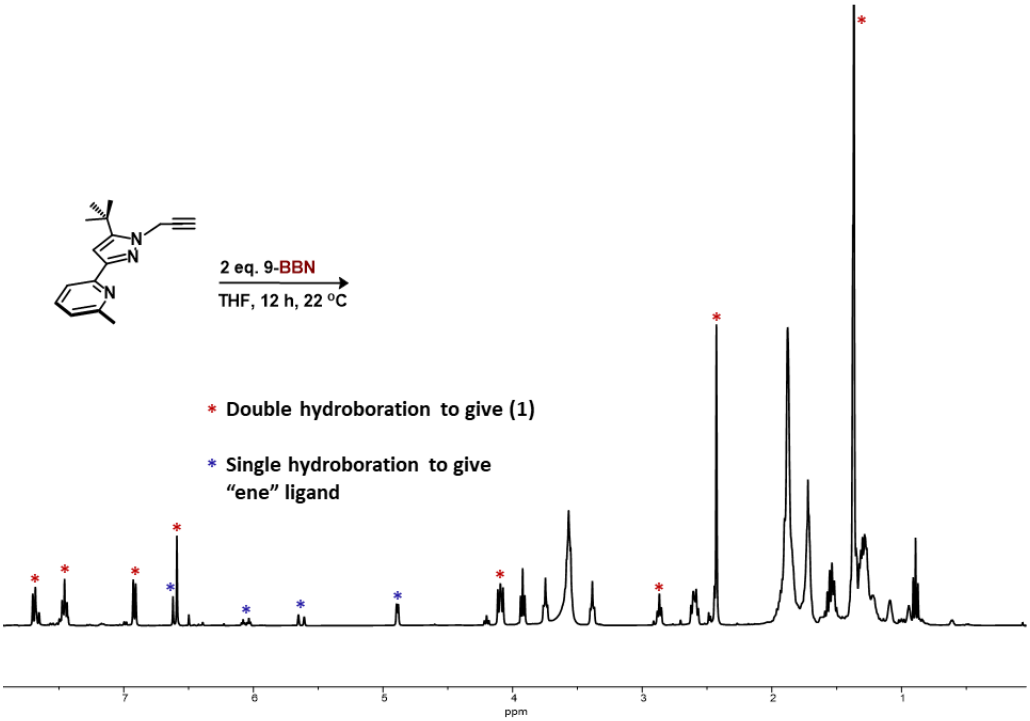

Figure S81. ^{1}H NMR spectrum (THF, 23 °C) of ^{propargyl}NN^{tBu} + 2 equiv. 9-BBN

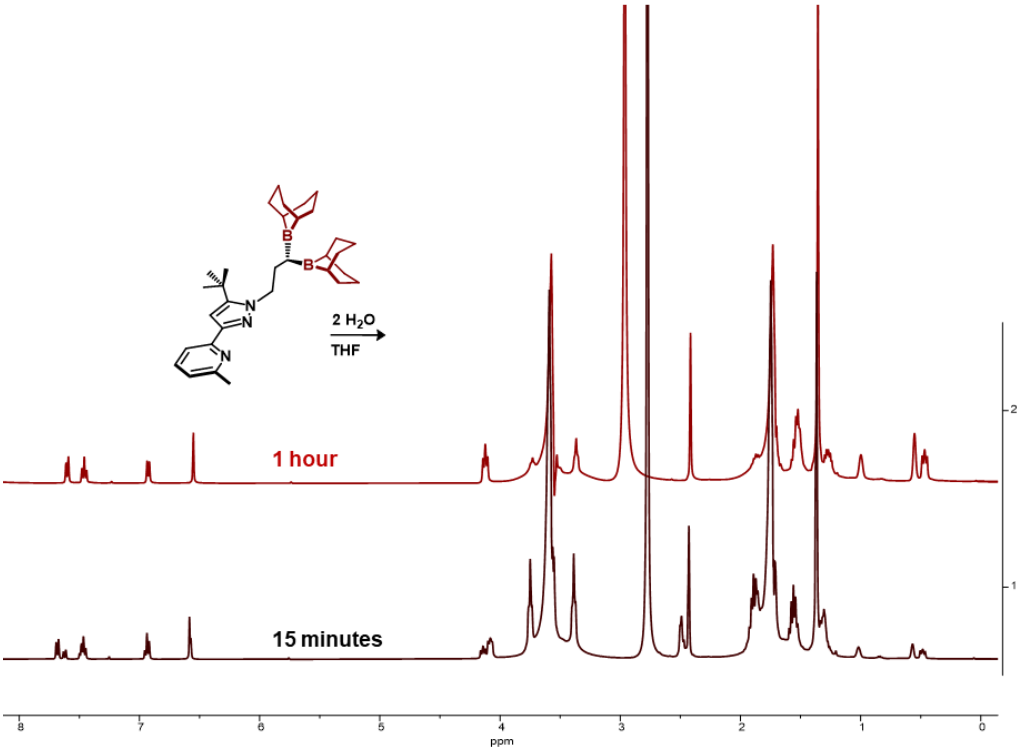

Figure S82. ^{1}H NMR spectrum (THF, 23 °C) of ($^{(BBN)2}$NN^{tBu}) + 2 equiv. H_2O.

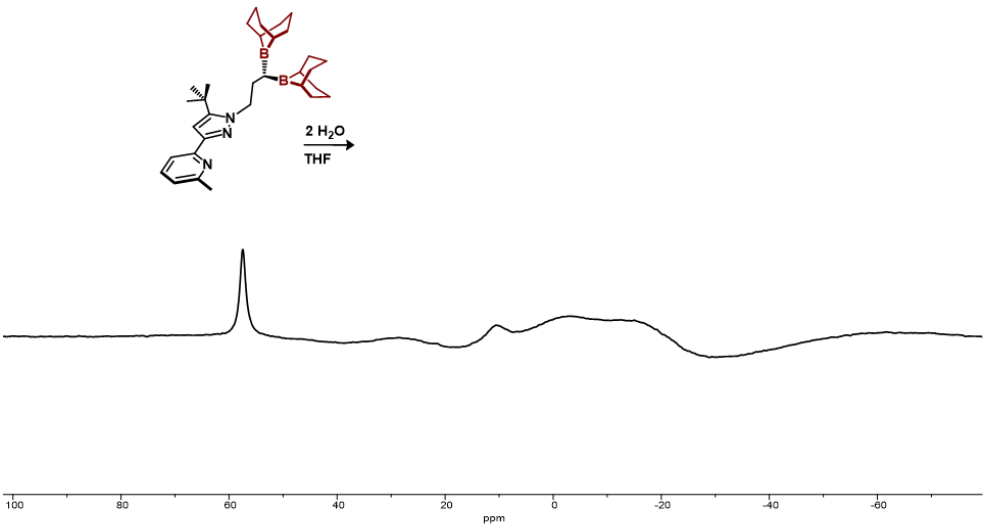

Figure S83. ^{11}B NMR spectrum (THF, 23 °C) of ($^{(BBN)2}$NN^{tBu}) + 2 equiv. H_2O.

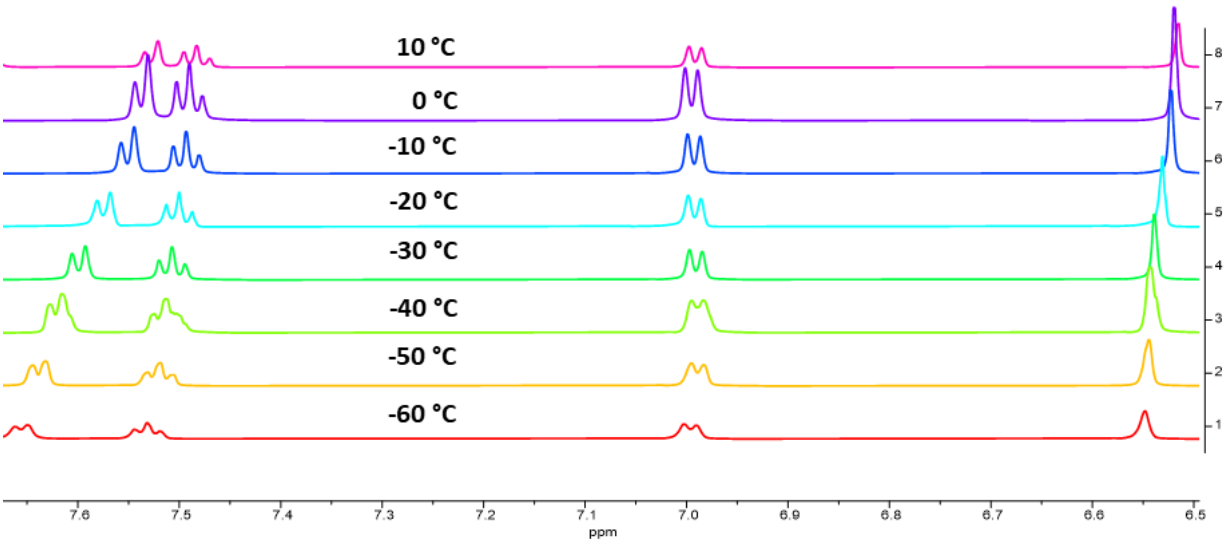

Figure S84. Aromatic region of variable temperature ^{1}H NMR spectra (THF) of ($^{(BBN)}$NN^{tBu}). Temperature dependent chemical shifts of the aromatic protons likely indicates fluxionality of the intramolecular Lewis acid/base adduct.

Determination of Acceptor Numbers

Acceptor numbers were determined by the Gutmann-Beckett method[9] via the equation:

$$\text{acceptor number} = 2.21 \times (\delta_{sample} - 41.0)$$

where δ_{sample} is the experimentally determined chemical shift in the ^{31}P NMR.

For each determination, 0.250 mL of a triethylphosphine oxide stock solution (0.1242 M, THF) were combined with an equimolar amount of substrate (either **1** or **1-mono**) in 0.500 mL THF and stirred at room temperature for 10 minutes before transfer of the solution to a J-Young tube. A sealed triethylphosphine oxide capillary was added and the ^{31}P NMR spectra were referenced to this internal standard (+43.36 ppm). The ^{31}P resonances are reported relative to phosphoric acid.

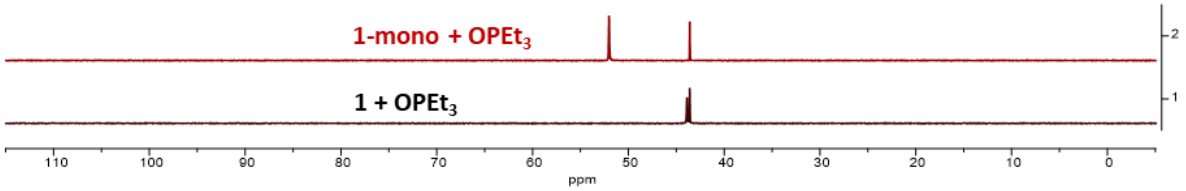

Figure S85. ^{31}P NMR spectrum of **1-mono** (top) and **1** (bottom) with 1 equiv. $OPEt_3$ for Lewis acid quantification using the Guttmann Beckett method.

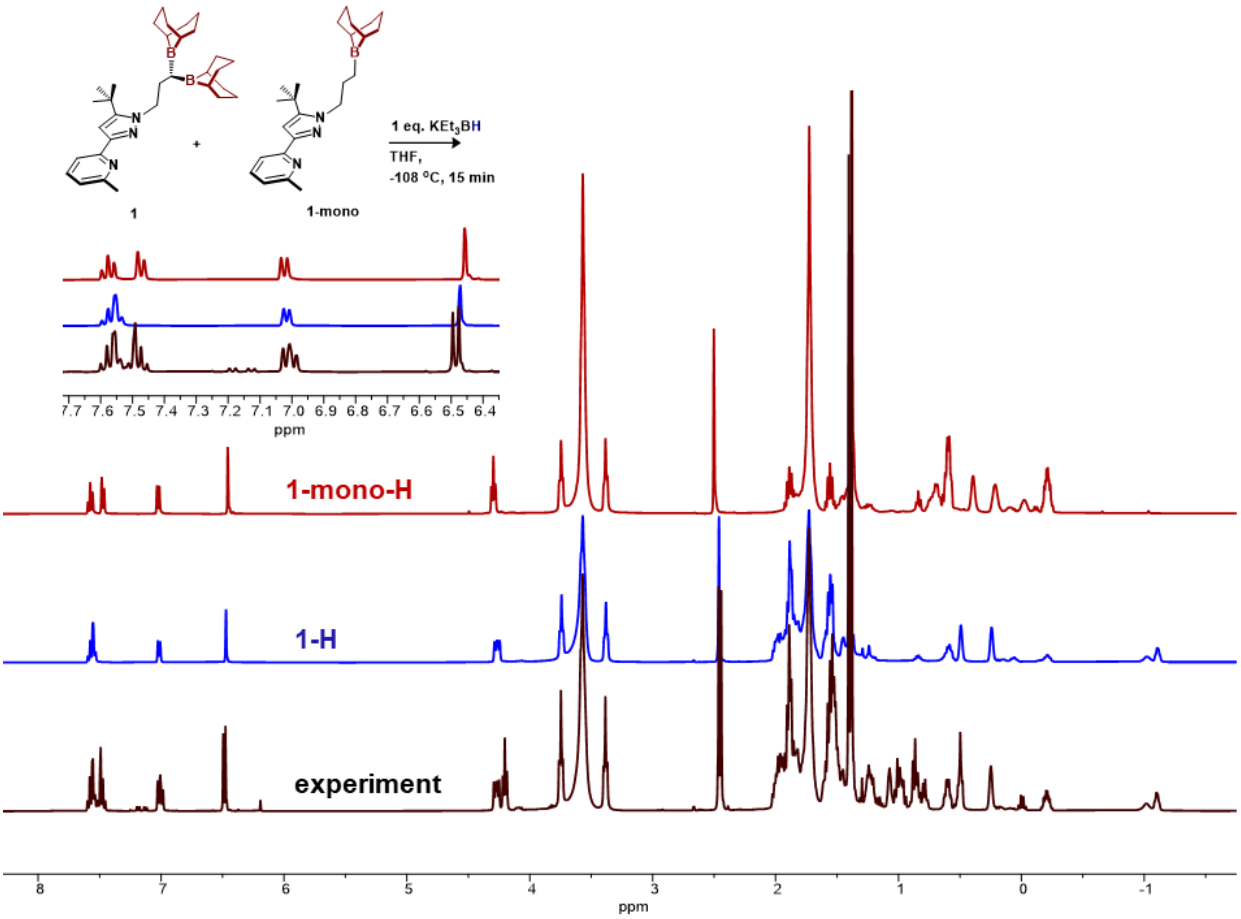

Figure S86. ^{1}H NMR spectrum of hydride competition experiment between **1** and **1-mono** (bottom), **1-H** (middle), and **1-mono-H** (top) showing selective conversion to **1-H** with unreacted **1-mono.** Inset shows aromatic region zoomed in. Small aromatic impurities were present in the starting materials used and do not affect hydride transfer experiment.

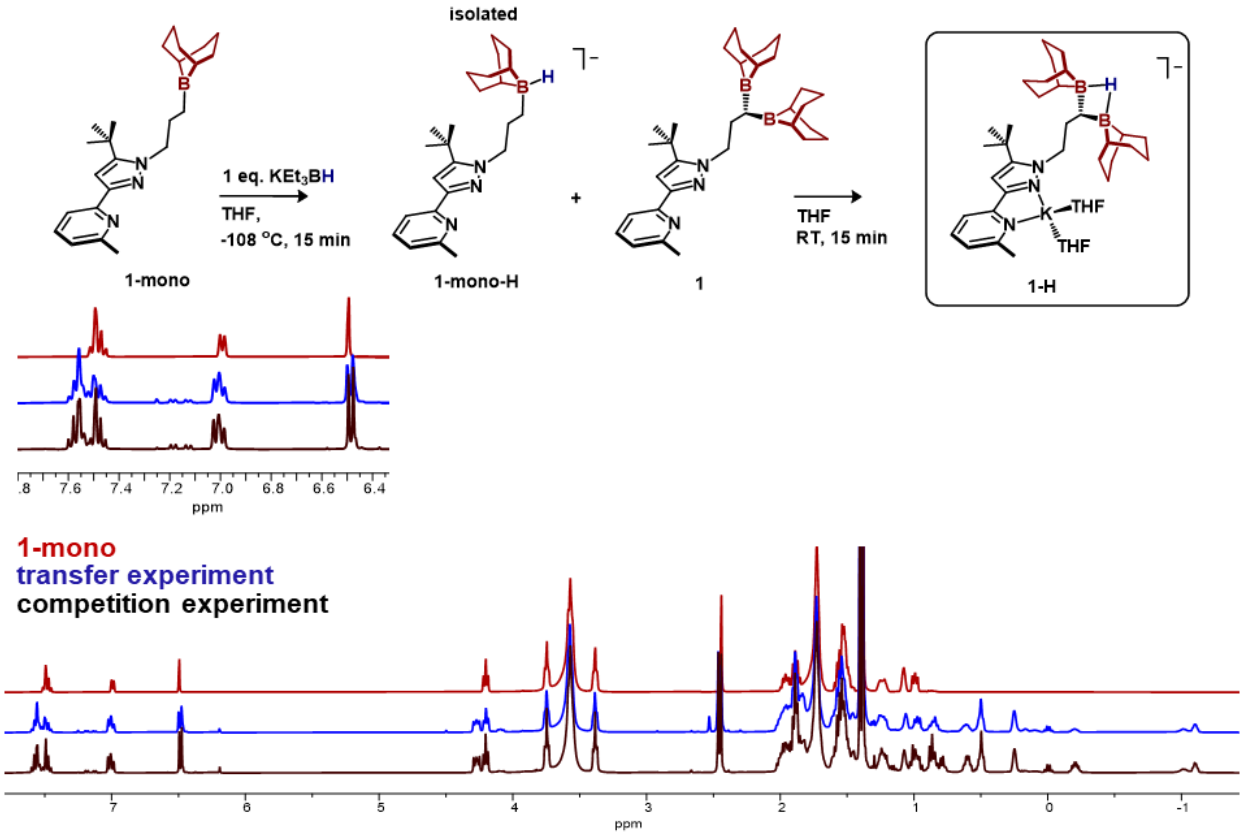

Figure S87. ^{1}H NMR spectrum of hydride competition experiment between **1** and **1-mono-H** (bottom), transfer experiment using **1-mono-H** (middle), and authentic **1-mono** (top) indicating only **1-mono** and **1-H** in solution. Inset shows aromatic region zoomed in. Small aromatic impurities were present in the starting materials used and do not affect hydride transfer experiment.

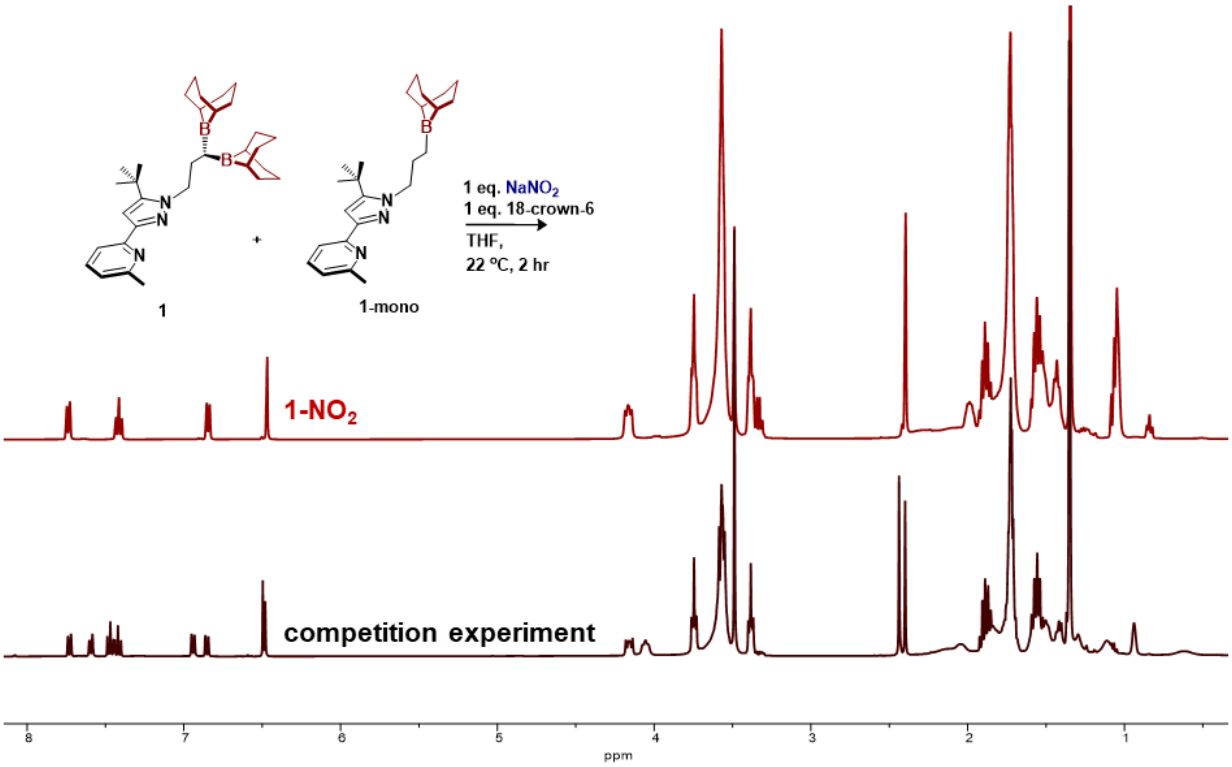

Figure S88. ^{1}H NMR spectrum of $NaNO_2$ competition experiment between **1** and **1-mono** (bottom) and authentic **1-NO_2** (top) showing selective conversion to **1-NO_2** with unreacted **1-mono**. Chemical shifts for **1-mono** are slightly shifted compared to authentic **1-mono**, likely due to an interaction of the 9-BBN boron with the uncoordinated nitrite oxygen in **1-NO_2**.

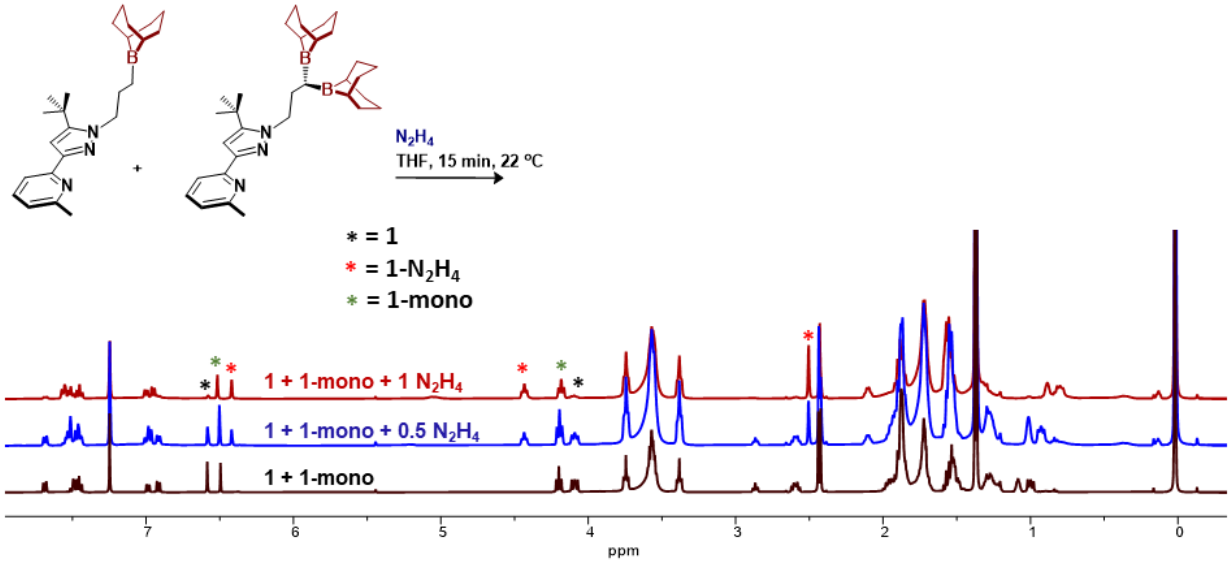

Figure S89. ^{1}H NMR spectrum of **1** + **1-mono** (bottom), **1** + **1-mono** + 0.5 equiv. N_2H_4 (middle) and **1** + **1-mono** + 1 equiv. N_2H_4 (top) showing selective conversion to **1-N_2H_4** with unreacted **1-mono**.

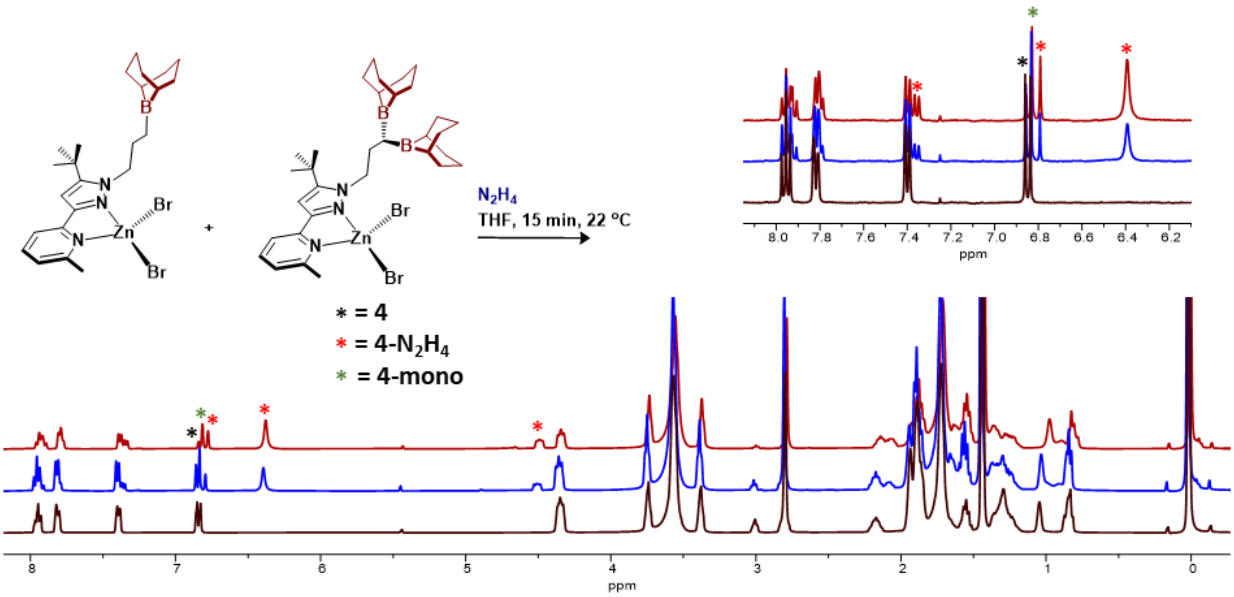

Figure S90. ^{1}H NMR spectrum of **4** + **4-mono** (bottom), **4** + **4-mono** + 0.5 equiv. N_2H_4 (middle) and **4** + **4-mono** + 1 equiv. N_2H_4 (top) showing selective conversion to **4-N_2H_4** with unreacted **4-mono**.

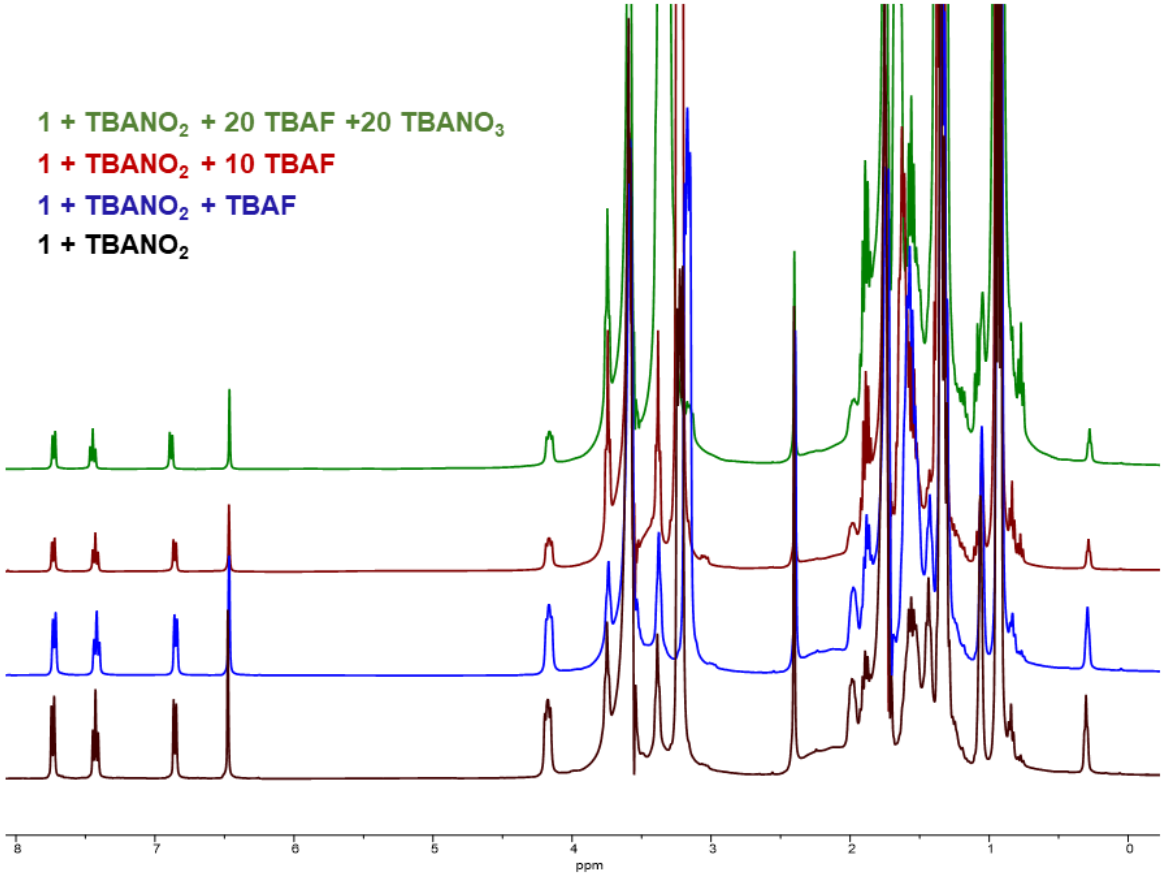

Figure S91. ^{1}H NMR spectrum of anion competition experiments. Bottom spectrum (black) is **1** + 1 equiv. $TBANO_2$, second from bottom (blue) is **1** + 1 equiv. $TBANO_2$ + 1 equiv. TBAF, third from bottom (red) is **1** + 1 equiv. $TBANO_2$ + 10 equiv. TBAF and top (green) is **1** + 1 equiv. $TBANO_2$ + 20 equiv. TBAF + 20 equiv. $TBANO_3$. Overlaid data shows each reaction forms the same selective product: **1-NO_2**, where the cation is NBu_4^+ instead of Na^+.

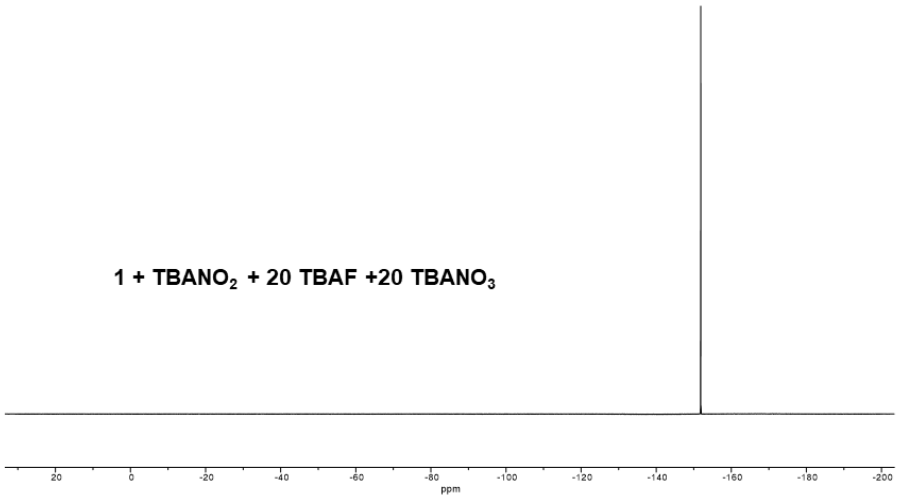

Figure S92. ^{19}F NMR spectrum of the reaction between **1**, $TBANO_2$, 20 equiv. TBAF and 20 equiv. $TBANO_3$ showing excess free fluoride in solution after formation of **1-NO$_2$**

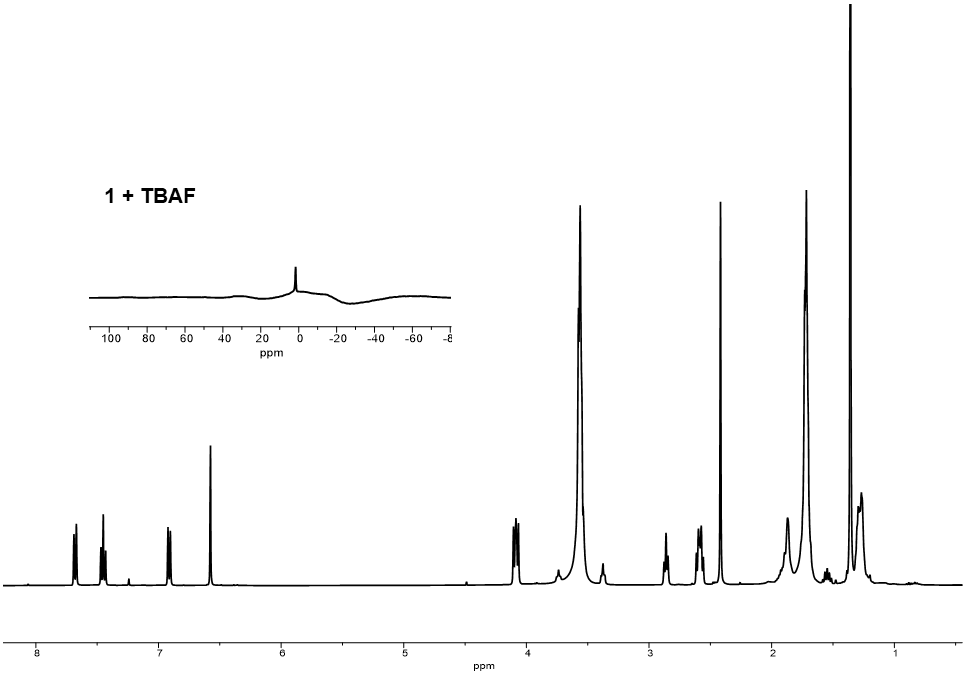

Figure S93. ^{1}H NMR spectrum of **1** + 1 equiv. TBAF showing clean conversion to a new species and ^{11}B NMR spectrum (inset) of the same reaction showing quenched boranes and no evidence for free ligand.

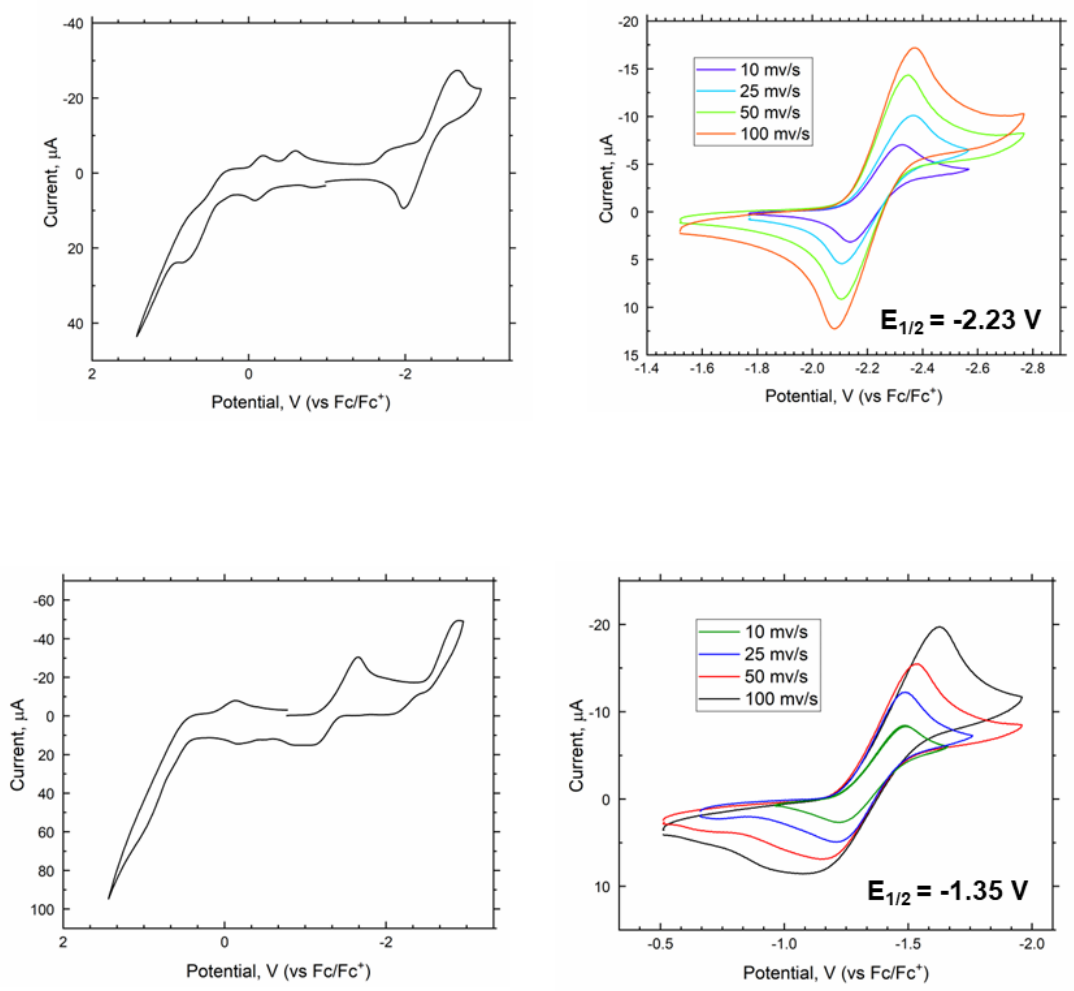

Figure S94. Cyclic voltammogram of **2-Br** (top left) and **3** (bottom left) and their respective isolated M(II/I) redox couples (**2-Br** = top right and **3** = bottom right) (vs. Fc/Fc+; 0.1M NBu_4PF_6 in THF)

Computational Details

DFT calculations were performed using the Gaussian 09 revD01 software package[10] using the B3LYP functional[11] and an ultrafine integration grid for all atoms. All reported compounds underwent geometry optimization with the 6-31G(d,p) basis set,[12] followed by vibrational frequency calculations. These were used to verify that the structures were truly local energetic minima by the absence of imaginary vibrational modes and to provide entropies of formation at 25 °C. Energies were determined by applying the free energy and enthalpy corrections from the frequency calculations to the scf energies from single point calculations of the optimized geometries using the higher-level 6-311G(d,p)[13] basis set for all atoms. For determination of Brønsted acidity, an acetonitrile solvation model was used with the same 6-311G(2d,p) basis set

for all atoms except Zn, which was treated with 6-311G(2d).[14] The calculated pKa values were calibrated to those of pyridine/pyridinium.[15]

To evaluate the extent to which functional choice changed thermodynamic values, we calculated ΔG values for hydride, fluoride, nitrite, and acetate addition to both **1** and **1-mono**. The optimized structures using B3LYP-D3BJ/6-31G(d,p) were used as the input geometries for single point calculations. We examined the single point energies using the functionals wb97xd, PBE1PBE, and bp86 all with the 6-311G(d,p) triple zeta basis set. Across all functionals, there is no significant change in the thermodynamic trends. The data is summarized below.

Table S1. Calculated energies (in hartrees) using various functionals for monotopic and ditopic ligands and their respective adducts with hydride, fluoride, acetate, and nitrite. NN represents ditopic ligand, while monoBBN represents monotopic ligand.

Species	wb97xd	PBE1PBE	bp86	B3LYP
F^-	-99.795527	-99.72261	-99.818075	-99.768247
monoBBN_F	-1225.268103	-1224.176231	-1225.593696	1225.005029
monoBBN_H	-1125.950587	-1124.923177	-1126.252616	1125.587483
monoBBN_NO2	-1330.511711	-1329.338888	-1330.896798	1330.252865
monoBBN_Oac	-1353.891244	-1352.68294	-1354.260956	1353.599052
monoBBN	-1125.300598	-1124.277907	-1125.598847	1125.041711
NN_F	-1562.814086	-1561.380274	-1563.185371	1562.420123
NN_H	-1463.523201	-1462.16513	-1463.881075	1463.022784
NN_NO2	-1668.075649	-1666.573719	-1668.520247	1667.693627
NN_OAc	-1691.456452	-1689.913982	-1691.877869	1691.043729
NN	-1462.848207	-1461.481641	-1463.189056	1462.467278
$NO2^-$	-205.11641	-204.967595	-205.207873	-205.11641
OAc^-	-228.496572	-228.316663	-228.580654	-228.496572

Table S2. Single point energies (in hartrees) used for the determination of pK_a values of hydrazine adducts on **1** and **1-mono**.

Species	Energy (SCF)
1-N2H4	-1575.198963
monoBBN_N2H3	-1237.075497
monoBBN_N2H4	-1237.577309
1_N2H3_2	-1574.711336
1_N2H3	-1574.709611
pyridine	-248.351805
pyridinium	-248.800979
monoBBN_N2H3_2	-1237.028834

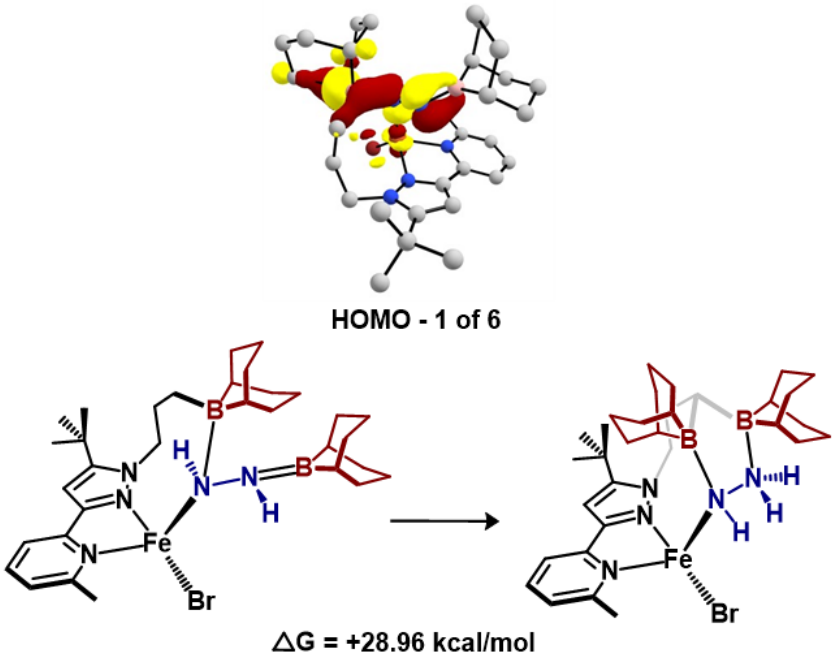

Figure S95. HOMO -1 of 6 showing B-N double bond and calculated DFT thermodynamics of isomerization from Fe-diazene to Fe-hydrazido indicating an endergonic process.

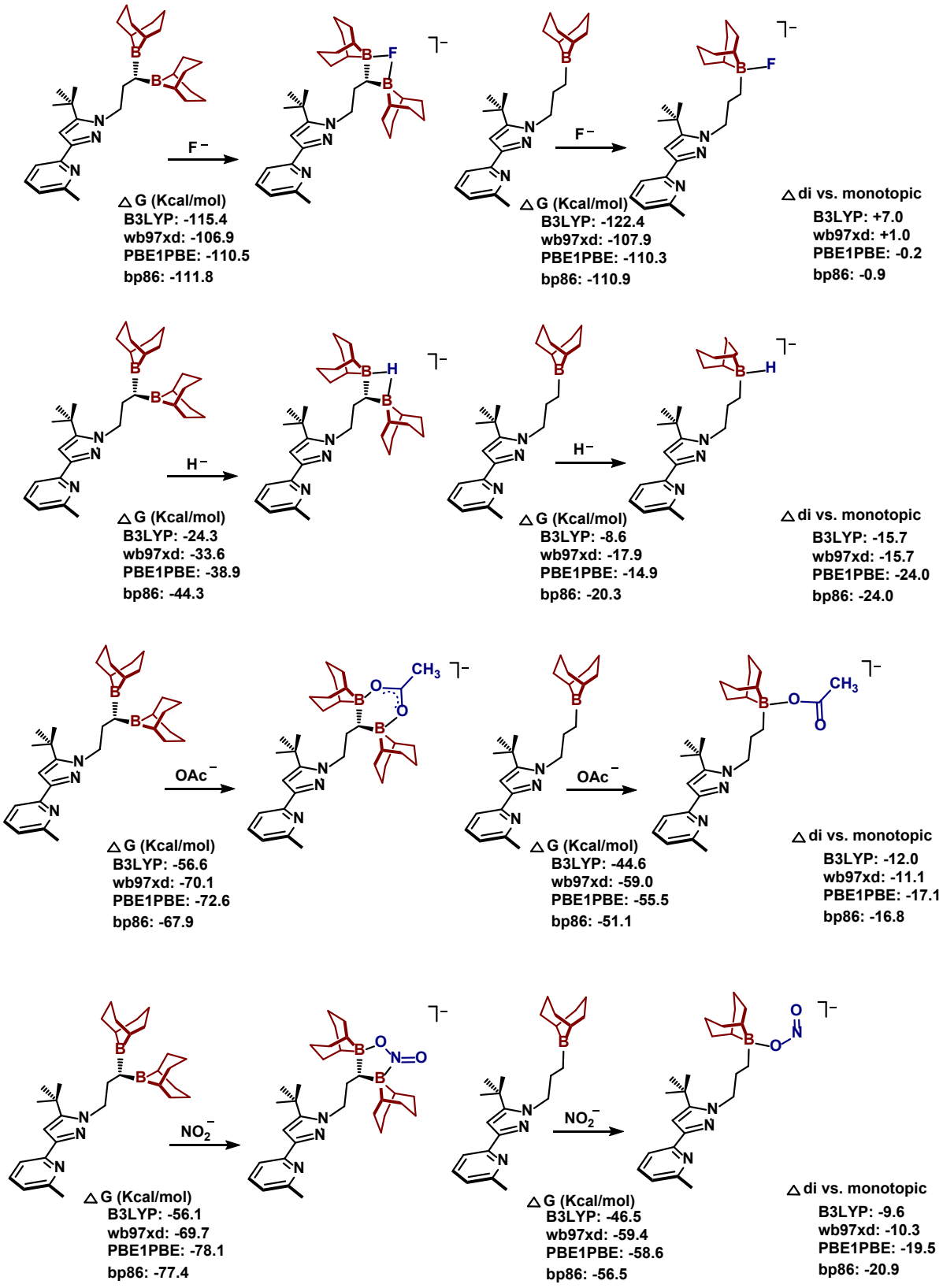

Figure S96. Reaction thermodynamics for hydride, fluoride, acetate, and nitrite capture by **1** and **1-mono** with varying functionals.

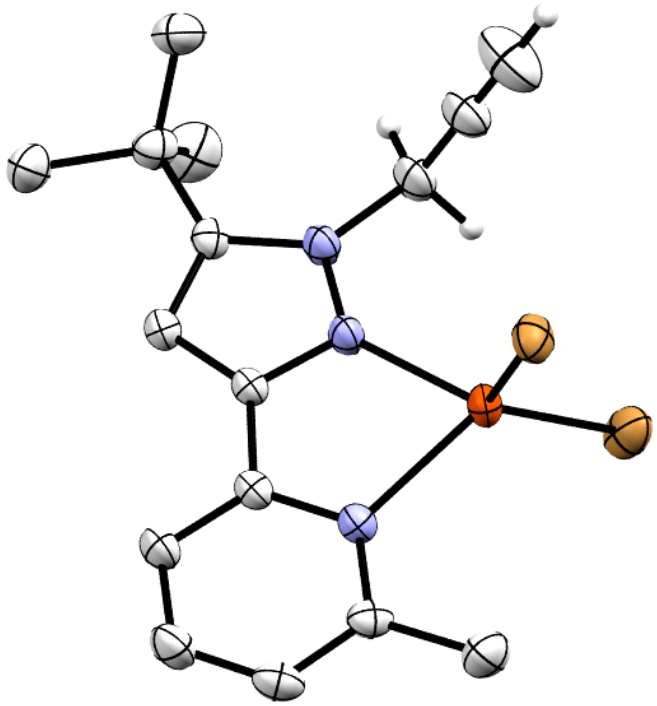

Figure S97. Molecular structure of ($^{(propargyl)}$NN^{tBu})FeBr$_2$ displayed with 50% probability ellipsoids. Hydrogen atoms not attached to propargyl group are omitted for clarity.

Complex: ($^{(propargyl)}$NN^{tBu})$FeBr_2$

Local name: JKE_32

CCDC: 2214460

Table S3. Crystallographic parameters for: ($^{(propargyl)}$NN^{tBu})$FeBr_2$.

Crystal data	
Chemical formula	$C_{16}H_{19}Br_2FeN_3$
M_r	469.01
Crystal system, space group	Monoclinic, $P2_1/c$
Temperature (K)	149
a, b, c (Å)	10.1248 (6), 11.3895 (7), 17.1674 (9)
β (°)	106.190 (2)
V (Å^3)	1901.18 (19)
Z	4
Radiation type	Mo $K\alpha$
μ (mm^{-1})	5.00
Crystal size (mm)	0.55 × 0.22 × 0.16
Data collection	
Diffractometer	Bruker AXS D8 Quest diffractometer with PhotonII charge-integrating pixel array detector (CPAD)
Absorption correction	Multi-scan *SADABS* 2016/2: Krause, L., Herbst-Irmer, R., Sheldrick G.M. & Stalke D., J. Appl. Cryst. 48 (2015) 3-10
T_{min}, T_{max}	0.415, 0.747
No. of measured, independent and observed [$I > 2\sigma(I)$] reflections	57794, 7268, 5311
R_{int}	0.054
$(\sin \theta/\lambda)_{max}$ (Å^{-1})	0.770
Refinement	
$R[F^2 > 2\sigma(F^2)]$, $wR(F^2)$, S	0.035, 0.090, 1.05
No. of reflections	7268
No. of parameters	203
H-atom treatment	H-atom parameters constrained
$\Delta\rho_{max}$, $\Delta\rho_{min}$ (e Å^{-3})	1.75, −1.44

Computer programs: Apex3 v2019.1-0 (Bruker, 2019), SAINT V8.40A (Bruker, 2019), SHELXS97 (Sheldrick, 2008), SHELXL2018/3 (Sheldrick, 2015, 2018), SHELXLE Rev1146 (Hübschle et al., 2011).

Refinement details:

One of the dangling side ligands was refined as disordered over two orientations by an approximate 2-fold rotation around the CH_2-CH_2 bond. The disorder extends to the entire side-ligand. The two disordered moieties were restrained to have similar geometries. The U^{ij} components of ADPs for disordered atoms closer to each other than 2.0 Angstrom were restrained to be similar. Subject to these conditions the occupancy ratio refined to 0.660(3) and 0.340(3).

A benzene solvate molecule is disordered around an inversion center. The disorder is partially correlated to the ligand disorder, but exactly 1:1. The benzene ring was constrained to resemble an ideal hexagon (AFIX 66). A rigid bond restraint (RIGU) was applied to its atoms.

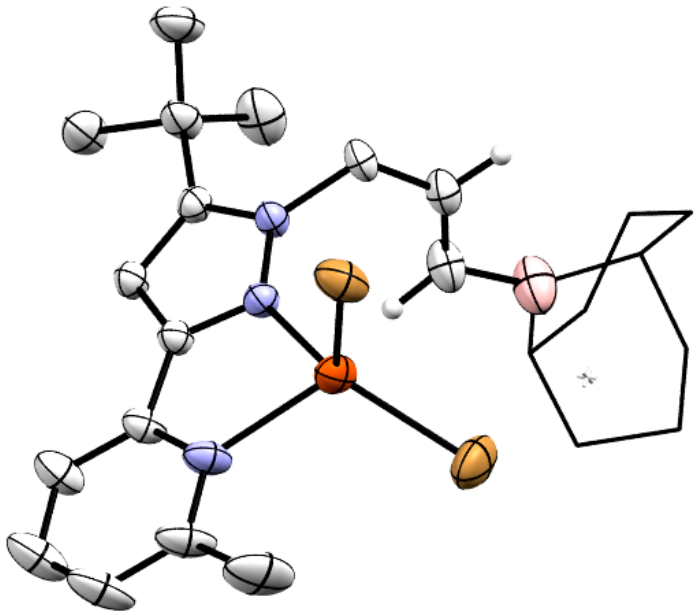

Figure S98. Molecular structure of ($^{(ene)}$NN$^{t\text{Bu}}$)$FeBr_2$ displayed with 50% probability ellipsoids. Hydrogen atoms not attached to alkene group are omitted for clarity. The 9-BBN substituent is displayed in wireframe for improved clarity.

Complex: ($^{(ene)}$NN$^{t\text{Bu}}$)FeBr$_2$

Local name: JKE_33

CCDC: 2214463

Table S4. Crystallographic parameters for: ($^{(ene)}$NN$^{t\text{Bu}}$)FeBr$_2$.

Crystal data	
Chemical formula	$C_{24}H_{34}BBr_2FeN_3 \cdot 1.5(C_6H_6)$
M_r	708.18
Crystal system, space group	Triclinic, *P*1
Temperature (K)	150
a, *b*, *c* (Å)	8.4908 (4), 14.6755 (7), 15.3739 (8)
α, β, γ (°)	115.9874 (19), 93.0230 (19), 97.5795 (17)
V (Å^3)	1693.77 (15)
Z	2
Radiation type	Mo *K*α
μ (mm^{-1})	2.83
Crystal size (mm)	0.33 × 0.30 × 0.17
Data collection	
Diffractometer	Bruker AXS D8 Quest diffractometer with PhotonII charge-integrating pixel array detector (CPAD)
Absorption correction	Multi-scan *SADABS* 2016/2: Krause, L., Herbst-Irmer, R., Sheldrick G.M. & Stalke D., J. Appl. Cryst. 48 (2015) 3-10
T_{min}, T_{max}	0.558, 0.747
No. of measured, independent and observed [$I > 2\sigma(I)$] reflections	62616, 12770, 7842
R_{int}	0.055
$(\sin \theta/\lambda)_{max}$ (Å^{-1})	0.771
Refinement	
$R[F^2 > 2\sigma(F^2)]$, $wR(F^2)$, S	0.043, 0.123, 1.01
No. of reflections	12770
No. of parameters	489
No. of restraints	438
H-atom treatment	H-atom parameters constrained
$\Delta\rho_{max}$, $\Delta\rho_{min}$ (e Å^{-3})	1.02, −0.96

Computer programs: Apex3 v2019.1-0 (Bruker, 2019), SAINT V8.40A (Bruker, 2019), SHELXS97 (Sheldrick, 2008), SHELXL2018/3 (Sheldrick, 2015, 2018), SHELXLE Rev1146 (Hübschle et al., 2011).

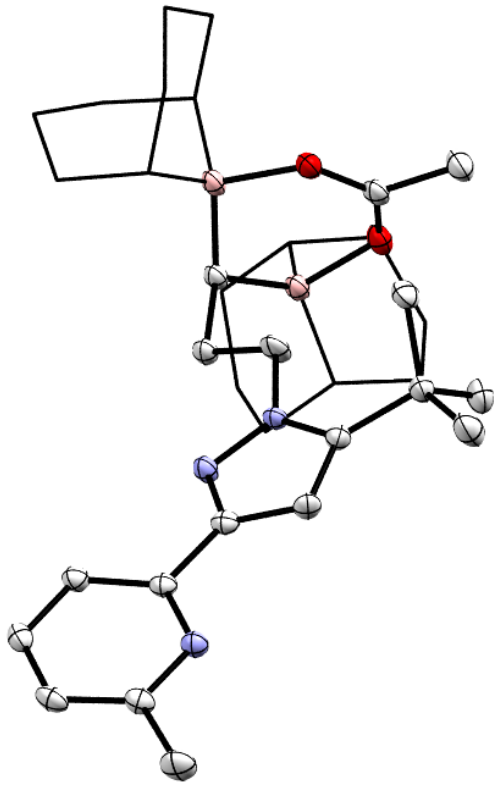

Figure S99. Molecular structure of [($^{(BBN)2}$NN^{tBu})(OAc)](K-18-crown-6) displayed with 50% probability ellipsoids. Hydrogen atoms, potassium counterion, and 18-crown-6 are omitted for clarity. The 9-BBN substituents are displayed in wireframe for improved clarity.

Complex: [($^{(BBN)2}$NN^{tBu})(OAc)](K-18-crown-6)

Local name: dmb_2_224

CCDC: 2214456

Table S5. Crystallographic parameters for: [($^{(BBN)2}$NN^{tBu})(OAc)](K-18-crown-6) 1-OAc.

Crystal data	
Chemical formula	$C_{20}H_{40}KO_8 \cdot C_{34}H_{52}B_2N_3O_2$
M_r	1004.02
Crystal system, space group	Triclinic, *P*1
Temperature (K)	85
a, *b*, *c* (Å)	10.4950 (2), 15.2279 (4), 19.6472 (3)
α, β, γ (°)	103.371 (2), 102.960 (2), 108.049 (2)
V (Å^3)	2751.92 (10)
Z	2
Radiation type	Cu *K*α
μ (mm^{-1})	1.31
Crystal size (mm)	0.17 × 0.16 × 0.06
Data collection	
Diffractometer	Dtrek-*CrysAlis PRO*-abstract goniometer imported rigaku-*D*TREK* images
Absorption correction	Multi-scan *CrysAlis PRO* 1.171.40.53 (Rigaku Oxford Diffraction, 2019) Empirical absorption correction using spherical harmonics, implemented in SCALE3 ABSPACK scaling algorithm.
T_{min}, T_{max}	0.852, 1.000
No. of measured, independent and observed [$I > 2\sigma(I)$] reflections	42374, 9960, 9488
R_{int}	0.046
$(\sin \theta/\lambda)_{max}$ (Å^{-1})	0.610
Refinement	
$R[F^2 > 2\sigma(F^2)]$, $wR(F^2)$, *S*	0.043, 0.117, 1.06
No. of reflections	9960
No. of parameters	825
No. of restraints	1003
H-atom treatment	H-atom parameters constrained
$\Delta\rho_{max}$, $\Delta\rho_{min}$ (e Å^{-3})	0.32, −0.41

Computer programs: CrysAlis PRO 1.171.42.61a (Rigaku OD, 2022), CrysAlis PRO 1.171.42.61a (Rigaku OD, 2022), SHELXT 2018/2 (Sheldrick, 2018), SHELXL2018/3 (Sheldrick, 2018).

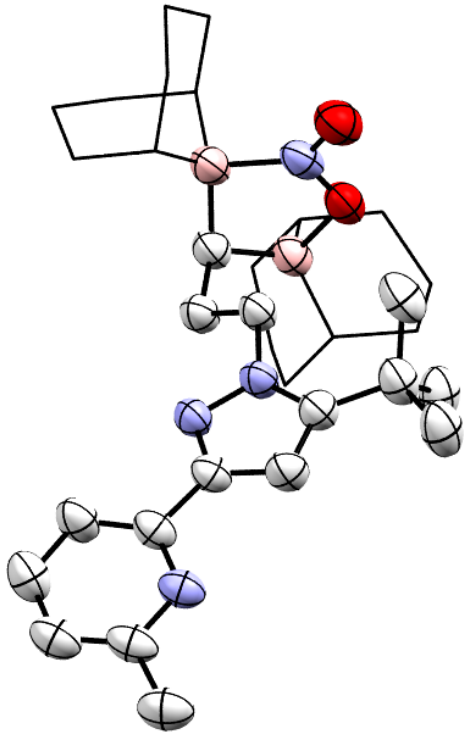

Figure S100. Molecular structure of [($^{(BBN)2}$NN^{tBu})(NO_2)](Na-18-crown-6) displayed with 50% probability ellipsoids. Hydrogen atoms, sodium counterion, and 18-crown-6 are omitted for clarity. The 9-BBN substituents are displayed in wireframe for improved clarity.

Complex: [($^{(BBN)2}$NN^{tBu})(NO_2)](Na-18-crown-6)

Local name: dmb_2_222

CCDC: 2214455

Table S6. Crystallographic parameters for: [($^{(BBN)2}$NN^{tBu})(NO_2)](Na-18-crown-6) 1-NO_2.

Crystal data	
Chemical formula	$C_{54}H_{93}B_2N_4NaO_{10.50}$
M_r	1010.93
Crystal system, space group	Monoclinic, $P2_1/n$
Temperature (K)	85
a, b, c (Å)	16.0543 (2), 12.3968 (2), 28.5954 (6)
β (°)	103.591 (2)
V (Å^3)	5531.74 (18)
Z	4
Radiation type	Cu $K\alpha$
μ (mm^{-1})	0.73
Crystal size (mm)	0.12 × 0.12 × 0.04
Data collection	
Diffractometer	Dtrek-*CrysAlis PRO*-abstract goniometer imported rigaku-*D*TREK* images
Absorption correction	Multi-scan *CrysAlis PRO* 1.171.40.53 (Rigaku Oxford Diffraction, 2019) Empirical absorption correction using spherical harmonics, implemented in SCALE3 ABSPACK scaling algorithm.
T_{min}, T_{max}	0.678, 1.000
No. of measured, independent and observed [$I > 2\sigma(I)$] reflections	84631, 10282, 7317
R_{int}	0.088
$(\sin \theta/\lambda)_{max}$ (Å^{-1})	0.608
Refinement	
$R[F^2 > 2\sigma(F^2)]$, $wR(F^2)$, S	0.062, 0.196, 1.03
No. of reflections	10282
No. of parameters	955
No. of restraints	804
H-atom treatment	H-atom parameters constrained
$\Delta\rho_{max}$, $\Delta\rho_{min}$ (e Å^{-3})	0.29, −0.31

Computer programs: CrysAlis PRO 1.171.42.61a (Rigaku OD, 2022), CrysAlis PRO 1.171.42.61a (Rigaku OD, 2022), SHELXT 2018/2 (Sheldrick, 2018), SHELXL2018/3 (Sheldrick, 2018).

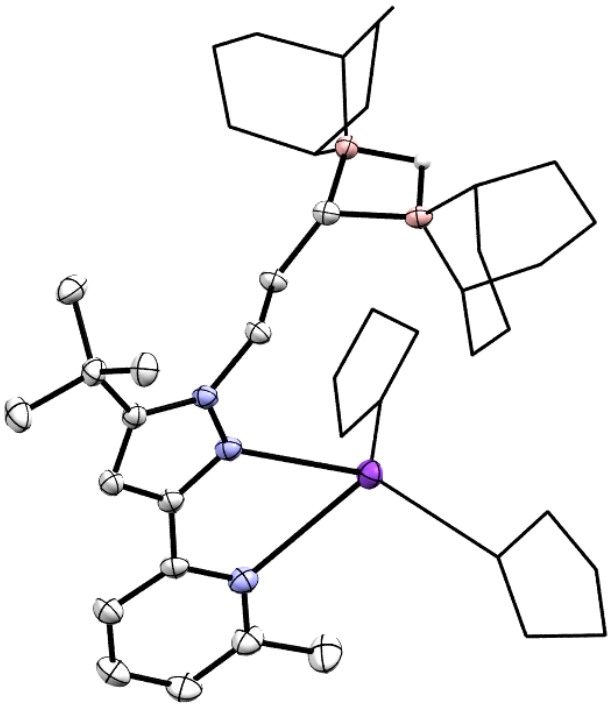

Figure S101. Molecular structure of [($^{(BBN)2}$NN^{tBu})(H)]K displayed with 50% probability ellipsoids. Hydrogen atoms not coordinate to boranes are omitted for clarity. The 9-BBN substituents and THF molecules coordinated to potassium are displayed in wireframe for improved clarity.

Complex: [($^{(BBN)2}$NN^{tBu})H]K

Local name: dmb_2_84

CCDC: 2214454

Table S7. Crystallographic parameters for: [($^{(BBN)2}$NN^{tBu})H]K 1-H.

Crystal data	
Chemical formula	$C_{40}H_{66}B_2KN_3O_2$
M_r	681.67
Crystal system, space group	Triclinic, *P*1
Temperature (K)	85
a, *b*, *c* (Å)	10.1073 (2), 11.5307 (3), 19.0899 (3)
α, β, γ (°)	74.937 (2), 81.981 (2), 66.504 (2)
V (Å^3)	1968.63 (7)
Z	2
Radiation type	Cu *K*α
μ (mm^{-1})	1.45
Crystal size (mm)	0.18 × 0.11 × 0.07
Data collection	
Diffractometer	Dtrek-*CrysAlis PRO*-abstract goniometer imported rigaku-*D*TREK* images
Absorption correction	Multi-scan *CrysAlis PRO* 1.171.42.61a (Rigaku Oxford Diffraction, 2022) Empirical absorption correction using spherical harmonics, implemented in SCALE3 ABSPACK scaling algorithm.
T_{min}, T_{max}	0.864, 1.000
No. of measured, independent and observed [$I > 2\sigma(I)$] reflections	30067, 7114, 6792
R_{int}	0.036
$(\sin \theta/\lambda)_{max}$ (Å^{-1})	0.609
Refinement	
$R[F^2 > 2\sigma(F^2)]$, $wR(F^2)$, *S*	0.040, 0.104, 1.07
No. of reflections	7114
No. of parameters	494
No. of restraints	180
H-atom treatment	H atoms treated by a mixture of independent and constrained refinement
$\Delta\rho_{max}$, $\Delta\rho_{min}$ (e Å^{-3})	0.28, −0.26

Computer programs: CrysAlis PRO 1.171.42.61a (Rigaku OD, 2022), CrysAlis PRO 1.171.42.61a (Rigaku OD, 2022), SHELXT 2018/2 (Sheldrick, 2018), SHELXL2018/3 (Sheldrick, 2018).

Refinement details:

The chloride atoms were modelled as disordered with bromide atoms (79% Cl and 21 % Br).

A THF molecule was refined as disordered. U^{ij} components of ADPs for disordered atoms closer to each other than 2.0 Angstrom were restrained to be similar.

A second THF molecule was refined as disordered with a pentane molecule. U^{ij} components of ADPs for disordered atoms closer to each other than 2.0 Angstrom were restrained to be similar.

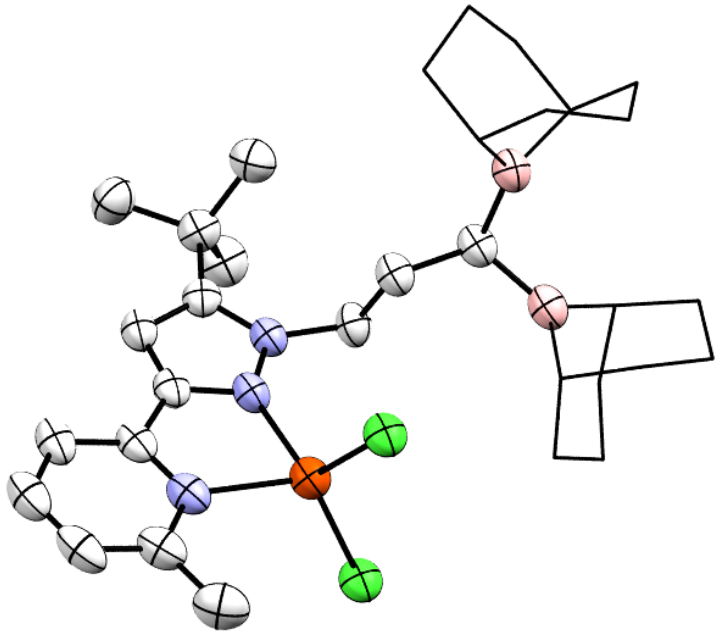

Figure S102. Molecular structure of ($^{(BBN)2}NN^{tBu}$)$FeCl_2$ displayed with 50% probability ellipsoids. Hydrogen atoms are omitted for clarity. The 9-BBN substituents are displayed in wireframe for improved clarity.

Complex: ($^{(BBN)2}NN^{tBu}$)$FeCl_2$

Local name: dmb_1_91

CCDC: 2214449

Table S8. Crystallographic parameters for: ($^{(BBN)2}NN^{tBu}$)$FeCl_2$ 2-Cl.

Crystal data	
Chemical formula	$C_{40}H_{63}B_2Br_{0.25}Cl_2FeN_3O_2$
M_r	786.28
Crystal system, space group	Monoclinic, $P2_1/n$
Temperature (K)	293
a, b, c (Å)	12.6903 (5), 12.6641 (4), 26.5743 (12)
β (°)	100.109 (4)
V (Å^3)	4204.5 (3)
Z	4
Radiation type	Cu $K\alpha$
μ (mm^{-1})	4.59
Crystal size (mm)	0.11 × 0.06 × 0.01
Data collection	
Diffractometer	Dtrek-*CrysAlis PRO*-abstract goniometer imported rigaku-*D*TREK* images
Absorption correction	Multi-scan *CrysAlis PRO* 1.171.40.53 (Rigaku Oxford Diffraction, 2019) Empirical absorption correction using spherical harmonics, implemented in SCALE3 ABSPACK scaling algorithm.
T_{min}, T_{max}	0.612, 1.000
No. of measured, independent and observed [$I > 2\sigma(I)$] reflections	60870, 7874, 5263
R_{int}	0.117
$(\sin \theta/\lambda)_{max}$ (Å^{-1})	0.609
Refinement	
$R[F^2 > 2\sigma(F^2)]$, $wR(F^2)$, S	0.069, 0.192, 1.04
No. of reflections	7874
No. of parameters	551
No. of restraints	356
H-atom treatment	H-atom parameters constrained
$\Delta\rho_{max}$, $\Delta\rho_{min}$ (e Å^{-3})	0.62, −0.49

Computer programs: CrysAlis PRO 1.171.40.53 (Rigaku OD, 2019), CrysAlis PRO 1.171.40.53 (Rigaku OD, 2019), SHELXT 2018/2 (Sheldrick, 2018), SHELXL2018/3 (Sheldrick, 2018).

Refinement details:

One methylene group is disordered over two positions. The disorder was extended to the two neighboring methylene groups. The two disordered moieties were restrained to have similar geometries as another not disordered THF molecule. The U^{ij} components of ADPs for disordered atoms closer to each other than 2.0 Angstrom were restrained to be similar. Subject to these conditions the occupancy ratio refined to 0.878(5) and 0.122(8).

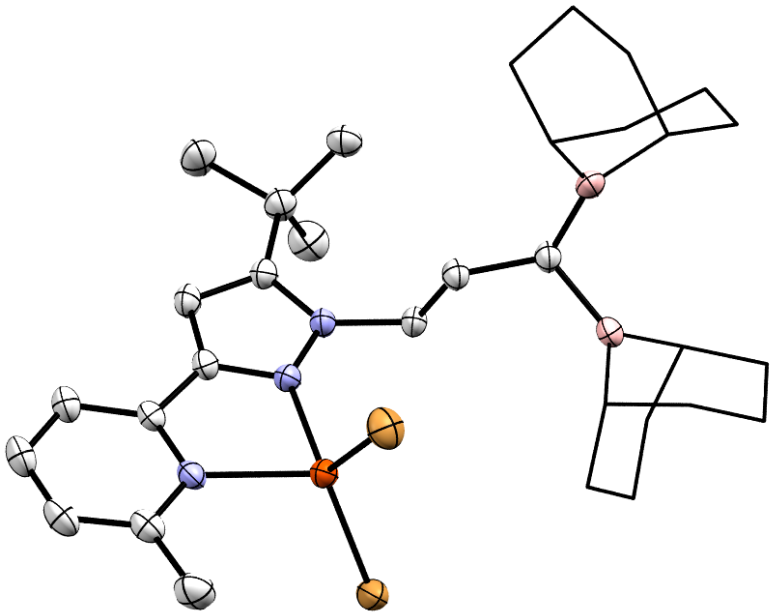

Figure S103. Molecular structure of ($^{(BBN)2}$NN^{tBu})$FeBr_2$ displayed with 50% probability ellipsoids. Hydrogen atoms are omitted for clarity. The 9-BBN substituents are displayed in wireframe for improved clarity.

Complex: $(^{(BBN)2}NN^{tBu})FeBr_2$

Local name: JK_E38

CCDC: 2214461

Table S9. Crystallographic parameters for: $(^{(BBN)2}NN^{tBu})FeBr_2$ 2-Br.

Crystal data	
Chemical formula	$C_{32}H_{49}B_2Br_2FeN_3 \cdot C_4H_8O$
M_r	785.13
Crystal system, space group	Monoclinic, $P2_1/n$
Temperature (K)	150
a, b, c (Å)	17.0839 (10), 12.4720 (8), 18.1445 (11)
β (°)	105.354 (2)
V (Å^3)	3728.1 (4)
Z	4
Radiation type	Cu $K\alpha$
μ (mm^{-1})	5.99
Crystal size (mm)	0.31 × 0.21 × 0.09
Data collection	
Diffractometer	Bruker AXS D8 Quest diffractometer with PhotonIII_C14 charge-integrating and photon counting pixel array detector
Absorption correction	Multi-scan *SADABS* 2016/2: Krause, L., Herbst-Irmer, R., Sheldrick G.M. & Stalke D., J. Appl. Cryst. 48 (2015) 3-10
T_{min}, T_{max}	0.532, 0.754
No. of measured, independent and observed [$I > 2\sigma(I)$] reflections	68866, 7991, 7444
R_{int}	0.038
$(\sin \theta/\lambda)_{max}$ (Å^{-1})	0.639
Refinement	
$R[F^2 > 2\sigma(F^2)]$, $wR(F^2)$, S	0.028, 0.070, 1.08
No. of reflections	7991
No. of parameters	439
No. of restraints	72
H-atom treatment	H-atom parameters constrained
$\Delta\rho_{max}$, $\Delta\rho_{min}$ (e Å^{-3})	0.34, −0.50

Computer programs: Apex3 v2019.1-0 (Bruker, 2019), *SAINT* V8.40A (Bruker, 2019), *SHELXS97* (Sheldrick, 2008), *SHELXL2018*/3 (Sheldrick, 2015, 2018), SHELXLE Rev1172 (Hübschle *et al.*, 2011).

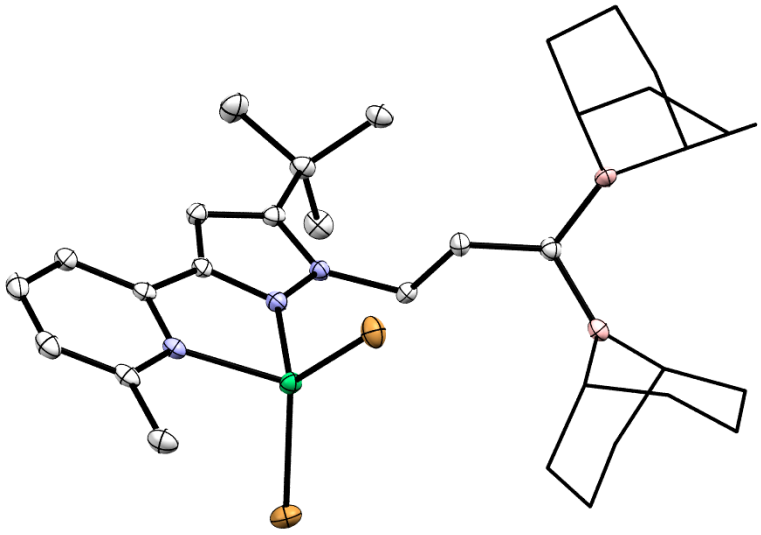

Figure S104. Molecular structure of ($^{(BBN)2}$NN^{tBu})NiBr$_2$ displayed with 50% probability ellipsoids. Hydrogen atoms are omitted for clarity. The 9-BBN substituents are displayed in wireframe for improved clarity.

Complex: ($^{(BBN)2}NN^{tBu}$)$NiBr_2$

Local name: dmb_1_008

CCDC: 2214450

Table S10. Crystallographic parameters for: ($^{(BBN)2}NN^{tBu}$)$NiBr_2$ 3.

Crystal data	
Chemical formula	$C_{36}H_{57}B_2Br_2N_3NiO$
M_r	787.99
Crystal system, space group	Monoclinic, $P2_1/n$
Temperature (K)	85
a, b, c (Å)	16.98046 (9), 12.46623 (7), 17.99373 (11)
β (°)	105.4470 (6)
V (Å^3)	3671.37 (4)
Z	4
Radiation type	Cu $K\alpha$
μ (mm^{-1})	3.55
Crystal size (mm)	0.16 × 0.07 × 0.03
Data collection	
Diffractometer	Dtrek-*CrysAlis PRO*-abstract goniometer imported rigaku-*D*TREK* images
Absorption correction	Multi-scan *CrysAlis PRO* 1.171.40.53 (Rigaku Oxford Diffraction, 2019) Empirical absorption correction using spherical harmonics, implemented in SCALE3 ABSPACK scaling algorithm.
T_{min}, T_{max}	0.505, 1.000
No. of measured, independent and observed [$I > 2\sigma(I)$] reflections	55032, 6793, 6655
R_{int}	0.052
$(\sin \theta/\lambda)_{max}$ (Å^{-1})	0.607
Refinement	
$R[F^2 > 2\sigma(F^2)]$, $wR(F^2)$, S	0.027, 0.070, 1.05
No. of reflections	6793
No. of parameters	410
H-atom treatment	H-atom parameters constrained
$\Delta\rho_{max}$, $\Delta\rho_{min}$ (e Å^{-3})	0.41, −0.46

Computer programs: CrysAlis PRO 1.171.40.53 (Rigaku OD, 2019), CrysAlis PRO 1.171.40.53 (Rigaku OD, 2019), SHELXT (G. Sheldrick), SHELXL2018/3 (Sheldrick, 2018).

Refinement details:

A THF molecule was refined as disordered. U^{ij} components of ADPs for disordered atoms closer to each other than 2.0 Angstrom were restrained to be similar.

A second THF molecule was refined as disordered with a pentane molecule. U^{ij} components of ADPs for disordered atoms closer to each other than 2.0 Angstrom were restrained to be similar.

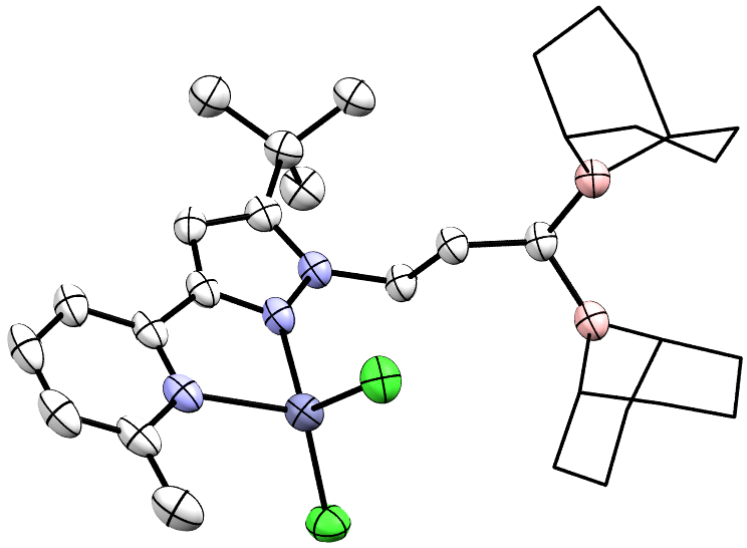

Figure S105. Molecular structure of $(^{(BBN)2}NN^{tBu})ZnCl_2$ displayed with 50% probability ellipsoids. Hydrogen atoms are omitted for clarity. The 9-BBN substituents are displayed in wireframe for improved clarity.

Complex: ($^{(BBN)2}NN^{tBu}$)$ZnCl_2$

Local name: dmb_1_68

CCDC: 2214452

Table S11. Crystallographic parameters for: ($^{(BBN)2}NN^{tBu}$)$ZnCl_2$ 4.

Crystal data	
Chemical formula	$C_{32}H_{49}B_2Cl_2N_3Zn \cdot 1.768(C_4H_8O) \cdot 0.232(C_5H_{12})$
M_r	777.85
Crystal system, space group	Monoclinic, $P2_1/n$
Temperature (K)	85
a, b, c (Å)	12.6463 (3), 12.6508 (2), 26.5526 (6)
β (°)	100.441 (2)
V (Å^3)	4177.74 (14)
Z	4
Radiation type	Cu $K\alpha$
μ (mm^{-1})	2.26
Crystal size (mm)	0.07 × 0.06 × 0.02
Data collection	
Diffractometer	Dtrek-*CrysAlis PRO*-abstract goniometer imported rigaku-*D*TREK* images
Absorption correction	Multi-scan *CrysAlis PRO* 1.171.40.53 (Rigaku Oxford Diffraction, 2019) Empirical absorption correction using spherical harmonics, implemented in SCALE3 ABSPACK scaling algorithm.
T_{min}, T_{max}	0.643, 1.000
No. of measured, independent and observed [$I > 2\sigma(I)$] reflections	62044, 7686, 6470
R_{int}	0.066
$(\sin \theta/\lambda)_{max}$ (Å^{-1})	0.608
Refinement	
$R[F^2 > 2\sigma(F^2)]$, $wR(F^2)$, S	0.053, 0.152, 1.08
No. of reflections	7686
No. of parameters	549
No. of restraints	328
H-atom treatment	H-atom parameters constrained
$\Delta\rho_{max}$, $\Delta\rho_{min}$ (e Å^{-3})	0.46, −0.83

Computer programs: CrysAlis PRO 1.171.40.53 (Rigaku OD, 2019), CrysAlis PRO 1.171.40.53 (Rigaku OD, 2019), SHELXT 2018/2 (Sheldrick, 2018), SHELXL2018/3 (Sheldrick, 2018).

Refinement details:

A THF molecule was refined as disordered. The two disordered moieties were restrained to have similar geometries as another not disordered THF molecule. U^{ij} components of ADPs for disordered atoms closer to each other than 2.0 Angstrom were restrained to be similar. Subject to these conditions the occupancy ratio refined to 0.564(9) and 0.436(9).

A pentane molecule was refinded as 1:1 disordered across an inversion center. Atom positions were freely refined. U^{ij} components of ADPs for disordered atoms closer to each other than 2.0 Angstrom were restrained to be similar.

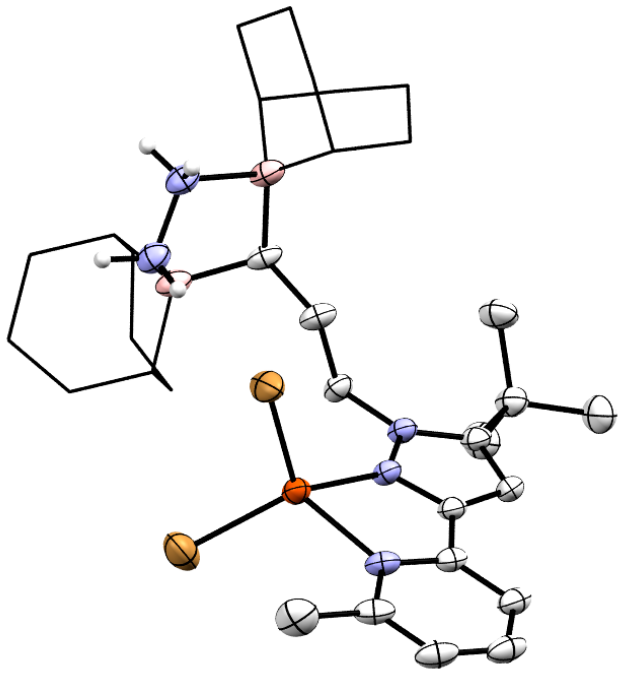

Figure S106. Molecular structure of ($^{(BBN)2}$NN^{tBu})FeBr$_2$(N$_2$H$_4$) displayed with 50% probability ellipsoids. Hydrogen atoms not attached to hydrazine unit are omitted for clarity. The 9-BBN substituents are displayed in wireframe for improved clarity.

Complex: $(^{(BBN)2}NN^{tBu})FeBr_2(N_2H_4)$

Local name: JK_E_080

CCDC: 2214463

Table S12. Crystallographic parameters for : $(^{(BBN)2}NN^{tBu})FeBr_2(N_2H_4)$ 2-N_2H_4

Crystal data	
Chemical formula	$2(C_{32}H_{53}B_2Br_2FeN_5)\cdot 6(C_4H_8O)\cdot C_5H_{12}$
M_r	1994.93
Crystal system, space group	Triclinic, *P*1
Temperature (K)	150
a, *b*, *c* (Å)	11.4942 (6), 11.5768 (6), 19.3917 (10)
α, β, γ (°)	95.397 (3), 96.278 (3), 91.068 (3)
V (Å^3)	2552.4 (2)
Z	1
Radiation type	Mo *K*α
μ (mm^{-1})	1.90
Crystal size (mm)	0.41 × 0.35 × 0.28
Data collection	
Diffractometer	Bruker AXS D8 Quest diffractometer with PhotonII charge-integrating pixel array detector (CPAD)
Absorption correction	Multi-scan *SADABS* 2016/2: Krause, L., Herbst-Irmer, R., Sheldrick G.M. & Stalke D., J. Appl. Cryst. 48 (2015) 3-10
T_{min}, T_{max}	0.599, 0.747
No. of measured, independent and observed [$I > 2\sigma(I)$] reflections	78595, 19504, 13477
R_{int}	0.051
$(\sin\theta/\lambda)_{max}$ (Å^{-1})	0.771
Refinement	
$R[F^2 > 2\sigma(F^2)]$, $wR(F^2)$, *S*	0.036, 0.089, 1.01
No. of reflections	19504
No. of parameters	623
No. of restraints	204
H-atom treatment	H atoms treated by a mixture of independent and constrained refinement
$\Delta\rho_{max}$, $\Delta\rho_{min}$ (e Å^{-3})	1.18, −0.64

Computer programs: Apex3 v2019.11-0 (Bruker, 2020), SAINT V8.40B (Bruker, 2020), SHELXT (Sheldrick, 2015), SHELXL2018/3 (Sheldrick, 2015, 2018), SHELXLE Rev1231(Hübschle et al., 2011).

Refinement details:

A THF molecule was refined as disordered. The two disordered moieties were restrained to have similar geometries as another not disordered THF molecule. U^{ij} components of ADPs for disordered atoms closer to each other than 2.0 Angstrom were restrained to be similar. Subject to these conditions the occupancy ratio refined to 0.583(8) and 0.425(4).

A pentane molecule was refinded as 1:1 disordered across an inversion center. Atom positions were freely refined. U^{ij} components of ADPs for disordered atoms closer to each other than 2.0 Angstrom were restrained to be similar.

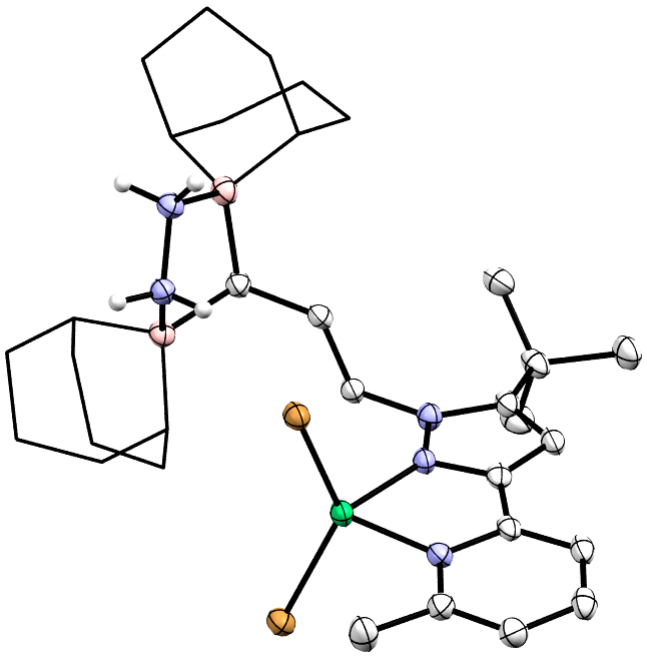

Figure S107. Molecular structure of ($^{(BBN)2}NN^{tBu}$)$NiBr_2(N_2H_4)$ displayed with 50% probability ellipsoids. Hydrogen atoms not attached to hydrazine unit are omitted for clarity. The 9-BBN substituents are displayed in wireframe for improved clarity.

Complex: ($^{(BBN)2}NN^{tBu}$)$NiBr_2(N_2H_4)$

Local name: dmb_1_017

CCDC: 2214451

Table S13. Crystallographic parameters for : ($^{(BBN)2}NN^{tBu}$)$NiBr_2(N_2H_4)$ 3-N_2H_4

Crystal data	
Chemical formula	$2(C_{32}H_{53}B_2Br_2N_5Ni)\cdot 6(C_4H_8O)\cdot C_5H_{12}$
M_r	1000.32
Crystal system, space group	Triclinic, *P*1
Temperature (K)	293
a, *b*, *c* (Å)	11.4884 (3), 11.5073 (3), 19.1225 (4)
α, β, γ (°)	95.093 (2), 96.331 (2), 91.211 (2)
V (Å^3)	2501.45 (12)
Z	2
Radiation type	Cu *K*α
μ (mm^{-1})	2.76
Crystal size (mm)	0.14 × 0.10 × 0.06
Data collection	
Diffractometer	Dtrek-*CrysAlis PRO*-abstract goniometer imported rigaku-*D*TREK* images
Absorption correction	Multi-scan *CrysAlis PRO* 1.171.40.53 (Rigaku Oxford Diffraction, 2019) Empirical absorption correction using spherical harmonics, implemented in SCALE3 ABSPACK scaling algorithm.
T_{min}, T_{max}	0.385, 1.000
No. of measured, independent and observed [$I > 2\sigma(I)$] reflections	35826, 9019, 8519
R_{int}	0.066
$(\sin\theta/\lambda)_{max}$ (Å^{-1})	0.607
Refinement	
$R[F^2 > 2\sigma(F^2)]$, $wR(F^2)$, *S*	0.062, 0.177, 1.07
No. of reflections	9019
No. of parameters	611
No. of restraints	182
H-atom treatment	H-atom parameters constrained
$\Delta\rho_{max}$, $\Delta\rho_{min}$ (e Å^{-3})	1.33, −1.56

Computer programs: CrysAlis PRO 1.171.40.53 (Rigaku OD, 2019), CrysAlis PRO 1.171.40.53 (Rigaku OD, 2019), SHELXT 2018/2 (Sheldrick, 2018), SHELXL2018/3 (Sheldrick, 2018).

Refinement details:

3 THF molecules were refined as disordered. U^{ij} components of ADPs for disordered atoms closer to each other than 2.0 Angstrom were restrained to be similar.

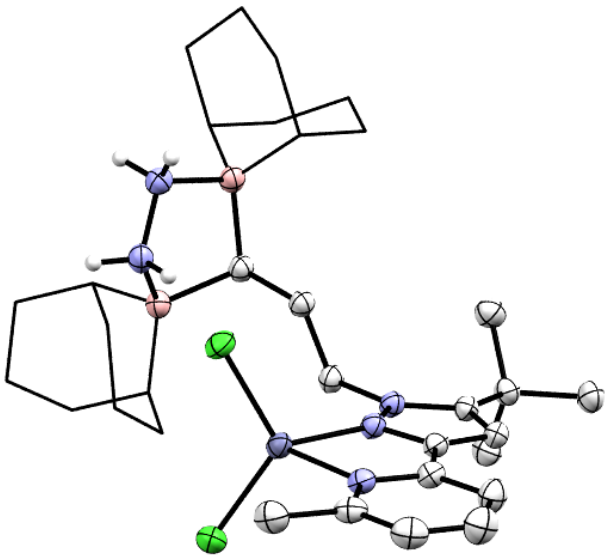

Figure S108. Molecular structure of $(^{(BBN)2}NN^{tBu})ZnCl_2(N_2H_4)$ displayed with 50% probability ellipsoids. Hydrogen atoms not attached to hydrazine unit are omitted for clarity. The 9-BBN substituents are displayed in wireframe for improved clarity.

Complex: ($^{(BBN)2}NN^{tBu}$)$ZnCl_2(N_2H_4)$

Local Name: dmb_1_81

CCDC: 2214453

Table S14. Crystallographic parameters for : ($^{(BBN)2}NN^{tBu}$)$ZnCl_2(N_2H_4)$ 4-N_2H_4

Crystal data	
Chemical formula	$C_{44}H_{78}B_2Cl_2N_5O_3Zn$
M_r	883.00
Crystal system, space group	Monoclinic, $P2_1/c$
Temperature (K)	85
a, b, c (Å)	24.4636 (2), 11.2506 (1), 18.4289 (1)
β (°)	109.297 (1)
V (Å^3)	4787.22 (6)
Z	4
Radiation type	Cu $K\alpha$
μ (mm^{-1})	2.06
Crystal size (mm)	0.18 × 0.18 × 0.15
Data collection	
Diffractometer	Dtrek-*CrysAlis PRO*-abstract goniometer imported rigaku-*D*TREK* images
Absorption correction	Multi-scan *CrysAlis PRO* 1.171.40.53 (Rigaku Oxford Diffraction, 2019) Empirical absorption correction using spherical harmonics, implemented in SCALE3 ABSPACK scaling algorithm.
T_{min}, T_{max}	0.683, 1.000
No. of measured, independent and observed [$I > 2\sigma(I)$] reflections	72778, 8938, 8504
R_{int}	0.039
$(\sin\theta/\lambda)_{max}$ (Å^{-1})	0.607
Refinement	
$R[F^2 > 2\sigma(F^2)]$, $wR(F^2)$, S	0.039, 0.113, 1.03
No. of reflections	8938
No. of parameters	722
No. of restraints	952
H-atom treatment	H atoms treated by a mixture of independent and constrained refinement
$\Delta\rho_{max}$, $\Delta\rho_{min}$ (e Å^{-3})	0.27, −0.44

Computer programs: CrysAlis PRO 1.171.40.53 (Rigaku OD, 2019), CrysAlis PRO 1.171.40.53 (Rigaku OD, 2019), SHELXT 2018/2 (Sheldrick, 2018), SHELXL2018/3 (Sheldrick, 2018).

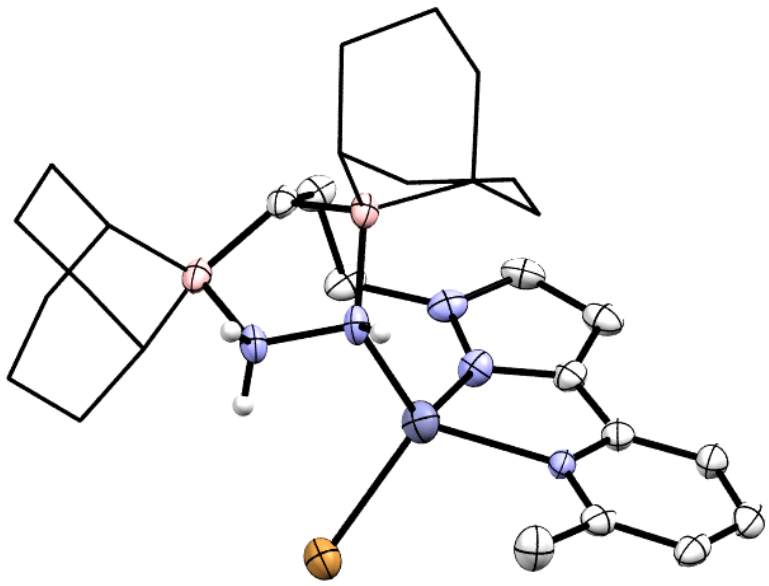

Figure S109. Molecular structure of ($^{(BBN)2}NN^{tBu}$)ZnBr(N_2H_3) displayed with 50% probability ellipsoids. Hydrogen atoms not attached to hydrazodp unit are omitted for clarity. The 9-BBN substituents are displayed in wireframe for improved clarity.

Complex: ($^{(BBN)2}NN^{tBu}$)ZnBr(N_2H_3)

Local Name: dmb_1_167

CCDC: 2214458

Table S15. Crystallographic parameters for ($^{(BBN)2}NN^{tBu}$)ZnBr(N_2H_3) 5-Br.

Crystal data	
Chemical formula	$C_{28}H_{48.67}B_{1.33}Br_{0.67}N_{3.33}O_{1.67}Zn_{0.67}$
M_r	569.97
Crystal system, space group	Monoclinic, $P2_1/c$
Temperature (K)	293
a, *b*, *c* (Å)	11.440 (2), 20.059 (4), 18.949 (4)
β (°)	95.55 (3)
V (Å^3)	4328.05 (4)
Z	2
Radiation type	Cu *K*α
μ (mm^{-1})	1.53
Crystal size (mm)	0.21 × 0.20 × 0.18
Data collection	
Diffractometer	Dtrek-*CrysAlis PRO*-abstract goniometer imported rigaku-*D*TREK* images
Absorption correction	Multi-scan *CrysAlis PRO* 1.171.42.61a (Rigaku Oxford Diffraction, 2022) Empirical absorption correction using spherical harmonics, implemented in SCALE3 ABSPACK scaling algorithm.
T_{min}, T_{max}	0.918, 1.000
No. of measured, independent and observed [$I > 2\sigma(I)$] reflections	65546, 7979, 7887
R_{int}	0.039
$(\sin \theta/\lambda)_{max}$ (Å^{-1})	0.607
Refinement	
$R[F^2 > 2\sigma(F^2)]$, $wR(F^2)$, S	0.043, 0.118, 1.07
No. of reflections	7979
No. of parameters	1050
No. of restraints	2309
H-atom treatment	H-atom parameters constrained
$\Delta\rho_{max}$, $\Delta\rho_{min}$ (e Å^{-3})	0.60, −0.64

Computer programs: CrysAlis PRO 1.171.40.53 (Rigaku OD, 2019), CrysAlis PRO 1.171.40.53 (Rigaku OD, 2019), SHELXT 2018/2 (Sheldrick, 2018), SHELXL2018/3 (Sheldrick, 2018).

Refinement details:

A THF molecule was refinded as 1:1 disordered across an inversion center. Atom positions were freely refined. U^{ij} components of ADPs for disordered atoms closer to each other than 2.0 Angstrom were restrained to be similar.

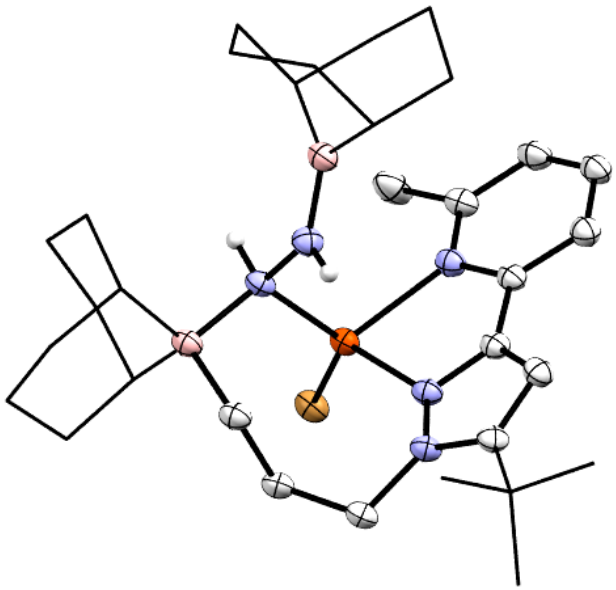

Figure S110. Molecular structure of ($^{(BBN)2}NN^{tBu}$)FeBr(N_2H_2) displayed with 50% probability ellipsoids. Hydrogen atoms not attached to diazene unit are omitted for clarity. The 9-BBN substituents and tert-butyl groups are displayed in wireframe for improved clarity.

Complex: ($^{(BBN)2}NN^{tBu}$)FeBr(N_2H_2)

Local name: dmb_1_131

CCDC: 2214457

Table S16. Crystallographic parameters for ($^{(BBN)2}NN^{tBu}$)FeBr(N_2H_2) 6.

Computer programs: CrysAlis PRO 1.171.40.53 (Rigaku OD, 2019), CrysAlis PRO 1.171.40.53 (Rigaku OD, 2019), SHELXT 2018/2 (Sheldrick, 2018), SHELXL2018/3 (Sheldrick, 2018).

Crystal data	
Chemical formula	$C_{32}H_{52}B_2BrFeN_5 \cdot O_{.5}(C_6H_6) \cdot C_4H_8O$
M_r	775.32
Crystal system, space group	Triclinic, *P*1
Temperature (K)	293
a, *b*, *c* (Å)	12.1486 (2), 12.2452 (2), 14.1823 (3)
α, β, γ (°)	72.016 (2), 77.781 (2), 88.918 (2)
V (Å^3)	1958.78 (7)
Z	2
Radiation type	Cu *K*α
μ (mm^{-1})	4.55
Crystal size (mm)	0.12 × 0.04 × 0.04
Data collection	
Diffractometer	Dtrek-*CrysAlis PRO*-abstract goniometer imported rigaku-*D*TREK* images
Absorption correction	Multi-scan *CrysAlis PRO* 1.171.40.53 (Rigaku Oxford Diffraction, 2019) Empirical absorption correction using spherical harmonics, implemented in SCALE3 ABSPACK scaling algorithm.
T_{min}, T_{max}	0.700, 1.000
No. of measured, independent and observed [$I > 2\sigma(I)$] reflections	29509, 7046, 6827
R_{int}	0.033
$(\sin \theta/\lambda)_{max}$ (Å^{-1})	0.607
Refinement	
$R[F^2 > 2\sigma(F^2)]$, $wR(F^2)$, *S*	0.034, 0.094, 1.05
No. of reflections	7046
No. of parameters	468
No. of restraints	40
H-atom treatment	H atoms treated by a mixture of independent and constrained refinement
$\Delta\rho_{max}$, $\Delta\rho_{min}$ (e Å^{-3})	0.46, −0.57

References

1) A. V. Polezhaev, C.-H. Chen, Y. Losovyj, K. G. Caulton, *Chem. Eur. J*., **2017**, 23, 8093.
2) J. J. Kiernicki, E. E. Norwine, Matthias Zeller, and N. K. Szymczak, *Chem. Commun*., **2019**, 55, 11896
3) CrysAlisPro 1.171.38.41 (Rigaku Oxford Diffraction, 2015).
4) CrystalClear Expert 2.0 r16, Rigaku Americas and Rigaku Corporation (2014), Rigaku Americas, 9009, TX, USA 77381-5209, Rigaku Tokyo, 196-8666. Japan
5) Bruker Advanced X-ray Solution, Apex3, SAINT, SADABS, Bruker AXS Inc.: Madison (WI), USA, 2018.
6) Sheldrick, G. M., A Short History of SHELX. *Acta Crystallogr., Sect. A.* **2008**, *64*, 112-122.
7) Sheldrick, G.M. Crystal structure refinement with SHELXL. *Acta Crystallogr. Sec.t C. Struct. Chem.* **2015**, *71*, 3–8.
8) Hübschle, C.B., Sheldrick, G.M., Dittrich, B. ShelXle: a Qt graphical user interface for SHELXL. *J. Appl. Crystallogr.* **2011**, *44*, 1281–1284.
9) M. A. Beckett, G. C. Strickland, J. R. Holland, V. K Sukumar, *Polymer*, **1996**, 37, 20, 4629.
10) Gaussian 09, Revision D.01, M. J. Frisch, G. W. Trucks, H. B. Schlegel, G. E. Scuseria, M. A. Robb, J. R. Cheeseman, G. Scalmani, V. Barone, G. A. Petersson, H. Nakatsuji, X. Li, M. Caricato, A. Marenich, J. Bloino, B. G. Janesko, R. Gomperts, B. Mennucci, H. P. Hratchian, J. V. Ortiz, A. F. Izmaylov, J. L. Sonnenberg, D. Williams-Young, F. Ding, F. Lipparini, F. Egidi, J. Goings, B. Peng, A. Petrone, T. Henderson, D. Ranasinghe, V. G. Zakrzewski, J. Gao, N. Rega, G. Zheng, W. Liang, M. Hada, M. Ehara, K. Toyota, R. Fukuda, J. Hasegawa, M. Ishida, T. Nakajima, Y. Honda, O. Kitao, H. Nakai, T. Vreven, K. Throssell, J. A. Montgomery, Jr., J. E. Peralta, F. Ogliaro, M. Bearpark, J. J. Heyd, E. Brothers, K. N. Kudin, V. N. Staroverov, T. Keith, R. Kobayashi, J. Normand, K. Raghavachari, A. Rendell, J. C. Burant, S. S. Iyengar, J. Tomasi, M. Cossi, J. M. Millam, M. Klene, C. Adamo, R. Cammi, J. W. Ochterski, R. L. Martin, K. Morokuma, O. Farkas, J. B. Foresman, and D. J. Fox, Gaussian, Inc., Wallingford CT, 2016.
11) Stephens, P. J.; Devlin, F. J.; Chabalowski, C. F.; Frisch, M. J. *Ab Initio* Calculation of Vibrational Absorption and Circular Dichroism Spectra using Density Functional Force Fields. *J. Phys. Chem.* **1994**, *98*, 11623-11627.
12) Rassolov, V. A.; Pople, J. A.; Ratner, M. A.; Windus, T. L. 6-31G* Basis Set for Atoms K through Zn. *J. Chem. Phys.* **1998**, *109*, 1223-1229.
13) Ditchfield, R.; Hehre, W. J.; Pople, J. A. Self-Consistent Molecular-Orbital Methods. IX. An Extended Gaussian-Type Basis for Molecular-Orbital Studies of Organic Molecules. *J. Chem. Phys.* **1971**, *54*, 724-728.
14) Rassolov, V. A.; Ratner, M. A.; Pople, J. A.; Redfern, P. C.; Curtiss, L. A. 6-31G* basis set for third-row atoms. *J. Comput. Chem.* **2001**, *22*, 976-984.
15) Lathem, A. P.; Heiden, Z. M. Quantification of Lewis Acid Induced Brønsted Acidity of Protogenic Lewis bases. *Dalton Trans.* **2017**, *46*, 5976-5985.